Speciation of and the effects of silver nanoparticles on the earthworm *Aporrectodea caliginosa*

A thesis

submitted in partial fulfilment

of the requirements for the Degree of

Masters of Applied Science

at

Lincoln University

by

Abby Bate

Lincoln University

2015

Abstract of a thesis submitted in partial fulfilment of the requirements for the Degree of Masters of Applied Science.

Speciation of and the effects of silver nanoparticles on the earthworm *Aporrectodea caliginosa*

by

Abby Bate

Silver nanoparticles (AgNPs) were first used as antimicrobial agents. Through technological development, AgNPs are now used in a wide range of applications across the commercial sector due to their beneficial antimicrobial and other desirable traits. However these traits are also what has generated great concern to environmental scientists. There are numerous suggested pathways that can cause AgNP soil contamination. This research was designed to compare the toxic effects of low environmentally relevant doses of AgNP and $AgNO_3$ on the earthworm species *A. caliginosa.* A total of 60 earthworms were DNA typed for the cytochrome oxidase I gene to identify *A. caliginosa* specimens. The genetically typed earthworms were then used to construct a breeding population of *A. caliginosa*. Citrate coated AgNPs were synthesised and characterised for soil exposure experiments. Earthworms were exposed to 0.3 $mgkg^{-1}$ AgNP, 30 $mgkg^{-1}$ AgNP, 3 $mgkg^{-1}$ $AgNO_3$ and 0 $mgkg^{-1}$ control in 600 g of organic soil. RNA samples and coelomocyte samples were removed from earthworms at 3 time points, 2, 7 and 14 d. Gene expression of catalase (CAT), superoxide dismutase (SOD) and metallothionein (MT), and also coelomocyte viability and differential coelomocyte cell counts were studied. CAT gene expressions were significant across treatments notably at the 14 d time point. SOD gene expressions were also significant across time, and several - fold inductions of SOD were measured across all the treatment conditions at the 14 d time point. There was no significant effect on coelomocyte cell viability. Among the coelomocytes, the amoeobocyte proportions were significantly higher on day 14 across all treatments and granulocytes were significantly higher on day 2 across all treatments. The research showed an effect on gene expression of CAT and SOD and also on coelomocyte cell

type proportion fluctuations following exposure to AgNP and $AgNO_3$. Overall, the threat of environmentally relevant AgNP doses in soil do not pose an immediate threat to the earthworm species *A. caliginosa* based on the few parameters studied.

Keywords: Aporrectodea caliginosa, cytochrom oxidase I, silver nanoparticle, flame atomic absorption spetrospcopy, silver nitrate, catalase, superoxide dismutase, metallothionein, quantitative PCR, coelomocyte, eleocyte, amoebocyte, granulocyte.

Acknowledgements

As this postgraduate research work comes to an end, I reflect on all of the obstacles and accomplishments I have encountered throughout this experience. As is the case with all research work, I faced difficult times where all practical and logical efforts were in vain. While these periods were testing of my character, I persevered and developed strong critical thinking skills as a result. This postgraduate research work has helped me evolve into a more confident and adaptable scientist.

To my two supervisors, Dr. Ravi Gooneratne and Dr. Victoria Metcalf, I would like to express earnest thanks for their support and encouragement throughout my research. Their collective experience and enthusiam in their fields of expertise were essential to my achievements. Both of my supervisors have gone over and above the requirements of postgraduate supervisors from the very beginning of my MApSc, for which I will always be grateful.

To the Don Hulston Foundation, I extend my thanks for awarding me the Don Hulston Foundation Scholarship. This generosity allowed me to dedicate my time to my demanding research and alleviated the burden of financial strain during my postgraduate research. I would also like to thank the Alma Baker Trust for awarding me the Alma Baker Trust postgraduate scholarship during the first theory based year of MApSci, again allowing me to concentrate fulltime on my studies.

To Dr. Christopher Winefield, who graciously found time to guide and advise me through the challenging genetic based obstacles I encountered. His support, guidance and enthusiaum inspired and encouraged me to perserve through the challenging genetic based complications experienced in this work.

To Scott Gregan and Dr. Darrell Lizamore, who both made the time to assist me with technical issues encountered during my qPCR analysis work. To fellow researcher Nadir Saleeb and Dr Craig Bunt for their helping with AgNP characterisation and experimental dose design.

To the entire department of RFH, thank you for the daily advice, laugther and encoragement. A special thank you to Martin Wellby for assistance with numerous tasks throughout my research.

To the research group at Université Lille 1 France, thank you for developing my skills and preparing me for my work in this field of research.

Finally to my friends and family, who were encouraging and supportive through this entire journey I extend my thanks.

Table of Contents

List of Tables

List of Figures

Chapter 1

Introduction

1.1 Silver Nanoparticles

A nanomaterial has been defined by the European Commission states as "A natural, incidental or manufactured material containing particles, in an unbound state or as an aggregate or as an agglomerate and where, for 50 % or more of the particles in the number size distribution, one or more external dimensions is in the size range 1 nm - 100 nm". Silver nanoparticles (AgNPs) are broad spectrum antimicrobial agents which were originally utilised as antiseptic agents over a century ago (Boese, 1920). Recently, through technological development, AgNPs are now widely used in a range of applications across the commercial sector including healthcare, appliances, food packaging and clothing. In addition to the efficient antimicrobial traits, the ease of AgNP incorporation into numerous materials has led to their increased manufacture for downstream applications. The ever-growing manufacture and the non-selective antimicrobial trait of AgNPs is generating great concern to environmental scientists since an adequate, robust environmental risk assessment has not been conducted (Nowack *et al.,* 2011).

Silver at the nanoscale no longer behaves as bulk Ag and there are numerous unique physio-chemical properties which distinguish AgNPs from the characteristics of bulk Ag (Fabrega *et al.,* 2011). It is some of these properties which are considered responsible for the toxicity AgNPs inflicts on biological life. Although larger particulates of Ag have been thoroughly researched and interactions with biological systems are well understood, the interactions

between AgNPs and biological systems are not well studied and remain unpredictable (Beer *et al.,* 2012).

1.2 Silver Nanoparticle Industry

The current technological age has seen the specialised use and complexity of nanomaterials increase and continue to evolve for many applications (Byrne *et al.,* 2008). These materials are xenobiotics with unique properties and are now entering the consumer market in large unregulated volumes (Wang *et al.,* 2010). According to the Woodrow Wilson International Centre for Scholars product inventory of nanomaterials (2010), in 2009 there were 1,015 products on the market containing nanomaterials, with the majority of these materials being metal-based NPs. Furthermore, it was reported that 25% of these were AgNPs (Yu *et al.,* 2013).

With these products presently in circulation, and the manufacture of them projected to steadily increase, researchers and environmental protection agencies are concerned by the uncertain effects these novel materials may exhibit on environmental health (Nowack *et al.,* 2011). The growing use of AgNPs and their antimicrobial behaviour on soil micro-organisms have been under immense scrutiny (Lorenz *et al.,* 2012). This has led to an increase in the amount of research on AgNP environmental release and subsequent environmental effects (Benn & Westerhoff, 2008). This is encouraging especially because an excess of 300 tons of AgNPs are produced and used annually worldwide and a significant proportion of those will enter the environment (Gottschalk *et al.,* 2010).

Manufacturers have been shifting away from organic chemical agents and opting for more effective additives of less toxicity and higher potency. AgNPs offer manufactures an advantageous alternative as low AgNP concentrations have a high impact and they can be

used across a variety of products. An attractive property of AgNPs is their tolerance to heat which is essential for incorporation into plastic and other products (Nowack *et al.,* 2011). AgNPs have a large surface area to volume ratio. This trait is hypothesised to provide greater surface contact to microbial cells and therefore greater antimicrobial activity. AgNPs are not microbial selective agents but rather express broad spectrum activity across a range of diverse species both of Gram negative and Gram positive bacteria and eukaryotic organisms (Marambio-Jones & Hoek, 2010). This has led to the recent claims made by manufacturers who use AgNP based products. These claims include statements such as ‘‘eliminate 99 % of bacteria’’, ‘‘permanently antimicrobial and antifungal’’, ‘‘kill approximately 650 kinds of harmful germs and viruses’’ and ‘‘kill bacteria in as short a time as 30 min” (Shahrokh & Emtiazi, 2009).

AgNPs have been commercially available for over 100 years but it is only in the modern day that the term “nano” has seen AgNPs perceived as a new and innovative substance. AgNPs have a long history of diverse commercial applications including use in synthesis of pigments, photographics, medical products, catalysts and biocides. In the USA, Ag impregnated water filters have been widely used in domestic applications for decades. Also Ag based algicides and disinfectants have been EPA registered since the 1950’s (Nowack *et al.,* 2011).

Emerging antibiotic resistance of various pathogenic bacteria has probably led to a resurgence of AgNP products. Applications within the medical sector account for a large proportion of current applications and developments (Rai *et al.,* 2009). These antimicrobial properties are considered to justify their application in over 250 consumer products. These include domestic appliances such as in washing machines and refrigerators, paints, clothing and food containers to name a few.

There is also growing use and interest of AgNP applications in agriculture, with an emphasis on phytopathogen management (Jo *et al.,* 2009). Based on then current usage, it was estimated that more than 1,120 tons of AgNPs would be synthesised before 2015 (Stensberg *et al.,* 2011).

1.3 Silver Nanoparticle Toxicity

It is believed that when AgNPs come into contact with moisture, toxic silver (Ag^+) ions are released. It has long been suggested that the antimicrobial capacity of Ag applications is directly proportional to the rate of Ag^+ formation (Egger *et al.,* 2009). Ag toxicity was described by Nowack *et al.* (2011) as having two opposite spectrums in terms of Ag^+ release and therefore toxicity. The low toxicity end of the spectrum is the formation of the compound Ag sulphide (Ag_2S). Ag_2S is well documented as a dominant chemical form when AgNPs are oxidised in the environment and waste water treatment plants (Lowry *et al.,* 2012a). The insoluble nature of Ag_2S not only reduces the rate of the Ag^+ release but also alters the surface chemistry and charge of AgNPs (Levard *et al.,* 2011), which correlates with its aggregate persistence (Lowry *et al.,* 2012b). At the high toxicity end of the spectrum is the high Ag^+ releasing, soluble Ag nitrate salt. AgNP toxicity resides between these two spectrums and numerous measurable parameters will affect how toxic a specific AgNP type will be (Nowack *et al.,* 2011).

The severity of AgNP toxicological effects on an organism is proportional to the size of the particles. Smaller sized AgNP have been shown to induce greater physiological effects. Lapied *et al.* (2010) found that the smaller colloidal AgNP (20 nm) induced a much higher rate of apoptosis in the earthworm *Lumbricus terretris* than the larger aggregated AgNP. Hu *et al.* (2012) demonstrated that both ~10nm and ~80nm AgNP generated inhibition of gene

expression of antioxidant enzymes such as superoxide dismutase in the earthworm *Eisenia fetida* with the effects of the ~10nm AgNP being much greater.

El Badawy *et al.* (2010) demonstrated that AgNP toxicity to *Bacillus* species is dependent on the surface charge and charge density of the particles ranging from highly positive to highly negative static potential. The charge density of AgNP is influenced by the capping agent or the reductant used during synthesis. El Badawy *et al*. (2010) showed that there is a direct correlation between the surface charge of AgNP and the degree of toxicity.

In a recent study investigating the toxic effects of AgNP based on size and charge, three differently coated AgNPs, citrate-coated AgNP, polyvinylpyrrolidone (PVP) -coated AgNP, and the branched polyethyleneimine-coated (BPEI) AgNP, each with different surface charges and particle sizes, were tested on two model organisms, *Escherichia coli* and *Daphnia magna* (Silva *et al.,* 2014). The toxicity for all of the AgNP types were compared to the toxicity of Ag^{+}, in the form of $AgNO_3$. Based on 100 % *D. magna* mortality and dose concentrations, Ag^{+} was the most toxic with at 3.26 μgL^{-1}, BPEI AgNPs second at 4.05 μgL^{-1} citrate coated AgNP third at 14.1 μgL^{-1} and PVP AgNPs the least toxic at 40.3 μgL^{-1}. Of the AgNPs, BPEI AgNPs were the most toxic of the three AgNP types. The BPEI AgNPs were the smallest of the AgNPs, with a 10 nm diameter, but possessed a high positive surface charge of + 28.8 mV. Citrate-coated AgNPs were the second most toxic of the AgNPs. Citrate AgNPs were the second largest with a diameter of 56 nm and had the highest negative surface charge of – 20.08 mV. PVP particles were shown to be the least toxic of the three, were the largest of the AgNPs with a diameter of 72 nm and had a surface charge of – 7.49 mV (Silva *et al.,* 2014).

1.4 Mechanisms of AgNP toxicity

The mechanisms of AgNP toxicity reported in the literature are associated with 1) redox activity: generation of reactive oxygen species (ROS), induction of oxidative stress and cell death (apoptosis); 2) cell and organelle membrane disruption: cell membrane punctures which can inhibit or limit physiological function or cause cell lysis; 3) electron transfer disruption: electrons retained by NP and processes such as phosphorylation and energy transfer are inhibited; and 4) sorption to proteins: NPs interfere with protein conformation and protein function. Direct interaction with proteins could disrupt bio-chemical signalling and gene transcription (Pan & Xing, 2010).

Limbach *et al.* (2007) have described the entry of a single AgNP into a cell as a 'Trojan Horse' model. A single AgNP enters a cell but has the potential to release thousands of toxic Ag^{+}. The delivery of such a large volume of Ag^{+} over a short period can result in marked oxidative stress and/or cell apoptosis. Several animal and human cell model studies have highlighted the cytotoxicity of AgNPs to cells, including disruption to cellular membranes and elevated ROS formation due to oxidative stress (Hussain *et al.,* 2005; Ahamed *et al.,* 2010; Umh & Kim, 2013).

1.5 Entry into Environment

Theoretically every product containing AgNPs will release varying amounts of Ag based on their use and these particles will ultimately enter the storm water drains, waste water treatment plants and/or landfills. Therefore these particles will ultimately gain entry into aquatic, marine and soil ecosystems (Lowery *et al.,* 2012). The used water from a commercially available Samsung washing machine, which releases AgNPs during each wash cycle, is reported to release an approximate AgNP concentration of 11 μgL^{-1} per cycle. Such a

concentration of AgNPs measured in a single wash cycle if released on a regular basis can lead to a negative impact on natural bacterial communities, thus significantly reducing bacterial multiplication (Farkas *et al.,* 2011). Benn & Westerhoff (2008) performed a similar study investigating the release of AgNPs from six types of socks containing AgNPs. A simulated washing machine cycle revealed that the socks released as much as 1.3 mg of Ag per litre of water. This amounted to 50% of the AgNP contained within the socks. The Ag was detected as both NP and ionic forms. El-Temsah & Joner (2012) reported that in USA, approximately 150 tons of AgNPs end up in sewage sludge and about 80 tons are released into surface waters annually.

AgNPs gain entry into terrestrial ecosystems from AgNP deposition (suspended in air from waste incineration plants), sewage sludge (biosolid) applications and AgNP containing consumer products (e.g. paints and pesticides) (VandeVoort *et al.,* 2012). The application of AgNP based fertiliser/pesticides would contribute a large volume of AgNPs into soils (Calder *et al.,* 2012).

A majority of literature available on environmental behaviour and toxicity of AgNPs is dominated by aquatic based research. Soil is and will continue to be a future sink for AgNPs. However studies focusing on AgNPs in terrestrial ecosystems are limited and considering the complexity of this system and there are many questions still to be answered through research (Pan & Xing, 2012).

Investigations have shown that AgNPs tend to accumulate in sewage sludge with less being suspended in the liquid effluent discharged to surface waters (Hou *et al.,* 2012; Wang *et al.,* 2012a). Therefore the majority of NPs will be present in the sludge following waste water treatment. This highlights a potential concern using biosolid fertiliser application on land.

Biosolids is the term used for organic sewage sludge applications as fertiliser. AgNPs in biosolids can interfere with soil microbial composition, function and overall soil ecosystem homeostasis. Therefore research is required to ensure that no ill effects will result following such applications (Gottschalk *et al.,* 2009; Gottschalk & Nowack, 2011).

As stated earlier, AgNP use in agriculture is projected to increase because of its antimicrobial and insecticidal properties (Zhang *et al.,* 2012). Global crop yields are annually reduced by 20-40% by pathogenic micro-organisms and other infectious pests (Strange & Scott, 2005). In recent years this has led to the development and use of a variety of pesticides containing AgNPs and other heavy metals (Bergeson, 2010).

1.6 Environmental Detection

Determining the environmental risks AgNPs pose to soil ecosystems and detecting AgNPs in soil is complicated due to their size, reactivity and lack of clear knowledge of dissolution chemistry (Benoit *et al.,* 2013). Based on their antimicrobial nature, AgNPs have been reported to threaten the stability of free-living nitrogen-fixing bacterial communities and other essential symbiotic cultures present in soil. Interference to these and other microbial soil inhabitants have been suggested to disrupt the soil physico-chemical properties (Klaine *et al.,* 2008).

To date, the majority of data available regarding AgNP concentrations in soils are based on predictions and measurements reported from studies. In 2008, USA soil concentrations of AgNPs were reported as between 0.02 and 0.1 $\mu g kg^{-1}$ (Mueller & Nowack, 2008). Subsequently, Gottschalk *et al.* (2009) reported that land fertilised with biosolids in the USA

has AgNP concentrations of up to 13 μgkg^{-1}, 130 times that predicted by Mueller & Nowack, (2008).

Detecting and monitoring AgNPs and their chemical derivatives in soil remains an obstacle (Glover *et al.,* 2011). It is possible to identify and quantify AgNPs by UV Vis spectrometry and this method is currently used in NP analysis. However, there are errors associated with UV-Vis spectrometric analyses. For example, NPs do not have a set molecular mass due to varying states of aggregation and chemical reactivity due to oxidation. To have confidence in this form of quantitative analysis, researchers need to have confidence that the NPs are chemically stable. This is an unrealistic expectation when analysing environmental samples (Pan & Xing, 2012). Less direct approaches are being applied to investigate levels of AgNP soil contamination, such as observations of adverse effects to soil health.

Soil health is determined by the biodiversity and bio-activity which are essentially responsible for sustaining the health of the soil system. Detectable disruptions to soil health could be utilised through the development of standardised, key bio-indicator measurements that could be applied to all soil metal-based NP toxicity studies (Pan & Xing, 2012).

1.7 Biomarkers and bioassays

Biomarkers and bioassays provide means of early detection of environmental impacts by chemicals on organisms, including NP pollution, and therefore can be used to detect and quantify the extent of AgNP contamination in ecosystems. A biomarker is defined as a measureable biological response to a chemical or stress. The rate and level of change detected in a biomarker is correlated to the exposure period and exposure dose. These quantifiable changes can be recognised in biomarkers at the molecular, cellular or physiological/ behavioural levels (Brulle *et al.,* 2006).

A limited number of studies have shown that the toxicity risk of AgNPs in soil is low compared to the risk to aquatic systems (Römer *et al.,* 2011; Kim *et al.,* 2011; Unrine *et al.,* 2012; Oukarroum *et al.,* 2013; Choi *et al.,* 2009). This statement is understandable as the charge expressed by NPs will interact with soil components and potentially decrease their overall toxicity.

Earthworms are predominantly used currently as bio-indicator models in NP soil toxicity research as they are fundamental soil dwelling invertebrates and easy to work with. It is also suggested that if ill effects are observed on earthworms following NP exposure in soils, then the entire soil ecosystem and soil productivity is at risk. Hu *et al.* (2010) showed that the mortality, growth and fertility of earthworms was affected at soil AgNP ≥1 g kg^{-1} soil. Some oppose such measurements, arguing that these endpoints (mortality, growth and fertility) are long-term effects and therefore not sensitive enough to identify a full complement of the negative effects and that experiments with lower dose exposures and more sensitive endpoints are more relevant. Lapied *et al.* (2010) highlighted this on exposure of earthworm *L. terrestris* in soil at doses of 4 mg kg^{-1} of AgNPs and a year later to 15 mg kg^{-1} titanium dioxde NPs (Lapied *et al.,* 2011). At these lower doses, Lapied *et al.* (2011) measured the frequency and specific tissue types that exhibited cellular apoptosis. Cellular apoptosis is a downstream effect of overwhelming oxidative stress. Apoptosis has been shown to be a sensitive biomarker for low dose NP exposures (Lapied *et al.,* 2011).

Tsyusko *et al.* (2012) showed that both gene induction and protein production are caused by oxidative stress to the earthworm *E. fetida* following exposure to AgNPs and Ag^{+} doses in soil. Similar studies have now highlighted 14 biomarker genes in *E. fetida* following exposures to Cd in soil. Gene expression changes were shown to be dose and time dependent (Brulle *et al.,* 2006). Molecular responses are now routinely used and have

become an essential tool to understanding metal and metal based NP toxicity in earthworms. The advances in molecular techniques applied in the above studies are an examples of the growing field of toxicogenomics. These approaches are a significant milestone in toxicological research. The information that can be obtained from a whole-genome, transcriptomics analysis can potentially identify toxic effects previously undiagnosed (Afshari *et al.,* 2011). Such information can be used to better understand mutations, chromosome breakages and other biological consequences to develop more robust hazard identification assessments and cancer risk estimations (Mahadevan *et al.,* 2011).

1.8 Research Aim and Objectives

1.8.1 Aim and context:

The aim of this research is to investigate and compare the effects of AgNPs and Ag^+ (in the form of $AgNO_3$), on the earthworm *Apporectodea caliginosa* exposed to chronic soil exposures through the use of selective oxidative stress gene expression levels and immunological cell compensation as biomarkers of toxicity.

1.8.2 Objectives:

1. Generate a homogenous population of *A. caliginosa* (speciation) through morphological and DNA analysis.
2. Establish and maintain optimum breeding conditions for a homogenous *A. caliginosa* population.
3. Expose *A. caliginosa* specimens to environmentally relevant and toxicologically comparative doses of AgNP and Ag^+ (in the form of $AgNO_3$) in soil over three time-points.
4. Amplify and sequence three genes of interest (GOI) (superoxide dismutase [SOD], catalase [CAT], metallothionein [MT]) and one reference gene (β-actin) from *A. caliginosa* cDNA.
5. Design qPCR primers within amplified GOI and reference gene sequences.
6. Perform quantitative analysis of GOI across all exposure treatments and time points.
7. Isolate coelomocytes from earthworms for viability and cellular differentiation following exposure to AgNP and Ag^+ (in the form of $AgNO_3$) in soil over three time-points counts.

1.8.3 Hypothesis:

i. The gene inductions in *A. caliginosa* following exposure to AgNP are dose dependent, reproducible and greater than on exposure to $AgNO_3$.

ii. Up-regulations pattern of GOI are similar across 3 $mgkg^{-1}$ $AgNO_3$ and 30 $mgkg^{-1}$ AgNP doses.

iii. A decrease in coelomocyte concentration and coelomocyte cell types in *A. caliginosa* following exposure to 3 $mgkg^{-1}$ $AgNO_3$ and 30 $mgkg^{-1}$ AgNP doses.

Chapter 2

Aporrectodea caliginosa Speciation

2.1 Introduction

It is estimated that there are between 3000 and 3500 valid earthworm species classified to date (Csuzdi *et al.,* 2012). Earthworms are essentially soil-dwelling engineers and are useful indicator organisms for soil toxicity studies. The most abundant earthworms found in grasslands and agricultural soils are the *A. caliginosa* species complex, which is actually reported to consist of four taxa: *A. caliginosa* (Savigny, 1826)*, A. trapezoids* (Perrier, 1872)*, A. tuberculate* (Eisen, 1874) and *A. nocturna* (Evans, 1946). Morphologically these species are very similar to each other, making species identification difficult (Pérez-Losada *et al.,* 2009). It is possible to identify species through male genitalia dissection (Tsai *et al.,* 2010). However, this technique is time consuming, can only be performed on adult earthworms, and requires familiarity and specialised skills (Klarica *et al.,* 2012). The most direct, robust and an accurate

Figure 1: Morphological Variation of *A. caliginosa* and *A. trapezoid.* The *A. trapezoid* specimen has a darker top surface colour compared to *A. caliginosa* specimen.

method for species identification is to differentiate sequence divergences of the mitochondrial DNA genealogies. The mitochondrial 16S ribosomal RNA (16S), is commonly used for this purpose (Sathis *et al.,* 2013). However, there is no variation or very little (single nucleotide polymorphisms) sequence variation in 16S within the *A. caliginosa* complex. In combination with 16S RNA sequencing, other mitochondrial genes such as cytochrome oxidase subunit I (COI), cytochrome oxidase subunit II (COII), mitochondrial 12S ribosomal RNA (12S), and NADH subunit 5 are also employed in speciation experiments (Caterino *et al.,* 2000).

This genomic exploitation of sequence diversity is a powerful tool in taxon diagnosis (Wilson, 1995). Mitochondrial DNA provides a genetic barcode that can be isolated and identified from any cell of an organism (Hebert *et al.,* 2003).

The objective of this work was to genetically identify 60 *A. caliginosa* (referring to the species from henceforth rather than the species complex unless indicated) earthworms from an earthworm colony by isolation, amplification and sequencing of two widely used speciation gene sequences, COI and 16S. The positively identified earthworms were then isolated and housed in optimum conditions for breeding.

2.2 Material and Methods

2.2.1 Speciation Experiments

During a three month internship at Universite Lille 1, Lille, France, I analysed seven earthworm specimens were analysed from the breeding population at Lincoln University for species identification. These seven earthworms were found to be a heterogeneous population, consisting of at least 3 *Aporrectodea* species: *A. caliginosa, A. trapezoid* and *A. rosea*. Species identification was determined through the amplification and sequencing of

the 16S and COI genes. Degenerate primers specifically designed for annelid speciation experiments were used for this analysis.

To establish a homogeneous breeding population of *A. caliginosa,* a further 60 earthworms were selected from an established Lincoln University population for screening. Although not entirely accurate, there are some morphological characteristics that can be used to eliminate selection of non *A. caliginosa* earthworms. *A. trapezoid* is darker in colour on the topside than *A. caliginosa.* *A. rosea* is thinner and dark red in colour compared to *A. caliginosa*. However, as stated earlier, these characteristics are difficult to differentiate and alone do not guarantee successful species identification.

2.2.1.1 DNA Extraction

Small sections (~5mm) of tissue were cut, using a sterile scalpel, from the posterior end of each earthworm and transferred into a sterile labelled 1.5 mL Eppendorf tube. After tissue removal, each earthworm was transferred into a labelled plastic container containing ~250 g of moist organic soil and held in isolation in containers (Fig 2). All earthworms were numbered from 1 to 60.

Figure 2: Speciation earthworms held independently.

DNA was extracted from the tissue samples using a Genomic DNA tissue Nucleospin tissue kit, (MACHEREY-NAGEL, Düran, Germany), and following the manufacturer's instructions. DNA was quantified using a 1 µL sample and measuring absorbance ratios at 260 nm and 280 nm wavelengths using a DeNovix Ds-11+Spectrophotometer (Denovix, Inc., Wilmington, USA).

2.2.1.2 Speciation PCR Amplifications

PCR was performed using Qiagen Taq DNA polymerase, Qiagen dNTPs (200 µM), Qiagen 10x buffer Mg^{2+} 3mM, primer pairs (0.4 µM), ~200 ng DNA template in a reaction volume 25 µL using molecular grade water. Preliminary DNA samples had both 16S RNA and cytochrome oxidase I genes amplified by PCR, using the annelid primers (Annelid 16S For: 5'- CGG TAT CCT AAC CGT GCA AA – 3', Annelid 16S Rev: 5'- TTC CCT AAG CCA ACA TCG AG -3' and Annelid COI For: 5'- CCA CGC CTT CGT CAT GAT NNN TTN NTT -3', Annelid COI Rev: 5'- CCG CCG GCG GGN NTC NNA ANN AA -3'), the expected fragment size was verified by 1.5 % agarose gel electrophoresis with Hyper Ladder I Bioline (Bioline (Aust) Pty. Ltd, Australia) and the products sequenced by ABI Big Dye Terminator v3.1.

The remaining speciation experiments were performed using the *A. caliginosa* COI specific primers, designed based on the speciation studies performed in Lille (*A. caliginosa* COI For: 5'- GAT AGC CCC TAG GAT GGA GG -3', *A. caliginosa* COI Rev: 5'- ATT GGT GGC TTT GGA AAC TG -3') as well as positive control primers Annelid 16S primers which were provided by the Unversite Lille 1, Lille, France. Sequence results were subjected to a BLAST analysis on the NCBI website to identify the species.

2.2.2 Husbandry Conditions

When an earthworm sample was not identified as *A. caliginosa*, another earthworm was collected from the current population at Lincoln University. Once 60 *A. caliginosa* earthworms had been positively identified, they were used to establish a breeding population.

Six, 10 L containers were prepared containing 7 kg of air dried soil hydrated with 2.56 L of water to achieve field capacity (Appendix 1). The soil was collected from the Lincoln University Biological Husbandry Unit (BHU) and air dried at 70 ^{o}C in a drying oven to kill any

potential earthworm cocoons. As a food source, 450 g of defrosted cow manure was mixed evenly through the saturated soil. The cow manure collected from the Lincoln University dairy farm were frozen for two days at -18 ^{o}C to kill any earthworms, earthworm cocoons and parasites present in it prior to use.

Six containers containing 7 kg of soil and 700 g of manure were labelled A to F and 10 *A. caliginosa* identified from the speciation studies were added to each container. Each month, 500 mL of water and 700 g of defrosted cow manure were added to each container. In addition, six new 10 L containers with identical conditions were set up every 6 weeks, into which the original 10 earthworms were transferred and the cocoons resident in the original containers were allowed to develop into adults. This process continued for one year until there was an adequate population of *A. caliginosa* for the experiments.

2.3 Results

2.3.1 *A. caliginosa* COI Specific Primer Design

The partial 16S rRNA and COI gene sequences from the seven earthworm specimens analysed at University of Lille, France, were aligned using MultAlin, Multiple sequence alignment software (Florence Corpet, Florence, Italy). Based on the genetic data obtained from the Lille speciation studies, it was apparent that the sequence variation across the

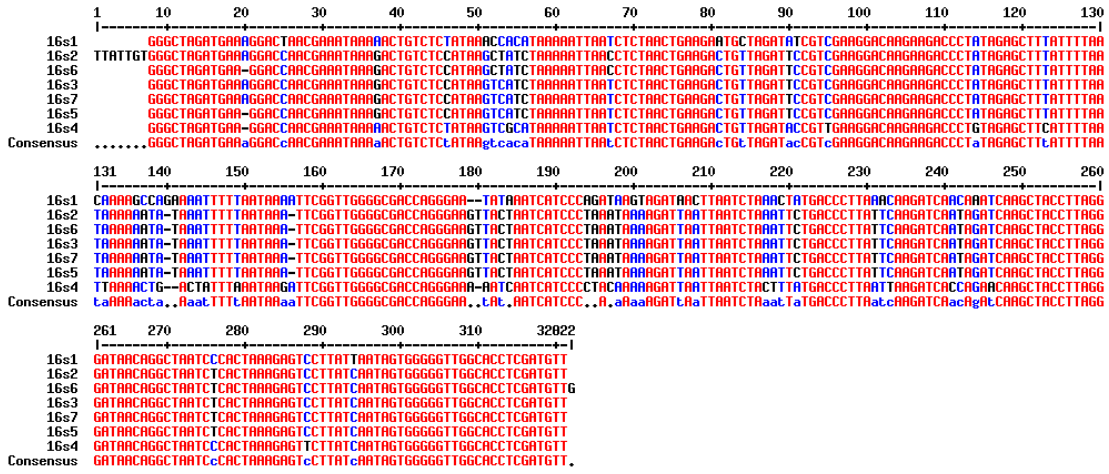

Figure 3: 16S sequence alignment from Lille speciation experiments.

three species identified was greater in the cytochrome oxidase I gene than 16S RNA. There was insufficient variation within the 16S RNA partial sequences from the different species to design *A. caliginosa*-specific primers (Fig 3). Red bases are conserved across all sequences, while the blue and black represent different bases, each colour being shared between sequences. This approach displays both sequence diversity and shared conservation. The variation within COI, determined from the Lille specimens, provided many sites within the sequence to design species-specific primers (Fig 4). The consensus COI sequence of the *A. caliginosa* samples was used to design *A. caliginosa*-specific COI primers. Figure 5 shows the primer locations within the COI sequence acquired (red, primer sequences; blue, amplification product).

Figure 5 shows the primer location within the COI sequence acquired.

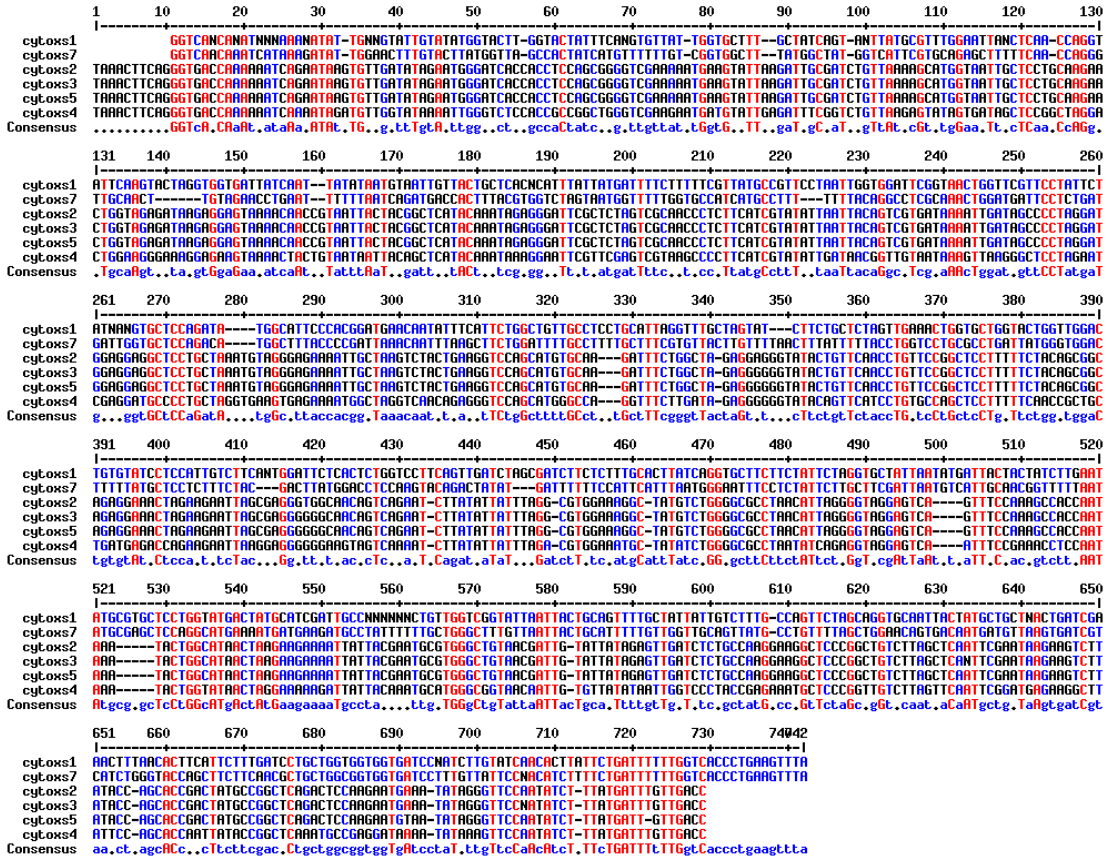

Figure 4: COI sequence alignment from University of Lille speciation experiments.

TAAACTTCAGGGTGACCAAAAAATCAGAATAAGTGTTGATATAGAATGGGATCACCACCTCCAGCGGGG
TCGAAAAATGAAGTATTAAGATTGCGATCTGTTAAAAGCATGGTAATTGCTCCTGCAAGAACTGGTAGA
GATAAGAGGAGTAAAACAACCGTAATTACTACGGCTCATACAAATAGAGGGATTCGCTCTAGTCGCAAC
CCTCTTCATCGTATATTAATTACAGTCGTGATAAAATTGATAGCCCCTAGGATGGAGGAGGCTCCTGCT
AAATGTAGGGAGAAAATTGCTAAGTCTACTGAAGGTCCAGCATGTGCAAGATTTCTGGCTAGAGGAGGG
TATACTGTTCAACCTGTTCCGGCTCCTTTTTCTACAGCGGCAGAGGAAACTAGAAGAATTAGCGAGGGT
GGCAACAGTCAGAATCTTATATTATTTAGGCGTGGAAAGGCTATGTCTGGGGCGCCTAACATTAGGGGT
AGGAGTCAGTTTCCAAAGCCACCAATAAATACTGGCATAACTAAGAAGAAAATTATTACGAATGCGTGG
GCTGTAACGATTGTATTATAGAGTTGATCTCTGCCAAGGAAGGCTCCCGGCTGTCTTAGCTCAATTCGA
ATAAGAAGTCTTATACCAGCACCGACTATGCCGGCTCAGACTCCAAGAATGAAATATAGGGTTCCAATA
TCTTTATGATTTGTTGACC

Figure 5: *A. caliginosa* COI sequence and *A. caliginosa* COI specific primer locations.

2.3.2 Speciation PCR Amplifications

All of the initial PCR products amplified from earthworm DNA samples using the University of Lille derived degenerate primers, were of the expected fragment size (16S: ~300 bp and COI: ~720 bp). Sequencing results were subjected to a nucleotide BLAST search on the NCBI website to confirm gene- and species-specific amplification. The 16S sequencing results of the first ten DNA samples identified one earthworm to be *A. trapezoid* and the remaining 9 earthworms as *A. caliginosa*. The same DNA samples were then amplified again using *A. caliginosa* specific COI primers. Only the samples previously identified as *A. caliginosa* produced a PCR product with the *A. caliginosa* specific primers (Fig 6). Therefore, the remaining earthworms of the speciation studies (total n=62), were amplified using 16S (positive control) and *A. caliginosa* specific COI primers. Only those DNA samples positive for both PCR products were submitted to sequencing to confirm *A. caliginosa* samples and only COI products were sequenced to save on resources.

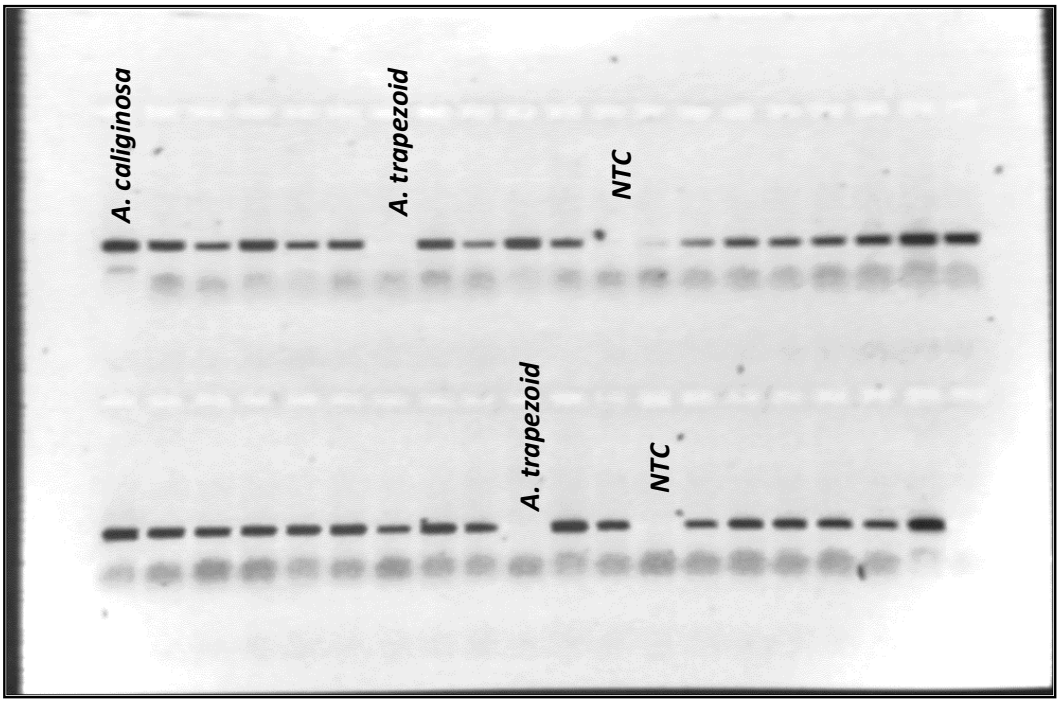

Figure 6: *A. caliginosa* specific COI PCR Products. All wells displaying bands are positive for *A. caliginosa* COI. Blank wells are *A. trapezoid* COI samples or NTC.

2.4 Discussion

For this nano-ecotoxicology based study, the taxonomy and positive genetic identification of the species being used was an essential part of the process, as these had not been published using the earthworm species *A. caliginosa* before. As this species is one of the dominant species found in New Zealand agricultural soils, it is a suitable model for soil toxicity studies in agricultural soil ecosystems. The speciation studies performed in France revealed that the breeding population at Lincoln University was heterogeneous, and consisted of at least three different species. The three species identified were morphologically similar, although subtle differences in colour and shape can assist in distinguishing them.

While performing this speciation work, earthworms were selected based on those factors. The COI sequences obtained were used to design

A. caliginosa specific primers, enabling identification of *A. caliginosa* specimens. Overall, 97.7 % of the earthworms morphologically selected as *A. caliginosa* were confirmed on PCR analysis as being *A. caliginosa,* with only 3.3% negative. The negative samples were

identified as being *A. trapezoid*. The 60 positively identified *A. caliginosa* thrived in the moist organic soil and rich manure conditions.

A phylogenetic study analysing the species variation of the *A. caliginosa* complex across Europe employed similar genetic methods (Pérez-Losada *et al.,* 2009). Earthworms (n=85) were collected from 27 different locations. To confirm the taxonomic status of each earthworm and phylogenetic relationships between locations, 6 genes were amplified and sequenced from these earthworms; COII, 12S and 16S RNA, NADH dehydrogenase 1 (ND1), tRNAs and 28S RNA and the sequencing data were analysed using Bayesian analysis and phylogenetic trees were constructed. This genomic evidence was combined with morphological and ecological evidence to determine species.

Comparing more genetically diverse earthworm species can be also achieved using COI as well as the 12S, 16S, and COII gene diversity used above. All of these genes were shown to be suitable genes for earthworm identification but with varying specificity. Klarcia *et al.* (2011), concluded 12S and 16S sequences are useful molecular markers for species identification while the COI gene is suited to identify genetic lineages and cryptic species. In my study, it was clear the genetic conservation of COI across even the closely related species, such as those three identified in the contained Lincoln population, was low. This allowed COI to be used for species selection via PCR amplification, whereas the 16S gene could only be used to confirm DNA integrity, but not to specifically identify of *A. caliginosa*. The results here ensured that all of the earthworm specimens used in the soil exposures (Chapter 3), the subsequent gene expression experiments (Chapter 4) and coelomocyte experiments (Chapter 5) were from a single species, *A. caliginosa*.

Chapter 3

Silver nanoparticle synthesis, characterisation and soil exposure studies

3.1 Introduction

Globally the rate of soil pollution has increased over the past 40 years through intensive agriculture, industrial activities and release of anthropological waste (Pan & Xing, 2012). Studies have shown that polluted soil threatens soil fertility; the sensitive balance of soil flora and fauna. Soil pollution can also alter soil structure, contaminate crops and ground water (Lionetto *et al.,* 2012).

With advances in nanotechnology, emerging pollutants include nanomaterials and these materials are entering soils through direct and indirect deposits. Keller *et al.* (2013) recently released estimates stating 63–91 % of the > 260,000–309,000 metric ton of global engineered NP-production in the year of 2010 ended up in landfills, with 8–28 % released into soils.

Most NP toxicity studies in soil compare the effects of both NP and also its equivalent dissolved ion at the same concentration (Pan & Xing, 2012). There is uncertainty over whether it is the NP or the released ions that inflict toxicity in soil models (Lubick, 2008). The toxicity of AgNPs is theorised to be caused by the release of Ag^{+}, therefore the difference in measured toxicity between ion and NP treatments can be used to indicate the amount of Ag^{+} released from NPs. Both AgNPs and Ag^{+} treatments have been shown to induce transcriptional fluctuations, in a dose dependent fashion (Gomes *et al.,* 2013).

The objective of the work contained within this Chapter was to: 1) synthesise, characterise and quantify citrate-coated AgNPs; 2) establish exposure conditions in soil; 3) the delivery of environmentally relevant AgNP doses to the earthworm species *A. caliginosa*. The results of this work provide the dosage amounts for exposure treatments for downstream gene expression (Chapter 4) and coelomocyte studies (Chapter 5).

3.2 Methods and Materials

3.2.1 Field Capacity Experiments

Organic soils were used in this work to eliminate any other chemical factors. The organic soil used for the treatment exposures was collected from the Biological Husbandry Unit (BHU), an organic farm at Lincoln University. The Ag treatment doses added to the soil were either via $AgNO_3$ or AgNP solutions. In order to determine the delivery volume of $AgNO_3$ or AgNP solutions to the soil, it is important to determine the field capacity of the organic soil being used. Field capacity is the amount of soil moisture or water content held in soil after excess water has drained away. To determine this, plastic rings, of known volume, with mesh bases were filled with the soil and saturated in water over night. Following saturation, the rings were transferred to tension tables for 24-48 hours. Tension tables are used in soil science experiments to drain away excess water in order to achieve field capacity. The tension tables provide the

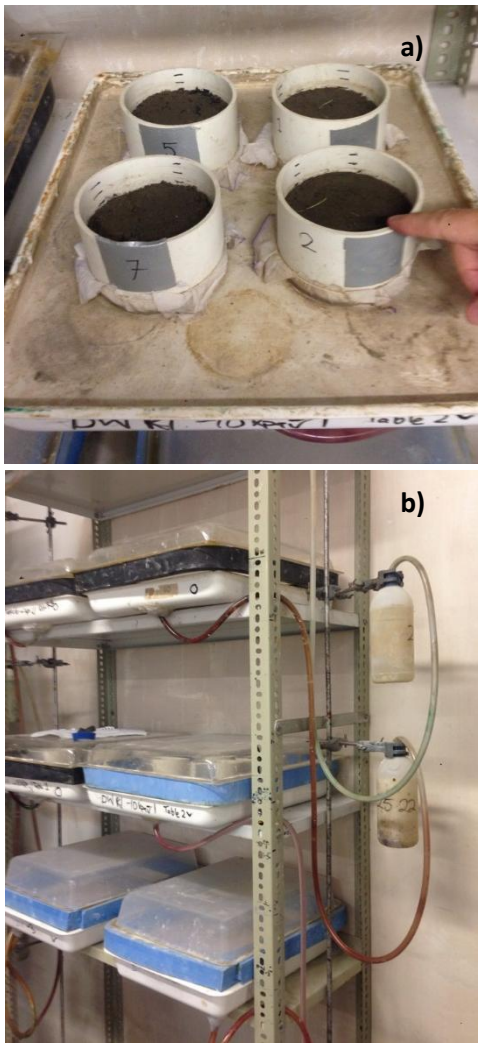

Figure 7: a) Plastic rings used to measure field capacity; b) Tension Table constructed to apply – 33 Jkg^{-1} suction pressure.

necessary – 33 Jkg^{-1} (field capacity unit of measure) suction pressure at which the bulk excess water content is retained in soil thus achieving field capacity. Following excess drainage, the weight of the wet soil was recorded. The wet soil was then oven dried at 60^{o}C for ~24 hours to constant weight and the soil weight was recorded. The field capacity results were calculated using the dry mass weight, wet mass weight and the total volume of the soil. This experiment was performed in triplicate. The moisture gravimetric % in the organic soil was calculated to be 36.6 %.

The plastic rings with soil within shown in Figure 7a are those following excess water drainage and before being transferred into the 60^{o}C oven for drying. The tension tables can be seen in Figure 7b connected to tubing draining the excess water at the necessary – 33 Jkg^{-1} suction pressure.

3.2.2 AgNP Synthesis and Quantification

3.2.2.1 Modified Carey Lea Method

Citrate coated AgNPs were synthesised using the original chemical reduction Carey Lea method first published in 1889. Carey Lea (1889) developed a AgNP production method synthesising a reddish-brown suspension of Ag through chemical reduction of $AgNO_3$ and peptization (dispersed as colloid) to create an Ag precipitate with citrate (Carey Lea, 1889). In my research, a modified Carey Lea (1889) method developed by Dr Brad Angel of CSIRO Land and Water, Sydney, Australia was used and is described below.

In a 25 mL beaker, 0.256 g of $AgNO_3$ was dissolved in 5 mL deionised water. A mixture of 2.5 mL of 1.076 M ferrous sulphate heptahydrate and 3.5 mL of 1.368 M trisodium citrate dehydrate was prepared and 6 mL of this mixture was added drop wise to the $AgNO_3$ solution with vigorous mixing using a magnetic stirrer. Instantly the colourless solution forms a dark brown precipitate. The solution is mixed for 5 min to produce an opaque

brown-black AgNP suspension. The AgNP suspension was transferred into a 50 mL falcon tube and centrifuged at 3000 rpm for 10 min. The supernatant was discarded and the black-blue pellet was re-suspended in 10 mL of 0.68 M trisodium citrate dihydrate. This step was repeated thrice. Following the fourth washing of the AgNP pellet, the supernatant was discarded and the pellet (Fig 8) re-suspended in 10 mL deionised water. The synthesised AgNPs were stored at 4^{o}C until being quantified and diluted for subsequent soil exposures.

3.2.2.2 AgNP morphology and size validation using TEM

The expected particle size distribution produced by the modified Carey Lea method range was approximately 2nm to 50nm, the majority of particles being from 10-30nm.The AgNPs synthesised by the modified Carey Lea method produce spherical shaped particles which will not aggregate due to the electrostatic repulsion of the citrate capping reagent (Carey Lea, 1889).

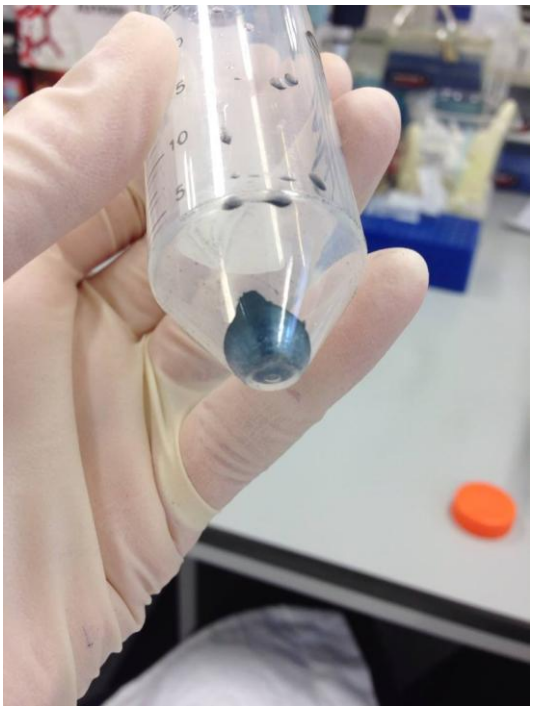

Figure 8: Carey Lea AgNP pellet.

The concentration of the AgNP suspension synthesised was too concentrated at 15gL^{-1} to be directly transferred onto a TEM gold-carbon grid for characterisation. Therefore, a 1:1000 dilution with deionised water was used (1µL in 1mL) for a more uniform distribution. Approximately, 10µL of the diluted sample was deposited onto each grid and left to air dry inside a fumehood to prevent dust contamination.

A transmission electron microscopy (TEM) technician at Canterbury University performed the analyses of the AgNP samples on the Philips CM200 high resolution analytical TEM (Amsterdam, Netherlands) fitted with a Gatan digital camera.

3.2.2.3 Ag Quantification

The modified Carey Lea states that a final Ag concentration of AgNP prepared by this method is approximately 15 gL^{-1}. The exact concentration of AgNP was determined by flame atomic absorption spectroscopy (FAAS) AA.6200 (Shimadzou, Japan). Calibration standards were serially diluted from a 1000ppm Ag Merck ICP certiPUR multi-element standard (Merck, Germany). The highest standard was 10 mgL^{-1}, taking 100 µL of Ag 1000 mgL^{-1} and making it up to 10 mL with deionised water. The following standards (5, 2.5 and 1.25 mgL^{-1}) were prepared by serial dilutions with deionised water.

Since the estimated Ag concentration stated by the modified Carey Lea method is 15 gL^{-1}, AgNP samples were diluted to fall within the standard range. A 35 µL aliquot of the AgNP sample (~15 gL^{-1}) was made up to 50 mL. Theoretically this dilution would equate to a AgNP concentration of ~10.5 mgL^{-1}. The actual concentrations varied between 9-10 mgL^{-1}.

3.2.2.4 Charge Measurement and Particle Size using Zetasizer

Zeta potential is a measure of the magnitude of the electrostatic or charge repulsion or attraction between particles, and is one of the fundamental parameters known to affect the stability of NP. Zetasizer can also measure the size distribution of the sample and is usually performed in conjunction with Dynamic Light Scattering (DLS) measurements to determine the accuracy between the two methods. Both zeta potential and size distribution of my AgNP were performed by Dr Craig Bunt (Lincoln University) at University of Auckland.

The zeta average mean particle size, Pdi and zeta potential of AgNP were determined using a Zetasizer Nano ZS (Malvern Instruments Ltd, Worcestershire, UK) at 25 °C. The conditions of measurement were: He/Ne laser (wavelength = 633 nm), scattering angle 90°, refractive index 1.33, and the viscosity 0.887 mPa s. Prior to the measurements, the concentration of AgNP was diluted 200 fold with water.

3.2.3 Exposure Doses

Enzyme assays perform by fellow student, N. Saleeb, identified that $AgNO_3$ was 10 fold more toxic than AgNPs to the earthworm *A. caliginosa.* Therefore, the concentrations of AgNP used in the study were at least 10 times higher than $AgNO_3$. Furthermore, the majority of literature investigating the toxicity of AgNPs to earthworms use relatively high doses which are not environmentally realistic. Therefore environmentally relevant doses were used. Doses were based on those reported by the United States EPA report cited in Coleman *et al.* (2013).

Figure 9: Experimental doses and biological replicates inside glass jars

Two AgNP doses were selected 0.3 $mgkg^{-1}$ and 30 $mgkg^{-1}$. The $AgNO_3$ dose was 3 $mgkg^{-1}$, 10 times less than the highest AgNP dose, based on the comparative toxicity finding made by N. Saleeb.

All of the AgNP doses were prepared using the FAAS quantified AgNP samples and diluted with deionised water. The $AgNO_3$ dose was calculated to deliver 3 $mgkg^{-1}$ of Ag not 3 $mgkg^{-1}$ of $AgNO_3$. Thus four treatments were used. Each of the four treatments consisted of four biological replicates and were prepared using 1 L glass jars (n=16 jars) (Fig 9). Each biological replicate contained 12 earthworms (12 x 16 = 192 earthworms). Two earthworm samples

from each jar were removed from each of the biological replicates at three time points (2 d, 7 d, 14 d) (2 x 16 x 3 = 96 earthworms). Thus only 50% of the 192 earthworms were used in the study. Excess earthworms were included in the study to compensate for any unexpected deaths.

Table 1: Experimental Exposures

Control 0 $mgkg^{-1}$ Replicate Jar 1	**$AgNO_3$** 3 $mgkg^{-1}$ Replicate Jar 1	**AgNP** 0.3 $mgkg^{-1}$ Replicate Jar 1	**AgNP** 30 $mgkg^{-1}$ Replicate Jar 1
Control 0 $mgkg^{-1}$ Replicate Jar 2	**$AgNO_3$** 3 $mgkg^{-1}$ Replicate Jar 2	**AgNP** 0.3 $mgkg^{-1}$ Replicate Jar 2	**AgNP** 30 $mgkg^{-1}$ Replicate Jar 2
Control 0 $mgkg^{-1}$ Replicate Jar 3	**$AgNO_3$** 3 $mgkg^{-1}$ Replicate Jar 3	**AgNP** 0.3 $mgkg^{-1}$ Replicate Jar 3	**AgNP** 30 $mgkg^{-1}$ Replicate Jar 3
Control 0 $mgkg^{-1}$ Replicate Jar 4	**$AgNO_3$** 3 $mgkg^{-1}$ Replicate Jar 4	**AgNP** 0.3 $mgkg^{-1}$ Replicate Jar 4	**AgNP** 30 $mgkg^{-1}$ Replicate Jar 4

3.3 Results

3.3.1 AgNP Characterisation

3.3.1.1 TEM AgNP morphology and size validation

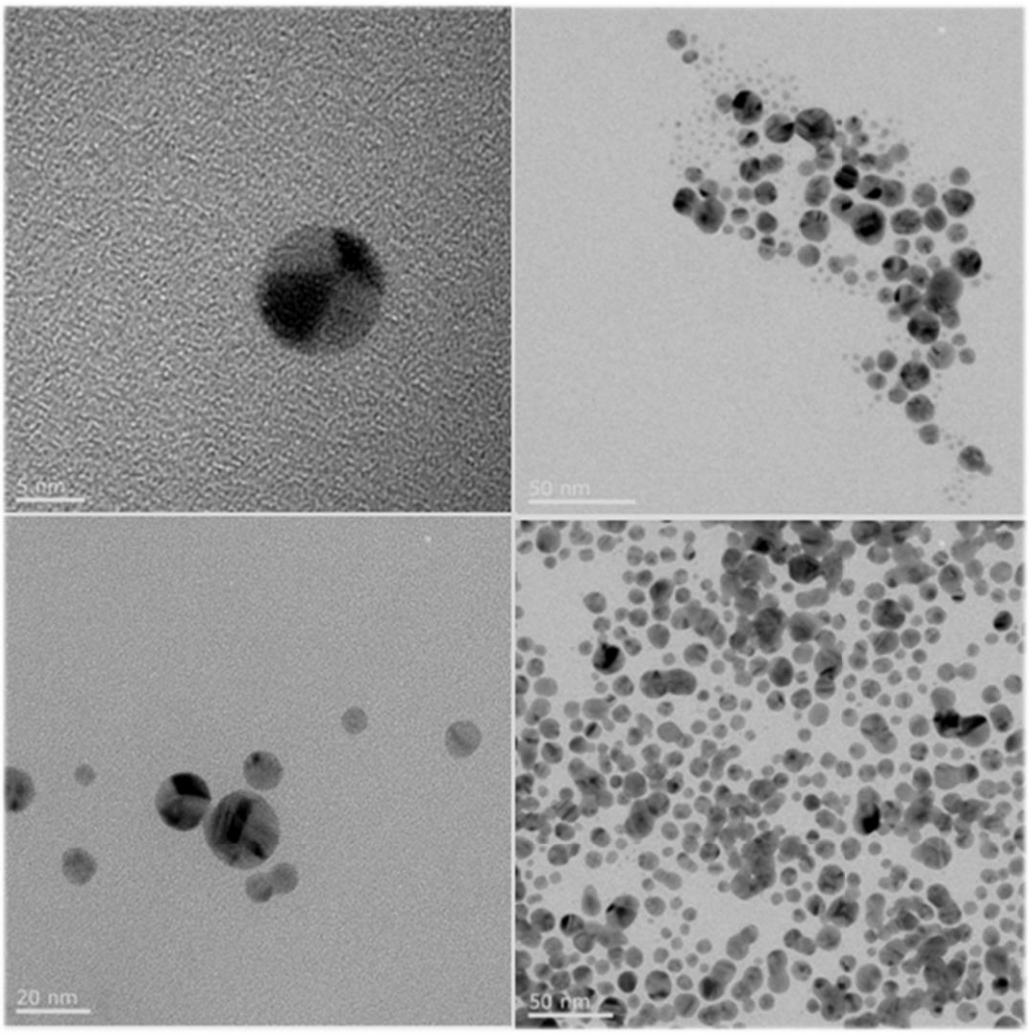

Figure 10: Transmission electron micrograph images of Carey Lea AgNPs synthesised at Lincoln University.

Preliminary TEM images collected from two independent samples showed the size and shape of the synthesised particles was consistent and met the expected morphology described by Carey (1889). The size distribution of the samples synthesised varied between 10 – 40 nm with the most frequent particle sizes ranging from 10-30 nm (Fig 10) and an average of ~ 25 nm. The AgNPs produced were spherical with a fairly high negative surface

charge and therefore will not aggregate or agglomerate due to the electrostatic repulsion of the citrate coating that forms a stable dispersion of AgNP in water (Carey Lea, 1889).

3.3.1.2 Charge Measurement and Particle Size using Zetasizer

Zetasizer Nano (Malvern Instrument, USA) used in the analyses of samples provided a simple, fast and accurate way to measure zeta potentials and NP diameters. It has a unique disposable capillary cell that ensures there is no cross contamination between samples, and also improves the simplicity, speed and accuracy of the measurements. Two peaks were observed and the average diameter of the AgNP measured was 20.81 (Fig 11).

Zeta potential provides an important criterion for estimating the stability of a colloid system (Hunter, 1981). The average zeta potential of the AgNP samples synthesised was ~ -60mV (Fig 12).

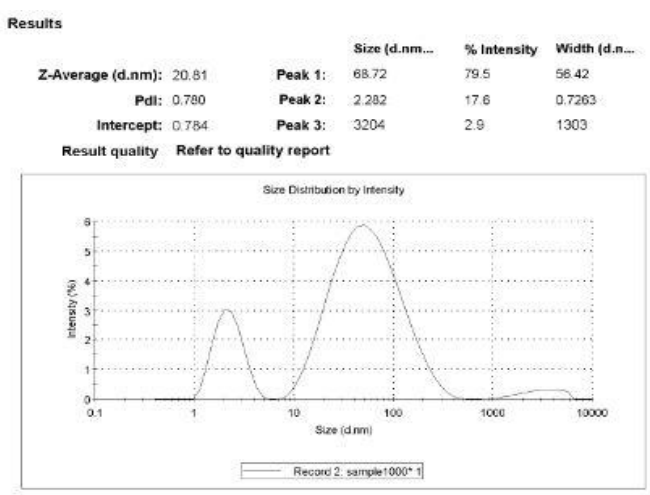

Figure 12: AgNP size measurement using Zetasizer

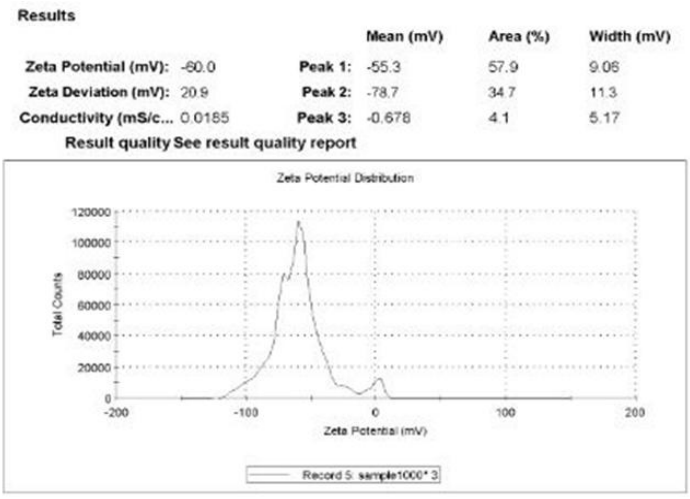

Figure 11: Zeta potential of AgNp using Zetasizer

3.3.1.3 Ag Quantification

The AgNPs synthesised for the soil exposure experiments were diluted and the quantified by FAAS in duplicate to have Ag concentrations of 9.4 mgL^{-1} and 9.9 mgL^{-1}. Based on the dilution factor (0.035 mL/50 mL) these equates to 13.4gL^{-1} and 14.1gL^{-1} respectively, with an

average concentration of ~ 13,.8gL^{-1}. The average Ag concentration of the duplicates was used to calculate the doses to be added for soil studies (Appendix A.2).

3.3.2 Exposure Doses

Each biological replicate jar was labelled and filled with 600 g of air dried soil which had been sieved to remove large stones and dried plant material.

The moisture gravimetric value for the organic soil was 36.6 % (Appendix 1). Therefore 219.6 mL of water added to the air dried 600 g of organic soil to achieve field capacity. The calculated $AgNO_3$ and AgNP solutions were added to soil through 219.6 mL to achieve the desired exposure concentrations and field capacity.

The stock AgNP solution synthesised contained 13.8gL^{-1} Ag (Appendix A.2). A 1.96 mL aliquot was made up to 900 mL with deionised water to make 30 mgL^{-1} AgNP solution. From the 30 mgL^{-1} solution, 9 mL was made up to 900 mL with deionised water to make a 0.3 mgL^{-1} AgNP solution. A 1000 mgL^{-1} solution of Ag^+ was prepared by dissolving 157.6 mg of $AgNO_3$ in 100 mL of deionised water and a 2.7 mL aliquot of the 1000 mgL^{-1} Ag^+ was made up to 900 mL with deionised water to make 3 mgL^{-1} Ag^+ solution. Controls were prepared using deionised water.

AgNP solutions were added to soil and mixed to prepare the 0.3 and 30 of AgNP $mgkg^{-1}$ samples and allowed to stand for 1 h. After 1 h, 12 earthworms were added to each biological replicate (12 x 16 = 192) for exposure studies. These earthworms were used for the subsequent studies on earthworm gene expression studies (Chapter 4) and coelomocytes (Chapter 5).

3.4 Discussion

While the exact toxic mechanism of AgNPs is still debated, research has highlighted that particle size (Carlson *et al.,* 2008; Park *et al.,* 2011), shape (Pal *et al.,* 2007) and surface charge relative to capping agent properties (El Badawy *et al.,* 2010; Silva *et al.,* 2014; Kvitek *et al.,* 2009) play vital roles in NP toxicity. Furthermore, AgNP suspensions will also contain Ag^{+} impurities as the result of incomplete reduction of the Ag salt employed during AgNP synthesis (Navarro *et al.,* 2008) and this will also add to the toxicity.

The characteristics of AgNPs used in toxicity studies need to be fully understood to be able to accurately interpret the toxicological endpoints being measured (Burleson *et al.,* 2004). Without sufficient knowledge, there is a possibility that the toxic effects being measured arise from factors besides the nanomaterial itself. Therefore it is necessary to acquire the critical details of the AgNPs being used particularly size, shape and surface charge (Sayes & Warheit, 2009).

The AgNPs synthesised in this work are citrate-coated AgNPs. When the citrate molecules are ionised these AgNPs have a surface potential of approximately -38 mV. In a toxicity study studying the effects of four differently capped AgNPs on *Bacillus* species, the surface charge of citrate-capped AgNPs was found to be equivalent to the surface charge of the *Bacillus* species cellular membrane - 37 mV(El Badawy *et al.,* 2010). The negative charge on the surface of the *Bacillus* species arises from the carboxyl, phosphate and amino acid groups located on the cellular membrane of the gram-positive bacteria (van der Wal et al., 1997). This equivalence of surface charge shared between the bacteria surface and the citrate-capped AgNPs generates a high degree of repulsion, which acts as a barrier limiting the rate of cell-particle interactions and thus reducing the toxicity. However, once the repulsive or electrostatic barrier is overcome, AgNPs will be able to interact with the cell

membrane (Fabrega *et al.,* 2009; Choi *et al.,* 2008). The surface charge behaviour also provides a useful tool for predicting the toxicological behaviour of various AgNPs.

Along with surface charge, the size of NPs has been demonstrated to affect the severity of AgNP toxicity. Studies suggest that the smaller the AgNP the greater the toxicity (Lapied *et al.*, 2010; El Badawy *et al.,* 2010). In a study using *D. magna* as a model species, lower concentrations of smaller 10 nm AgNPs (4.05 μgL^{-1}) lead to 100 % mortality compared to the concentration of 72 nm AgNPs (40.3 μgL^{-1}) necessary to achieve the same effect (Silva *et al.,* 2014). The AgNPs in this study were shown to have a median diameter of 25 nm, at the smaller end of the size spectrum and therefore can be considered relatively toxic based on size.

While the earthworm cell to citrate-coated AgNP charge compatibility and AgNP cell uptake rate based on size were not investigated directly, the results of the toxicity parameters measured in Chapter 4 and Chapter 5 are reflective of the AgNP characteristics measured in this chapter.

The majority of literature available for AgNP soil toxicity employing earthworms as model species uses high dose PVP-AgNPs purchased from a manufacturer. The research here is unique as the AgNPs were citrate coated, were synthesised fresh before use and the doses applied were based on environmentally relevant concentrations.

Further research on toxic responses beyond what is reported in Chapter 4 and Chapter 5 may include: 1) identifying the surface charge of *A. caliginosa* coelomocyte cell types; 2) the conditions within the earthworm coelomic cavity and its effects of citrate-capped AgNP surface charge; 3) the interactions between citrate-capped AgNPs and soil compounds and 4) the comparison of the toxicological effects across a range of different AgNP sizes and surface charges (capping agent applied).

Chapter 4

Gene Expression in earthworms exposed to silver nanoparticles

4.1 Introduction

The development of genomic technologies in the past decade has allowed scientists to understand and investigate molecular mechanisms that support biological structure and function (Afshari *et al.,* 2011). Genetic techniques and technologies are used increasingly in the field of toxicology to understand the impact various chemical and environmental conditions have on cellular and molecular machineries (Nuwaysir *et al.,* 1999). Significant molecular events induced by exposure to chemical or environmental stressors can now be measured in real time, across single or multiple species and genes (Sawada *et al.,* 2005). AgNPs have been shown at the cellular level to inflict apoptosis, suggestively induced by overwhelming oxidative stress, in the earthworm species *L. terretris* (Lapied *et al.,* 2011). Omic-based technologies allow cellular oxidative stress to be measured through quantitative gene expression analysis of antioxidant enzymes and stress signalling responses. This approach has been utilised in annelids and nematodes, following exposure to AgNP doses (Lim *et al.,* 2012; Hayashi *et al.,* 2012 & 2013; Ahn *et al.,* 2014).

The objective of the present study was to develop, validate, and optimise RT-qPCR assays to measure the expression of genes of interest, namely catalase, superoxide dismutase, metallothionein and reference gene β actin, in *A. caliginosa* following soil exposures to environmentally relevant doses of AgNPs (0.3 $mgkg^{-1}$, 30 $mgkg^{-1}$) and compare with exposure to a mid-range dose of $AgNO_3$ (3 $mgkg^{-1}$ Ag) over three time points (2 d, 7 d and 14 d).

4.2 Material and Methods

4.2.1 Earthworm experiments

The biological replicates and treatment doses reported in chapter 3 were used for this gene expression work. Individual earthworms were isolated from each biological replicate and treatment across the three time points (n= 4 treatments x 4 jars x 3 time points= 48).

Each biological replicate earthworm specimen was removed from the corresponding treatment at the corresponding time point. The gut contents were voided by gently applying pressure and stroking the intestinal section. The earthworms were then rinsed in deionised water before being transferred to labelled 2 mL Cryo-vials (Tarsons). Cryo-vials were suspended in liquid nitrogen (N_2) to snap freeze earthworms, (Fig 13) and each earthworm sample was clearly labelled, then stored at -80 ^{o}C until RNA extraction.

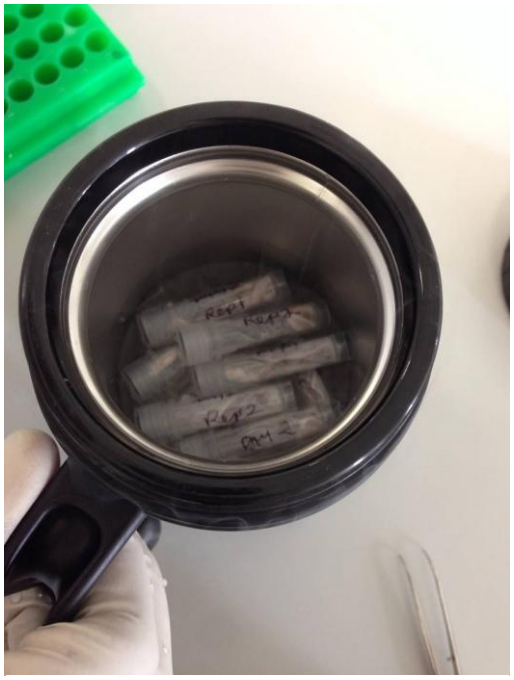

Figure 13: Cryo-vials suspended in liquid N2, snap freezing biological replicates

4.2.2 Gene of Interest Amplification

4.2.2.1 RNA Extractions

RNA extractions were performed separately for each time point (2 d, 7 d, 14 d) on every biological replicate from every treatment (n=16).

Earthworm samples were removed from -80 ^{o}C and held on ice. Inside a fumehood, earthworm samples were individually homogenised (dry) using liquid N_2 and a sterile ceramic mortar and pestle. Approximately 30 mg of homogenised tissue was transferred into a sterile 1.5 mL Eppendorf tubes. RNA was then extracted from samples using the E.Z.N.A. Mollusc RNA Isolation Kit (Omegabiotek) following the manufacturer's instructions.

RNA was quantified using a Qubit RNA assay kit and Qubit 2.0 Fluorometer. RNA quality was determined via the $^{260}/_{280}$ ratio measured in DeNovix Ds-11+ Spectrophotometer (Appendix C.1). Extracted RNA was eluted into molecular grade water and held at -80 ^{o}C in two separate 20 µL aliquots for each sample.

4.2.2.2 cDNA Synthesis

Following RNA quantification and quality measurements, RNA samples were treated to remove any DNA contamination that may have occurred during RNA extraction, using TURBO DNA-*free* (Life technologies, CA, USA). cDNA was synthesised using the PrimeScript RT reagent Kit (TaKara,CA, USA) following manufacturer's instructions. The synthesised cDNA was quality tested by PCR using SOD *A. caliginosa* primers (see below) and 0.5 µL of cDNA. The cDNA concentration is theoretically equivalent to the concentration of RNA converted. Based on that, the cDNA samples were diluted to 5 ngµL^{-1} with molecular grade water and stored at -18 ^{o}C.

4.2.2.3 One-step RT-PCR Degenerate Primer Trial

Degenerate primers for all three of the genes of interest (SOD, CAT, MT) were supplied by researchers at Universite Lille 1, Lille, France. These primers were designed to amplify the genes from annelid species and had been successful in amplifying the genes in the earthworm species *E. fetida.*

Using extracted RNA from *A. caliginosa*, each of the degenerate primer sets (MT_Ann For: 5'-AAG SWT TGC TGT GST GRH RC -3', MT_Ann Rev: 5'- ACR YKC TTY CCY ACG ACA C -3'; Catalase_For: 5'- GCG GCC CGA GAC CAC NCA YCA RGT -3', Catalase_Rev: 5'- GAT CTG CTC CAC CTC GGC RAA RWA RTT -3'; Sod_Ann For: 5'- TGT CCG CCG GCC CNC AYT TYA AYC -3', Sod_Ann Rev: 5'- CGG CCT CGA TGT TGC CAN RRT CNC C -3') were trialled using a QIAGEN Onestep RT-PCR kit (QIAGEN) following manufacturer's instructions.

Each QIAGEN One-step RT-PCR contained QIAGEN5x buffer, Mg^{2+} (2.5 mM), QIAGEN RT Enzyme mix, QIAGEN dNTPs (400 µM), primer pairs (0.6 µM), 200 ng of RNA template in a reaction volume of 10 µL with molecular grade water. Reactions were performed using a Gene Pro thermal cycler (BIOER), 50^{o}C, 30 min, 95^{o}C for 15 min, cycle reactions (94^{o}C, 30 sec, 50-65^{o}C gradient, 30 sec, 72^{o}C, 1 min) repeated 30 times and 72^{o}C, 10 min. PCR products were run through a 2% agarose gel, 100 V, 30 min. PCR product sizes determined using a0.5 kb indicator Hyper Ladder V (Bioline). Each primer pair was run parallel with a non-template control (NTC) to insure there was no contamination in the primer pairs. β-actin primers were used as the control (ACT_A For: 5'- CAG ATC ATG TTC GAG ACC -3', ACT_A Rev: 5'- TAC TCC TGC TTG CTG ATC C -3').. The primers were designed based on the β-actin sequence generated by Bernardi (2012), and have been shown previously to amplify a β-actin fragment of ~720 bp from *A. caliginosa* RNA samples using the QIAGEN Onestep RT-PCR kit. The 1 kb Hyper Ladder I (Bioline) was used to determine the β-actin fragment size.

4.2.2.4 GOI Primer Design

Earthworm sequences for CAT and MT were retrieved from the NCBI GenBank database. A general gene search was performed and then search parameters narrowed using the taxonomic function. The sequence search was narrowed to segmented worms and then *Lumbricidae*. SOD sequences were retrieved for the SOD primer pair provided by Zhan, (2012).

CAT Primers

An alignment of *L. rubellus* CAT mRNA (GenBank accession number: EU407494.1) with other sequences was used to design primers for CAT. The other sequences aligned were partial sequence from *A. caliginosa* (JQ782655.1), *L. terretris* (EU407496.1) and *E. fetida*

(DQ286713). The CAT primers (CAT_caliginosa For: 5'- GGC CTT AAG AAT TTG TCG GC -3', CAT_caliginosa Rev: 5'- TCG AAT GGA TTC GAG CGG -3') were positioned within the partial catalase sequences where there was conservation with other earthworm species to generate a product of ~170 bp. See Appendix 3.1 for CAT sequence alignments and primer sites within sequences.

SOD Primers

The sequence for a set of SOD primers previously used on suspected *A. caliginosa* samples were obtained from Y. Zhan, (2012). The validity of these primers was tested by constructing a SOD mRNA alignment using

L. terretris (EU407497.1), *L. rubellus* (EU407495.1) and *E. fetida* (DQ286712.1) to locate the sites of primer binding in order to determine the expected fragment length. The primer sequences were SOD_*caliginosa* For: 5'- GTG CTC ACT TCA ACC CAT T -3', SOD_*caliginosa* Rev: 5'- AGA TCR CCA CCA GCT CAT GT -3' and were shown to generate a product of ~200bp. See Appendix 3.2 for SOD sequence alignments and primer sites within sequences.

MT Primers

Three sets of MT primers were designed to amplify MT in *A. caliginosa.* The literature of MT evolution and conservation states that the genetic variation of this protein is extensive and there are numerous isoforms (Capdevila & Atrian, 2011).

Both partial and complete isoforms of MT mRNA sequences of *Lumbricidae* were retrieved and aligned for primer design. These sequences were *L. rubellus* isoform 1 (AJ005823.1), *L. rubellus* isoform 2 (AJ005822.1), *E. fetida* (AJ236886.1), *L. castaneus* (AJ010264.1), *L. terretris* (AJ010263.1) and *Allolobophora chlorotica* (HM014116.1). There were limited stretches of MT sequences conserved across the partial sequences collected from NCBI. Using these limited stretches of conservation, degenerate MT primers were designed

(MT_Ann For: 5'- AAG SWT TGC TGT GST GRH RC -3', MT_Ann Rev: 5'- ACR YKC TTY CCY ACG ACA C -3') which would generate a fragment of ~120 bp. See Appendix 3.3 for MT mRNA sequence alignments and MT_Ann primer sites within sequences.

Further MT primers were designed based on *Lumbricidae* MT protein alignments using *L. rubellus* (CAA06720.1), *L. rubellus* (CAA06719.1), *A. chlorotica* (ADK62365.1), *Eisenia fetida* (CAA15423.1), *L. castaneus* (CAA09057.1), *L. terrestris* (CAA09056.1), *Lumbricus friendi* (ADW27175.1), *L. rubellus* 2C (CAC14314.1), *L. rubellus* 2B (CAC14313.1) and *L. rubellus* 2A (CAC14312.1). Primers were designed across sites where 4-5 amino acids were conserved. Two forward primers were designed to compensate for all possible nucleotide preferences and the amino acids, across various species (MT.CW1 For: 5'- TGC TCC AAA TGC AGG TGC -3', MT.CW2 For: 5'- TGC TCA AAA TGC AGG TGT -3', MT.CW1 Rev: 5'- AGT CAC CAC AGC ATC CT -3'). The product length expected from each combination was ~170 bp. See appendix 3.5 for MT protein sequence alignments, MT CW primer sites within sequences and the primer nucleotide translation alignments (Appendix 3.6).

Bernardi, (2012) reported that *A. caliginosa* shares the same super phylum as the mollusc, *Mytilus* species. Primers were also designed based on *Mytilus* species MT protein sequences (P80258.1; P69154.2; P80252.2; CAA06553.1; P80249.2; CAA07546.1; P80248.2; CAA06551.1; O62554.3; CAA06549.1; P80246.2; CAA06548.1; P80247.3; CAA06550.1) and *Mytilus edulis* mRNA MT isoform sequences (AJ005453.1; AJ005452.1; AJ005451.1; AJ005456.1; AJ005454.1; AJ007506.1) collected from NCBI and aligned (M.edulis_MT For: 5'- GAA ACA AAT GTG TGT ATC TG -3', M.edulis_MT Rev: 5'- AAC ATTT TGC AAA CAA CTT TA -3'). See Appendix 3.7 for *Mytilus* species MT protein sequence alignments, *M. edulis* MT primer sites within the sequences (Appendix 3.8) and the nucleotide translation alignments.

A set of RT-qPCR MT primers designed for *E.fetida* (E.fetida_MT For: 5'- TCG CAA GAG AGG GAT CAA CT -3', E.fetida_MT Rev: 5'- CAT TTC CAC ATT TGC CCT TC -3'). They were shown to generate an expected product of ~120bp from within *E. fetida* mRNA MT sequences. See Appendix 3.5 for *E. fetida* MT primer location within the *Lumbricidae* MT protein alignments and Appendix 4 with a *E. fetida* MT mRNA sequence.

PCR for each primer pair was performed using Qiagen Taq DNA polymerase, QIAGEN dNTPs (200 µM), Qiagen 10x buffer (Mg^{2+}, 3mM), primer pairs (0.4 µM), ~200 ng *A. caliginosa* cDNA) template made up to reaction volume of 10 µL using molecular grade water. PCR products were run through a 2% agarose gel, 100 V, 30 min. Product sizes were determined by comparison with the indicator Hyper Ladder V and I (Bioline). Each primer pair was run parallel with a NTC to ensure there was no contamination in the primer pairs. Each PCR product generated that met the expected size range was sequenced and validated using the NCBI gene database.

4.2.3 Quantitative PCR Experiments

4.2.3.1 RT-qPCR Primer Design

The gene fragments generated from *A. caliginosa* cDNA which were successfully amplified, sequenced and identified were used as the templates for RT-qPCR primer design. The RT-qPCR primers were designed to bind to locations within the template fragments. Therefore, standards for each genes of interest and the reference gene could be constructed, using the PCR templates generated in 4.2.2.4, to generate known template concentrations.

The RT-qPCR primer sets were designed using IDT Primer Quest software (Coralville, USA). Assays were designed to have a primer melting temperature of 60 ^{o}C and yield a product of ~100 bp.

The SOD RT-qPCR primers (SODq_For: 5'-CCC AGT CAA ATT GAG GAG TTT AT -3', SODq_Rev: 5'- AAG ATC AGG AGA GGC ATG TT -3') yield a 100bp amplicon. The CAT RT-qPCR primers (CATq_For: 5'- CGT TCC TGA CCC AGA CTA TG -3', CATq_Rev: 5'- AAC GTC ATC ACC TGG ATG T -3') yield a 103bp amplicon. The ACT RT-qPCR primers (ACTq_G For: 5'- CTC GAG AAG AGC TAC GAG C -3', ACTq_G Rev: 5'- GGC GTA CAG ATC CTT ACG G -3') were obtained from a previous postgraduate student at Lincoln University, Bernardi (2012), to yield a 180bp amplicon RT-qPCR amplicon, which falls inside of the ACT template and shares the same melting profile of 60 ^{o}C.

MT RT-qPCR primers were designed to fall within a trimmed sequence which shared a 68% query cover with *E. fetida* partial MT mRNA sequence. The MT RT-qPCR primers (MT_qPCR For: 5'- TTT CGC AAG AGA GGG ATC AAC -3', MT_qPCR Rev: 5'- ATG AGA TTT GGT GGG CAT TCA -3') yield a ~75bp amplicon.

All RT-qPCR primers were tested on *A. caliginosa* cDNA by endpoint PCR. PCR was performed using Qiagen Taq DNA polymerase, QIAGEN dNTPs (200 µM), Qiagen 10x buffer (Mg^{2+},3mM), primer pairs (0.4 µM), ~200 ng DNA template made up to reaction volume of 10 µL using molecular grade water. PCR products were run through a 2% agarose gel at 100 V, 30 min with a PCR product size indicator Hyper Ladder V (Bioline). Each primer pair was run next to a NTC to ensure that there was no contamination in the primer pairs.

See Appendix 5 for RT-qPCR primer sites within sequenced templates.

4.2.3.2 RT-qPCR Primer Standards Efficiency Test

Standard curves were constructed for each RT-qPCR primer pair (ACTq, CATq, SODq, MTq) to test the amplification efficiencies. Each of the sequenced PCR product templates (ACT, CAT, MT, SOD) was quantified using the DeNovix Ds-11+ Spectrophotometer and each template sample diluted to 1 ngμL^{-1}. Serial dilutions of each diluted template were prepared

using the Eppendorf epMotion 5070 robot, Eppendorf epBlue software and molecular grade water. Serial dilutions were prepared using the diluted template of 1 $ngμL^{-1}$, through to $1x10^{-8}$ $ngμL^{-1}$. Dilutions of $1x10^{-1}$ $ngμL^{-1}$, $1x10^{-3}$ $ngμL^{-1}$, $1x10^{-5}$ $ngμL^{-1}$, $1x10^{-6}$ $ngμL^{-1}$ and $1x10^{-8}$ $ngμL^{-1}$ were used to construct standard curves to test amplification efficiency for each RT-qPCR primer pair. Standards were loaded onto a 48 well plate using the Eppendorf epMotion 5070 robot. Standards were run in duplicates with a NTC to identify any contamination.

Each RT-qPCR was performed using 5μL SYBR *Premix Ex Taq* II (Til RNaseH Plus), TaKaRa, RT-qPCR primers (4 μM), 3μL of serial dilution template and made up to volume (10μL) with molecular grade water. Experiments were performed using Illumina Eco Real Time thermal cycler with RT-qPCR conditions of 95 ^{o}C for 5 sec, then 40 cycles of 95 ^{o}C, 30 sec, 60 ^{o}C, 30 sec and 95 ^{o}C for15 sec and 55 ^{o}C for 15 sec. Data were collected using Eco Real Time Version 5.0 and analysed using Eco study software.

4.2.2.3 Exposure RT-qPCR Experiments

Each biological replicate cDNA sample (total n= 48) had been diluted to 5 $ngμL^{-1}$ following cDNA synthesis and stored at -18 ^{o}C. Each sample was run in triplicate for each gene of interest and reference β-actin. Standards used for each corresponding analysis (ACTq, CATq, MTq, SODq) were run in duplicate, using serial dilutions prepared on the day and dilutions $1x10^{-1}$ $ngμL^{-1}$, $1x10^{-5}$ $ngμL^{-1}$, and $1x10^{-8}$ $ngμL^{-1}$ were run in parallel with the exposure *A. caliginosa* cDNA samples. Plate control duplicates (SODq Primers with control *A. caliginosa* cDNA) and a NTC to the corresponding primer pair were applied to each plate. Any large variation between plate control cycle threshold (Cq) values was used to highlight any technical difficulties which may have affected sample Cq values between plates.

Each RT-qPCR was performed using 5µL SYBR *Premix Ex Taq* II (Til RNaseH Plus), TaKaRa, RT-qPCR primers (10mM), 3µL cDNA (5ngμL^{-1}) and made up to 10µLwith molecular grade water. Experiments were performed using Illumina Eco Real Time thermal cycler with RT-qPCR conditions of 95 ^{o}C for 5 sec, 40 cycles of 95 ^{o}C for 30 sec, 60 ^{o}C for 30 sec then 95 ^{o}C for 15 sec and 55 ^{o}C for 15 sec. The data were collected using Eco Real Time Version 5.0 and analysed using Eco study software.

Relative quantification was used to analyse the gene expression in each sample relative to the reference gene and an untreated sample (0 $mgkg^{-1}$). This approach is useful when measuring and comparing the response of an organism following exposure to a toxin. The relative quantification was calculated using the standard curve method.

4.3 Results

4.3.1 One-step RT-PCR Degenerate Primer Trial

There was no PCR product produced from any of the genes of interest (SOD, CAT, MT) degenerate primers provided by Universite Lille 1, Lille, France.. These primers were successfully used to amplify SOD, CAT and MT fragments in the earthworm *E. fetida*. PCR optimisation methods were applied (annealing temperature gradients, Mg^{2+} gradients, primer concentration gradients & template gradients) to identify ideal conditions but to no avail. The RNA integrity was not responsible for the lack of amplification as the β-actin fragment successfully amplified and the non-template controls (NTC) for the β-actin primer pairs were blank, which ruled out contamination in β-actin primers.

New primers were designed for the GOI (CAT, MT) and SOD primers used by Zhan (2011), who had worked with suspected *A. caliginosa* specimens, were trialled Fresh cDNA was synthesised for the following primer trials. OneStep RT-PCR requires large volumes of RNA.

It was more efficient to synthesise cDNA and run traditional PCR reactions to preserve *A. caliginosa* RNA samples.

4.3.2 GOI Primer Design

Because of the lack of *A. caliginosa* sequences available, CAT and MT primer pairs were designed using mRNA and protein sequences of *Lumbricidae* species. The SOD primer pair was acquired from previous researcher Zhan (2012) of Lincoln University.

The CAT and SOD primers amplified products of the expected fragment sizes from *A. caliginosa* (Fig 14) and each GOI product was verified by

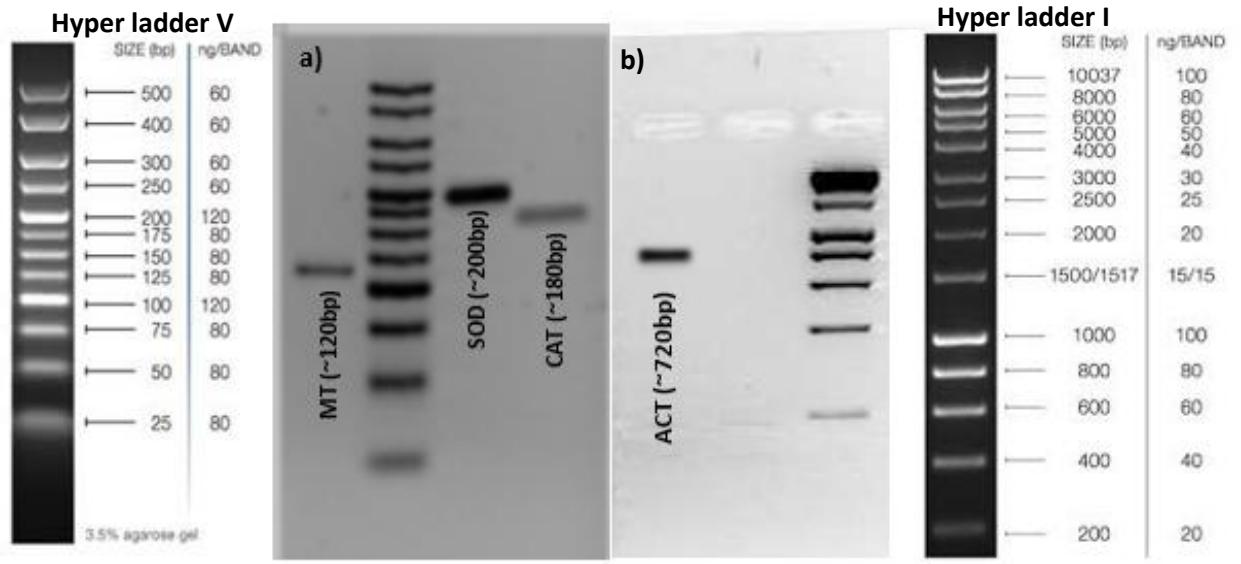

Figure 14: GOI Fragments in 3.5% agarose gel; a) hyper ladder V with GOI fragments MT, SOD and CAT, b) hyper ladder I with reference fragment β actin.

sequencing and nucleotide sequence BLAST searches. The NCBI BLAST result for the sequenced CAT PCR product showed 100 % query cover with the *A. caliginosa* (JQ782655.1) catalase sequence. The NCBI BLAST results for the sequenced SOD product showed 95% query cover for *Tubifex tubifex* SOD (GU592913.1) and *E. fetida* SOD (JN579648.1; DQ286712.1). As no *A. caliginosa* SOD sequence was available, the cDNA used originated from a genetically confirmed *A. caliginosa* specimen (see Chapter 2 for method) and thus,

this BLAST result could be considered positive for SOD.

No product was generated using *A. caliginosa* cDNA for the MT_Ann degenerate designed primers or the MT.CW primer combinations. Extensive PCR optimisation methods were applied (annealing temperature gradients, Mg^{2+} gradients, primer concentration gradients & template gradients) to identify ideal conditions to no avail for both the MT_Ann and MT.CW primer pairs.

The RT-qPCR MT primers designed and used previously on *E.fetida* (E.fetida_MT For: 5'- TCG CAA GAG AGG GAT CAA CT -3', E.fetida_MT Rev: 5'- CAT TTC CAC ATT TGC CCT TC -3') were then trialled and generated a product of the expected fragment size of ~120bp in *A. caliginosa* cDNA (Fig 14). Direct sequencing results of this product were inconclusive with a 210bp product being consistently produced. Initially NCBI BLAST searches using the entire 210bp sequence showed no results. However, when the sequence was trimmed, starting at the location of the reverse primer binding site to a 86bp fragment, the BLAST search of this attenuated fragment gave 68% query cover with *E. fetida* partial MT mRNA (DQ286714.1), suggesting the amplified product was partial *A. caliginosa* MT cDNA.

β-actin was selected as the reference gene as it is used in many earthworm gene expression studies as theoretically its expression profile stable and is unaffected by treatments (Chen *et al.,* 2011; Homa *et al.,* 2010; Liang *et al.,* 2011; Brulle *et al.,* 2006). However, this stability of expression was not validated in the present study.

4.3.3 RT-qPCR Primer Validation and Standards Efficiency Test

The RT-qPCR primers for each GOI and the reference gene β actin were shown to generate fragments of the expected size range following PCR with *A. caliginosa* cDNA and the corresponding template (Fig 15). The efficiencies of the RT-qPCR primers were tested using serial dilutions of the PCR products of each GOI (CAT, MT and SOD) and the reference gene (ACT) as a template. The Illumina Eco Real-time System User guide (2013), states that the slope of the standard curve is related to the efficiency and should be between -3.1 and -3.6. It also states the efficiency should be between 90-110 %. There should also be only a single peak of amplification observed. All of the RT-qPCR primer pairs designed met these requirements. Cq variation between standard duplicates were equal to 0.55 or less of a Cq. Refer to Appendix C.5 for raw data and for RT-qPCR primer melt curves.

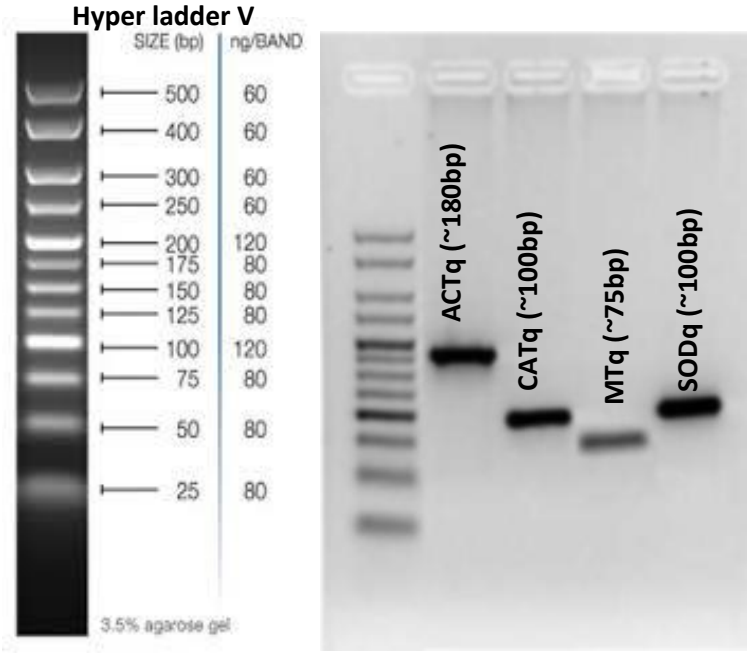

Figure 15: RT-qPCR Fragments in 3.5% agarose gel with hyper ladder V

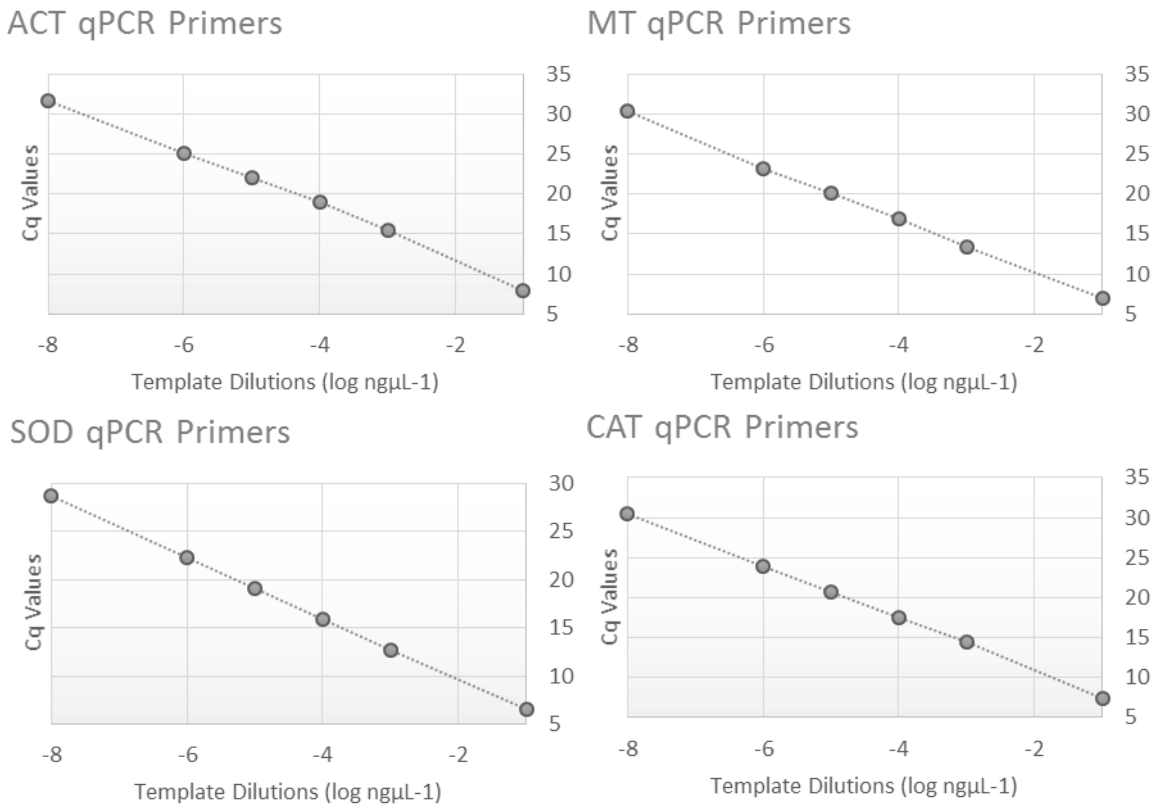

Figure 16: RT-qPCR Primer Standards Efficiency Results

	ACTq	CATq	SODq	MTq
Efficiency %	98.45	101.88	106.54	99.79
Error %	36.85	18.79	30.1	37.28
Equation	y=-3.36x+5.09	y=-3.28x+4.34	y=-3.17x+3.23	y=-3.33x+3.51
R2	0.9977348	0.999457	0.998753	0.997756

Table 2: RT-qPCR Primer Standards Efficiency Results

4.3.4 Earthworm Ag Exposure RT-qPCR Results

All the exposure biological replicates from the four treatments (0 $mgkg^{-1}$-control, 3 $mgkg^{-1}$-$AgNO_3$, 0.3 $mgkg^{-1}$- AgNP, 30 $mgkg^{-1}$- AgNP) and three time points (2 d, 7 d, 14 d) (n= 48) were analysed for gene expression one gene at a time. Each biological replicate was analysed in triplicate(n=144). Each analysis consisted of four 48 well plates, each plate containing a NTC for the corresponding primer pairs and two plate controls. A standard curve was also constructed for each gene analysis using three dilution factors of the corresponding template. Standards were analysed in duplicates and used to calculate the relative gene expressions.

Table 3: Exposure Experiment Standards

ACT Standards		CAT Standards		SOD Standards		MT Standards	
log ng cDNA	Cq	log ng cDNA	Cq	log ng cDNA	Cq	log ng cDNA	Cq
-1	7.07	-1	7.92	-1	6.68	-1	8.43
-1	6.83	-1	8.66	-1	6.50	-1	7.45
-5	21.49	-5	21.84	-5	20.79	-5	21.19
-5	21.73	-5	21.49	-5	21.03	-5	21.39
-8	30.83	-8	30.90	-8	31.99	-8	30.18
-8	28.72	-8	30.29	-8	31.90	-8	30.08

1

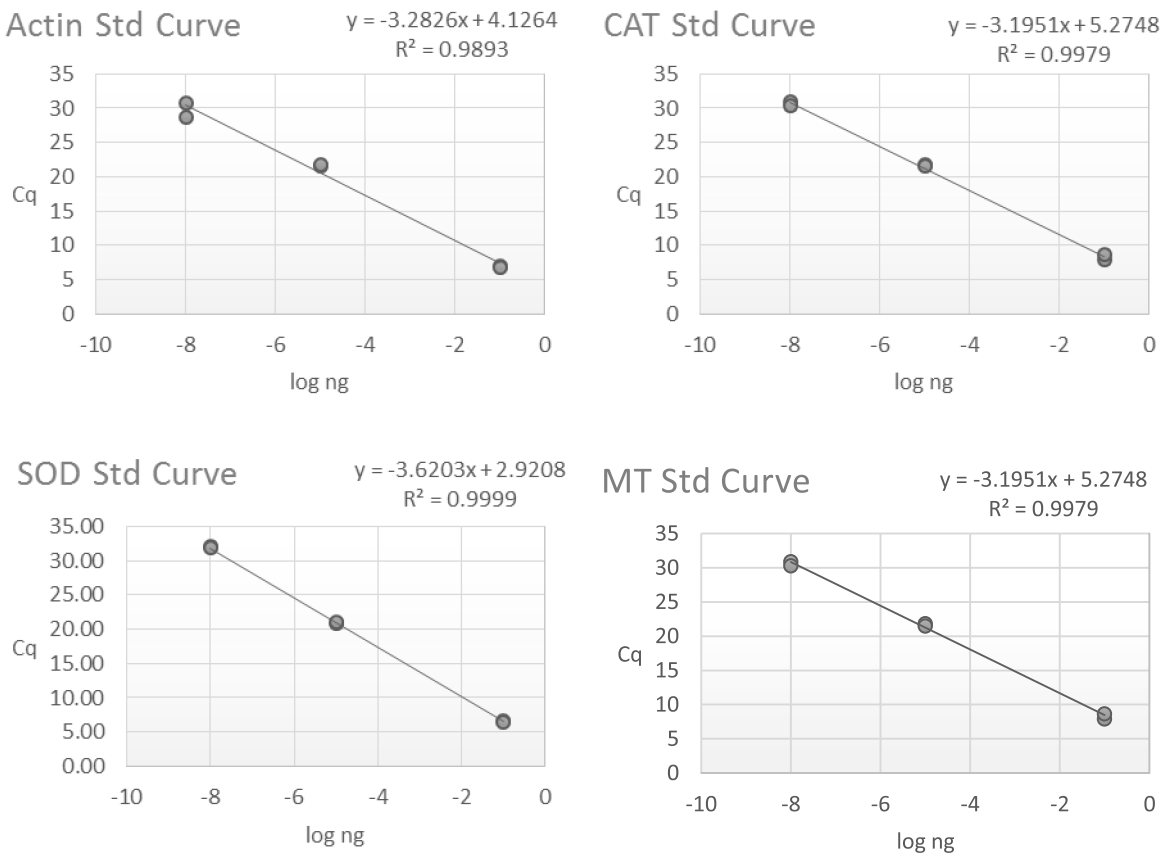

Figure 17: Exposure Experiment Standard Curves

The results of each biological replicate from all of the four treatments (n=48) analysed in triplicate (n=144), for each of the four gene analyses (n= 576) were analysed using Eco Study software. The melt curve for each gene analysis was analysed to verify single product amplification (Appendix C.5). Any samples with Cq values exceeding that of NTC (>30) were deemed inconclusive or negative results, suggesting nonspecific amplification due to 1) GOI not being present in the sample; 2) GOI present but at undetectable concentrations; or 3) no cDNA present in the sample.

The optimum standard deviation between technical replicates should not exceed 0.5 of a Cq. Only two out of the three technical replicate Cq values are required for relative quantification analysis. The standard deviations for the biological replicates were analysed to identify any samples with standard deviations > 0.5. When identified, the technical triplicate Cq values were compared individually to identify a potential outlier Cq value.

Each biological replicate was analysed using two Cq values. Relative quantification was calculated for each, relative to the reference gene and the calibrator sample.

The relative standard curve method was used to determine gene expression for each GOI, expressed as n-fold difference to the untreated calibrator sample which was selected to be the second biological replicate, 2 d, 0 $mgkg^{-1}$ sample. The standard curves for each gene composed of three known concentrations. Each sample fold was determined by interpolating the concentration from the corresponding standard curve and then dividing by the calibrator. The calibrator has a fold expression of 1 and all the samples folds are then expressed as n-fold difference relative to the calibrator.

Means and standard deviations were determined for each biological replicate. Each sample was then normalised by division with the corresponding expression value of the reference gene, β-actin, for that sample. The standard deviation of the normalised sample value was calculated. The fold difference of the normalised sample was then calculated by division with normalised calibrator value.

Analysis of variance (ANOVA) was performed for each GOI and the least significant difference (LSD) between treatments and time points calculated. The average of the biological replicates for each treatment and time point are described below. Refer to

Appendix C.2 for independent biological replicate results and Appendix A.3 and A.4 for statistics.

The RT-qPCR results for MT were all negative. Cq values were greater than the NTC. This result suggested there was no significant induction or any detectable expression across all treatments and time points. To validate the MT gene sequenced and the subsequent MT qPCR primers were representing a potential MT gene involved in heavy metal detoxification, two *A. caliginosa* specimens were exposed to a 80 $mgkg^{-1}$ dose of cadmium chloride ($CdCl_2$) on filter paper for 48 hours, which has been shown to induce MT induction in *E. fetida* (Brulle *et al.,* 2006). These two samples were processed following the same protocol as the soil exposure samples. The RT-qPCR results of the $CdCl_2$ exposed samples generated the same negative results as the soil exposure samples. This result suggests the MT isoform amplified and sequenced from the *E. fetida* MT primers was not the MT isoform involved in heavy metal detoxification in *A. caliginosa*.

Table 4: Relative Quantification of CAT and SOD

Treatment	Time	log CAT	log SOD
0mgkg^{-1}	2 days	-0.5373	-1.1349
0mgkg^{-1}	7 days	-0.079	0.0388
0mgkg^{-1}	14 days	-1.1683	0.9962
$AgNO_3$ 3mgkg^{-1}	2 days	-0.0366	-0.1814
$AgNO_3$ 3mgkg^{-1}	7 days	-0.3585	-0.0821
$AgNO_3$ 3mgkg^{-1}	14 days	0.3824	2.6494
AgNP 0.3mgkg^{-1}	2 days	0.3869	-0.0914
AgNP 0.3mgkg^{-1}	7 days	-0.3431	0.0541
AgNP 0.3mgkg^{-1}	14 days	0.1889	2.2955
AgNP 30mgkg^{-1}	2 days	0.2393	-0.1247
AgNP 30mgkg^{-1}	7 days	-0.2349	0.2412
AgNP 30mgkg^{-1}	14 days	-0.0926	1.3746

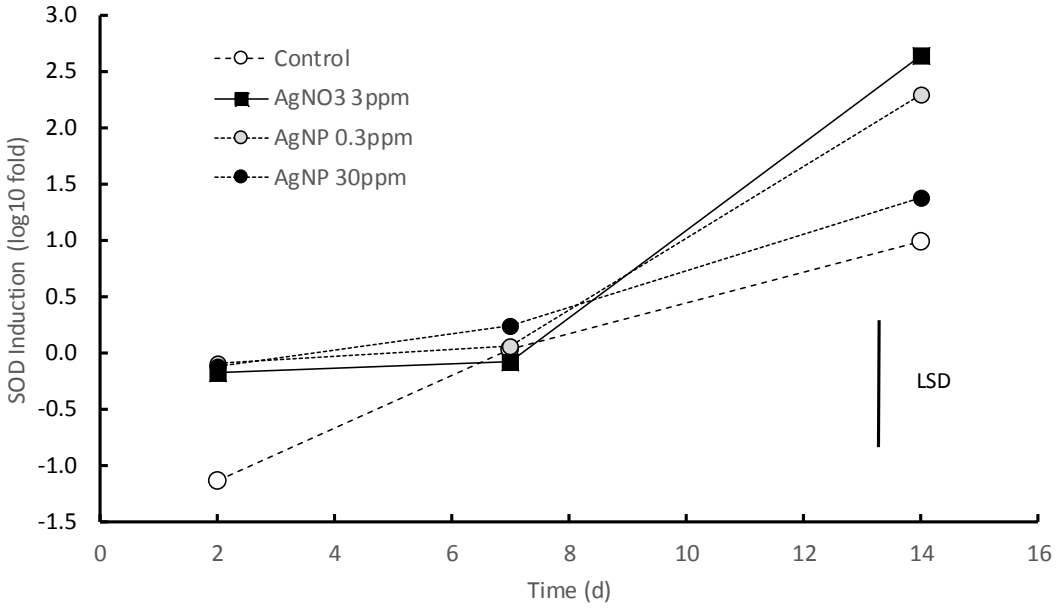

Figure 18: Relative Quantification Results for SOD Induction

ANOVA analysis showed a significant effect at 5% for CAT expression across treatments. At the 14 d time point, CAT expression was up-regulated compared with the control (0mgkg-^{1}) by ~1.2 fold (Fig 19). ANOVA analysis also showed a significant effect at 5% for SOD

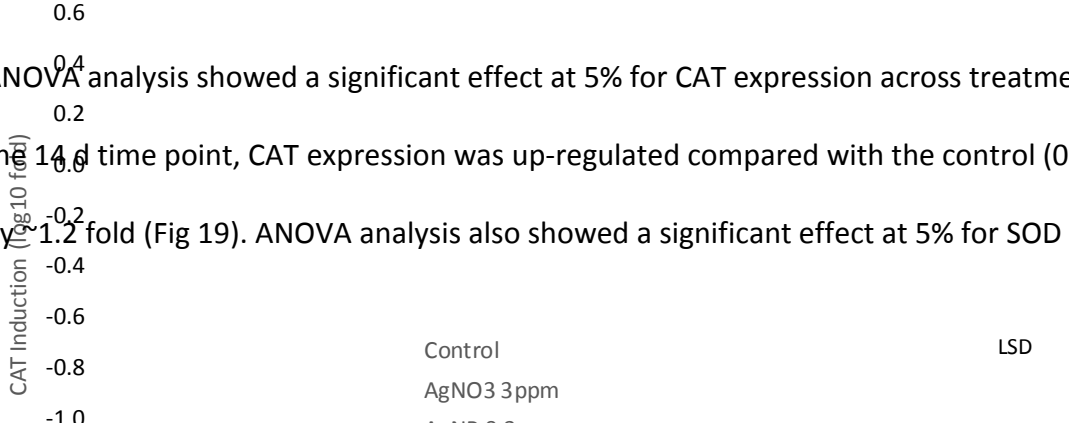

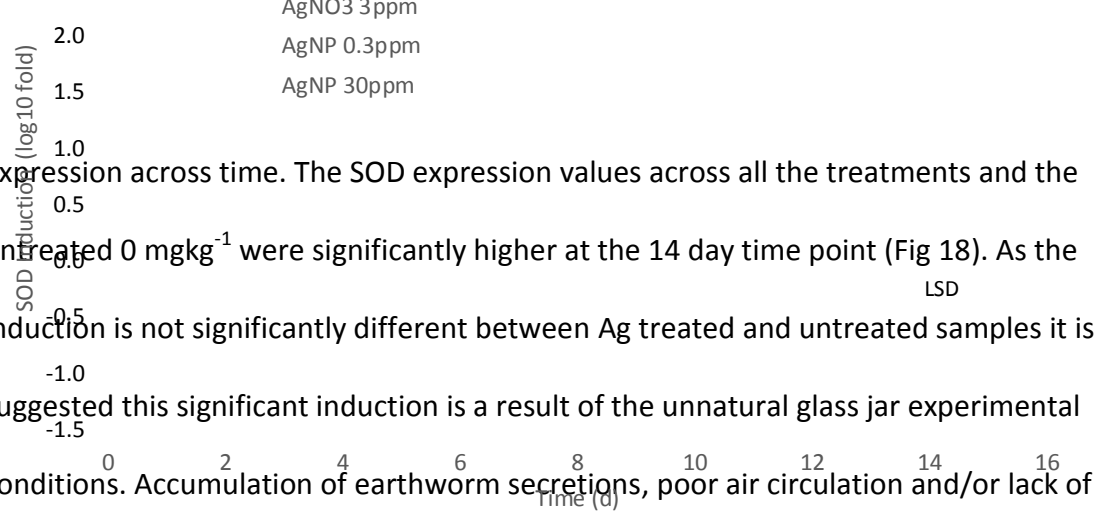

expression across time. The SOD expression values across all the treatments and the untreated 0 $mgkg^{-1}$ were significantly higher at the 14 day time point (Fig 18). As the induction is not significantly different between Ag treated and untreated samples it is suggested this significant induction is a result of the unnatural glass jar experimental conditions. Accumulation of earthworm secretions, poor air circulation and/or lack of

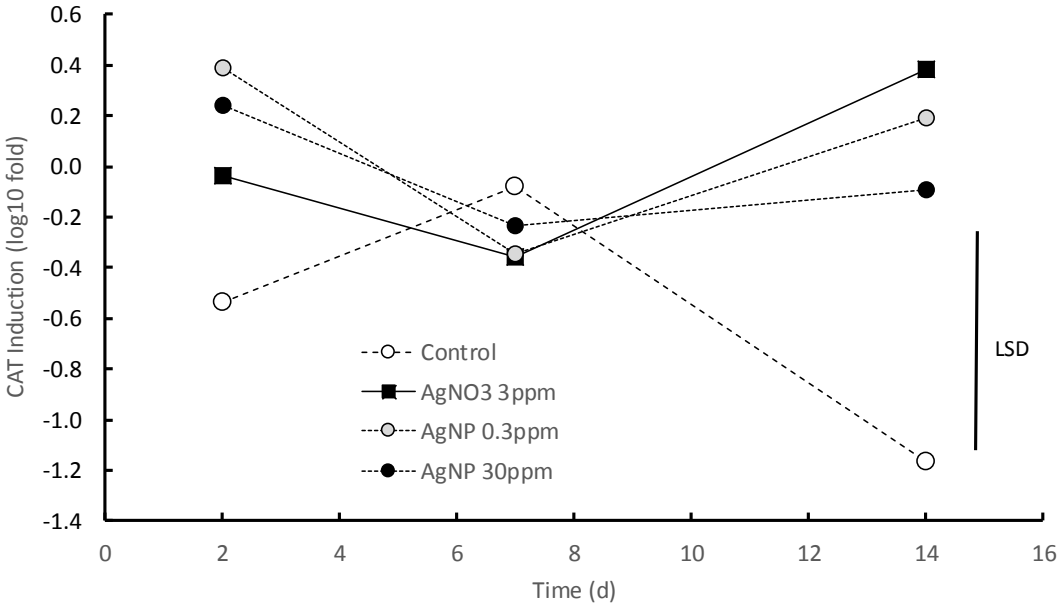

Figure 19: Relative Quantification Results for CAT Induction

nutrients could be responsible for the effect. Refer to Appendix 10 and 11 for raw statistical data of SOD and CAT expressions.

4.4 Discussion

Some heavy metals are essential for metabolic and signalling pathways, such as Cu and Zn, although high dose exposures result in toxicity. The non-essential heavy metals, such as Cd and Hg, are toxic to organisms even at low doses. These non-essential metals tend to persist and accumulate in the environment, which can cause numerous detrimental effects on the functionality of an ecosystem (Hooper *et al.,* 2012).

Molecular genetics have been applied in ecotoxicological research to advance the detection and understanding of the adverse effects of metal contamination on the environment (Stürzenbaum *et al.,* 2009). Earthworm species are commonly used as the indicator organism in soil ecosystem monitoring (Nahmani *et al.,* 2007).

Currently there is no published literature that has measured the gene expression of the GOIs of this chapter (CAT, SOD and MT) in the earthworm species *A. caliginosa* following exposure to high or low AgNP doses in soil.

Metallothioniens (MT) were first identified in earthworms by Stürzenbaum *et al.* (1998). The family of MT proteins are metal managing and metal tolerant proteins which are involved in both non-essential metal detoxification and essential metal regulation (Valko *et al.,* 2005). Metallothioneins have been studied in a few earthworm species including *L. rubellus* (Burgos *et al.,* 2005; Spurgeon *et al.,* 2005; Bundy *et al.,* 2008), *L. terrestris* (Calisi *et al.,* 2013), *E. fetida* (Gruber *et al.,* 2000; Brulle *et al.,* 2006, 2007, 2011; Demuynck *et al.,* 2007; Asensio *et al.,* 2013) and *Dendrobaena octaedra* (Fisker *et al.,* 2013). Some of these studies have demonstrated a clear time-dose dependent response to the heavy metal exposure, especially for non-essential metals like Cd, and MT gene expression.(Gruber *et al.,* 2000; Brulle *et al.,* 2006; Demuynck *et al.,* 2007). Therefore, based on literature, MT is considered a useful biomarker for the investigation of sub-lethal heavy metal contamination effects in earthworms.

Along with MT gene expression responses, oxidative stress responses, immune system responses and signal transductions have been applied in AgNP toxicity studies using whole earthworms and isolated earthworm coelomocytes (Hayashi *et al.,* 2012, 2014). In a cell culture study, coelomocytes were harvested from adult *E. fetida* and exposed to varying doses of AgNPs over three short-term time points. At a low AgNP (5.91 mgL^{-1}) dose coelomocyte viability was shown to be unaffected across the 1, 3 and 6 h time points.

However transcriptomic responses from the coelomocytes were shown to correspond with exposure time, with up-regulation of the oxidative stress related gene CAT at 1 h exposure with subsequent down-regulation at 3 h. Genes associated with cellular function and immune regulation were also shown to be up regulated at the 6 h time point (Hayashi *et al.,* 2012).

In a published soil exposure study conducted on adult *E. fetida* earthworms exposed to high concentrations (500 $mgkg^{-1}$) of AgNP and Ag^{+} (as $AgNO_3$) across four time points (1, 2, 7, 14 d), the gene expression of potential cross-talk between oxidative stress responses and downstream immunity responses were analysed. The 1 d profile of the $AgNO_3$ exposures were found to be associated with oxidative stress (SOD), immune (Lyz) and signal transduction (PKC1) inductions. These initial inductions were then shown to be down-regulated at the 2 d time point. The 2 d profile of the $AgNO_3$ exposures showed induction of metal detoxification (MT), immune response (MyD88) and signal transduction (MEKK1). The induction of both MT and MyD88 showed a 42-fold induction compared to the controls. No earthworms survived to take measurements for $AgNO_3$ at the 7 and 14 d time points.

The gene expression profiles of the AgNP exposures correlated with time points, 2 d and 7 d profiles were similar to the inductions associated with the oxidative stress responses (CAT, SOD, HSP70 and MEKK1) while 1 d and 14 d profiles corresponded with metal detoxification and immunity (MT, CCF1, Lyz and MyD88). These gene expression patterns related to exposure time, highlighting a complex cellular response following exposure to high doses of AgNP in soil. When one group of genes (2d and 7 d profiles) were up regulated, the other genes (1d and 14 d profiles) appeared to be down-regulated (Hayashi *et al.,* 2014).

This present study is the first investigation of the gene expression response of CAT, SOD or MT in the earthworm *A. caliginosa* following exposure to chemicals, including AgNPs. As

these earthworms are abundant in agricultural soils and as the threat of AgNP contamination increases, it is important to investigate the toxic effects of AgNPs and develop suitable biological assay systems.

This study was designed to investigate the effect of environmentally relevant doses of AgNPs on selective antioxidant gene expression profiles in the earthworm *A. caliginosa* over a 14 day period. Earthworm samples were exposed to two AgNP doses, (0.3 $mgkg^{-1}$, 30 $mgkg^{-1}$) across three time points (2 d, 7 d, 14 d) to observe the effects of dose and time on GOI expression. The $AgNO_3$ treatment (3 $mgkg^{-1}$) provided a positive control for Ag^{+}. Fellow Lincoln researcher N. Saleeb found that the $AgNO_3$ is at least 10 fold more toxic compared with citrate AgNPs, based on enzyme assay results. This finding was investigated, hence the $AgNO_3$ control dose was 3 $mgkg^{1}$, approximately corresponding to the 30 $mgkg^{1}$ AgNP treatment. Theoretically these treatments intended to generate similar effects. However, these two treatments generated the same effect only once across the experiment, at 2 d for CAT expression, with a fold induction of 1.8.

There was only one significant effect associated with treatment. The CAT expressions for the 2 d and 14 d samples showed that the untreated 0 $mgkg^{-1}$ biological replicates collectively had a CAT expression lower than the treated samples. Furthermore, the CAT expressions for the 7 d samples showed that the untreated 0 $mgkg^{-1}$ biological replicates collectively had a CAT expression higher than the treated samples but this was not significant. This pattern suggests that there is an inhibitory effect on exposure to the Ag treatments.

The results of the SOD expressions are less clear. There was a significant effect on SOD expression with time but not treatment. All the 14 d samples, both treated and untreated samples displayed an intensive SOD induction. This suggests that it was the exposure conditions which were responsible for the changes in gene expression and not necessarily the Ag treatment.

Interestingly, the lower of the AgNP doses (0.3 $mgkg^{-1}$) showed a higher expression for both CAT and SOD than the higher dose AgNP (30 $mgkg^{-1}$) at 2 d and 14 d, but was lower at 7 d.

While a MT sequence was isolated, sequenced and identified as MT with a 68% query cover to *E. fetida*, it was found not to be the valid isoform regarding metal detoxification in *A. caliginosa*. The high $CdCl_2$ exposure over 48 h is suggested by literature to induce a detectable MT expression, had this isolated sequence been the correct MT isoform.

A previous study, on the expression of MT, compared specimens of the earthworm species *D. octaedra* collected from a heavy metal (Cu and Zn) contaminated site and an uncontaminated site (Mustonen *et al.,* 2014). These earthworms collected from different sites were both then exposed to varying conditions of Cu (50, 100 or 200 $mgkg^{-1}$) or Zn (75, 150 or 300 $mgkg^{-1}$) for 7, 14 or 28 d.

It was found that the MT expression was higher in the earthworms originally from the contaminated site across all treatments. It was suggested the earthworms originating from the metal contaminated sites expressed greater baseline levels of MT than the population of earthworms originating from the uncontaminated site. The uncontaminated site specimens lacked previous metal exposure which is suggested to be the reason for the variation. The MT expression for the contaminated population was stably expressed regardless of exposure concentration or duration. The MT expression for the uncontaminated population was shown to increase over time (Fisker *et al.,* 2013).

The findings of the above study suggest that earthworms exposed to heavy metals for prolonged periods of time will have a consistently higher MT expression rate. This potential phenomenon could be utilised in future research when attempting to isolate and amplify the correct MT isoform in *A. caliginosa*.

The gene expression profiles of this chapter are in contrast to the hypothesis that toxicity equivalent doses of $AgNO_3$ (3 $mgkg^{-1}$) and AgNP (30 $mgkg^{-1}$) produce similar expression profiles. Unexpectedly, it was the lower AgNP dose (0.3 $mgkg^{-1}$) that shared a gene expression profile similar to that of the $AgNO_3$ dose. However, there was only one treatment effect that was significantly different for CAT expression which was the control, so technically all of the exposure treatments produced similar gene expression profiles.

Chapter 5

Coelomocyte Studies

5.1 Introduction

The immune system of any organism is fundamental for the maintenance of good health. In toxicological studies, it serves as a sensitive physiological indicator of exposure. There is now evidence that nanomaterials influence the immune response in invertebrates. A majority of these studies have used earthworm species as the invertebrate model (Hayashi *et al.,* 2012; van der Ploeg *et al.,* 2013; van der Ploeg *et al.,* 2012; Hooper *et al.,* 2011). Earthworms of all species have chloragogenous tissue, which resides between the intestinal epithelial tissue and the coelom cavity (Fig 20). This tissue is central to immune defences and comprises a variety of cells, collectively called coelomocytes. Coelomocytes are released from the chloragogenous tissue into the coelomic fluid, where they circulate to provide an immune function to repel infectious agents as well as a detoxification function (Hayashi *et al.,* 2012). There are three coelomocyte cell type classifications: eleocytes, amoebocytes and granulocytes (Hostetter & Cooper, 1974). All three cell types can recognise foreign matter and initiate or perform phagocytosis or encapsulation (Engelmann *et al.,* 2004). Coelomocytes are similar to vertebrate immune cells as they have the capacity to combat pathogens using reactive metabolites such as superoxide radicals, hydroxyl radicals and

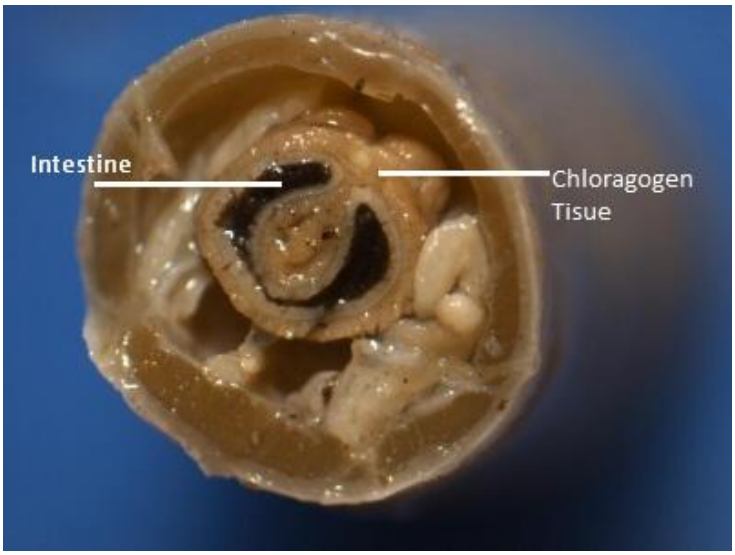

Figure 20: *A. caliginosa* transverse section to illustrate the intestinal cavity and chloragogen tissue

nitric oxide (Rivero, 2006). The proportions of the different coelomocyte cell types varies depending on the species being analysed (Kurek *et al.,* 2002).

Coelomocytes are classified largely by differential staining and ultrastructural morphology. Coelomocyte types can be differentiated based on cell size, nucleus size, shape and location and also subcellular organelles present (Hamed *et al.,* 2002).

Eleocytes are the largest of the coelomocyte cell types with a surface area of approximately 1800 μm^2. They contain a spherical nucleus which is small and eccentrically located within the cell. The cytoplasm contains no organelles. Typically, eleocytes account for about 30% of the circulating coelomocyte population (Adamowicz, 2005). The functions of eleocytes are regulatory and metabolic, maintaining the coelomic fluid pH, and providing storage for glycogen and lipids (Homa *et al.,* 2013).

Amoebocytes have multiple functions in the coelomic fluid. There are many sub-classifications of amoebocytes across the members of the *Lumbricidae* family. Collectively, amoebocytes perform the majority of immune reactions including phagocytosis, encapsulation, nodulation and humoral immune responses (Çotuk & Dales, 1984). Amoebocytes are polymorphic in nature, with a surface area ranging from 112–270 μm^2. Amoebocytes form aggregates which are composed of a few to over a dozen cells making them easy to identify when staining. Their nucleus is large and oval in shape, and generally localised in the centre of the cell. They account for approximately 40% of the circulating coelomocyte population (Adamowicz, 2005).

Granulocytes are similar in size to amoebocytes with an average surface area of 180 μm^2. They are spherical in shape and have a small oval shaped eccentric nucleus. Granulocytes account for 30% of circulating coelomocytes and do not appear to form aggregates. (Adamowicz, 2005).

There is currently no published literature that investigates changes in coelomocyte cell type proportions as a means of measuring toxicity. The extraction and processing of coelomocytes is simple and reproducible. Flow cytometry applications could be developed if changes in coelomocyte cell type proportions are found to be a direct dose response to a toxin.

The objective of this work was to isolate, identify, quantify and differentiate both viable coelomocytes and coelomocyte cell types following exposure to environmentally relevant soil treatments of AgNP (0.3 $mgkg^{-1}$,30 $mgkg^{-1}$) and $AgNO_3$ (3 $mgkg^{-1}$). Any significant changes in coelomocyte viability or coelomocyte cell type proportions observed in the treated samples in comparison to the untreated samples could then lead to the development of an assay for AgNP and $AgNO_3$ environmental contamination analysis.

5.2 Materials and Methods

5.2.1 Coelomocyte Extrusion

Biological replicates were collected from each treatment (0 $mgkg^{-1}$- untreated, 3 $mgkg^{-1}$-$AgNO_3$, 0.3 $mgkg^{-1}$- AgNP, 30 $mgkg^{-1}$- AgNP) across the three time points (2 d, 7 d, 14 d). Each earthworm sample was washed in deionised water to remove surface soil before the coelomocyte extrusion procedure. Coelomocytes were extruded from each earthworm individually by electrocution as describe below. Earthworms were immersed in 2 mL of ice cold extrusion buffer [5 mM EGTA, 71.2 mM NaCl, 50.4 mM guaiacol glyceryl ether, 5% ($^{v}/_{v}$)

Figure 21: Coelomocyte Extrusion Materials.

ethanol] in a glass petri-dish and held suspended for 2 minutes. After the two minute soak period, a 9 V current was applied to the solution in 5 second bursts, 10 times over a 1 minute (Muangphra & Gooneratne, 2011).

The extrusion buffer, containing the extruded coelomocytes, was removed from the petri-dish and transferred into a 1.5 mL Eppendorf tube. The extruded coelomocytes were mixed by pipette for even cell distribution. Cell viability counts and differential cell counts were performed immediately on each extruded coelomocyte sample.

5.2.2 Viable Cell Count

A 1:1 mixture containing a 50 µL aliquot of extruded coelomocytes and 50 µL HyClone Trypan blue solution (Thermo Scientific Inc.) was mixed thoroughly and allowed to rest for 15 minutes, and two 10 µL aliquots were loaded into two separate chambers of a haemocytometer (Clay Adams, Parsippany, N.J., USA).

Viable cells do not absorb the Trypan blue dye, while non-viable cells do. This principle was used to differentiated the viable (blue halo cells) from the non-viable (dark blue cells). Viable cells were counted from five of the 25 haemocytometer squares bounded by triple lines. Viable cell counts for the two chambers were recorded. The average of the two chambers was used to calculate the coelomocyte viable cell count for each biological replicate.

5.2.3 Differential Cell Counts

Differential cell counts were performed using 20 µL of the extruded coelomocyte samples spread onto glass slides and the Wright-Giemsa stain solution protocol (Sigma-aldrich Inc.). The 20 µL samples were spread evenly across microscope glass slides and allowed to air dry. Slides were then fixed by immersion in methanol for 5 minutes, suspended in 1:1 Wright-Giemsa stain (1.53 gL^{-1} Wright's stain, 2.50 gL^{-1} Giemsa stain, 10% ($^{v}/_{v}$) glycerin) and

phosphate buffer solution (50.1 % ($^{w}/_{w}$) monobasic potassium phosphate, 49.9 % ($^{w}/_{w}$) dibasic sodium phosphate) (PBS) for 2 minutes, and then rinsed in PBS and blotted dry and allowed to air dry.

Figure 22: Wrights-Giemsa staining process

Microscopy studies were performed on a Nikon H55OS microscope, using bright field and the NIS Elements BR 3.2 programme. The images of different cell types were collected and analysed for observable variations which can be utilised in the experimental differential cell counts.

Differential cell counts were performed on each biological replicate using a binocular light microscope and coelomocyte classifications were allocated based on the previous microscopy studies and characteristics provided by Adamowicz (2005). Cell counts began at the bottom left hand corner of each slide and 40 cells were counted for each biological replicate slide. Each slide was counted in the same manner, vertically scrolling up and down the slide from left to right.

5.3 Results

5.3.1 Viable Cell Counts

Viable coelomocytes were distinguished from non-viable cells by a bright white cell centre surrounded by a dark blue halo. The Trypan blue dye does not penetrate a viable cell but

does stain the external cellular membrane.

Ideally when counting the viable cells of each sample, the centre square and the four corners of the triple lined bound squares of the haemocytometer are used. Therefore any viable cells that fell within these five squares would be counted. However this was not possible for some samples which had viscous aggregates of cells, occupying an entire square and were impossible to count. In this situation the next closest horizontally neighbouring square was counted. See Appendix C.3 for individual biological replicate counts.

Table 5: Average Viable Cell Counts of Exposures

Treatment	Time	Average Viable Cell Count (per mL)
0ppm	2 days	35,500,000
0ppm	7 days	43,000,000
0ppm	14 days	55,500,000
AgNO3 3ppm	2 days	38,000,000
AgNO3 3ppm	7 days	46,500,000
AgNO3 3ppm	14 days	46,000,000
AgNP 0.3ppm	2 days	38,000,000
AgNP 0.3ppm	7 days	51,000,000
AgNP 0.3ppm	14 days	39,000,000
AgNP 30ppm	2 days	47,500,000
AgNP 30ppm	7 days	36,000,000
AgNP 30ppm	14 days	46,500,000

There was no significant effect ($p < 0.05$) for any of the treatments on viable cell counts at any time point (Appendix A.6).

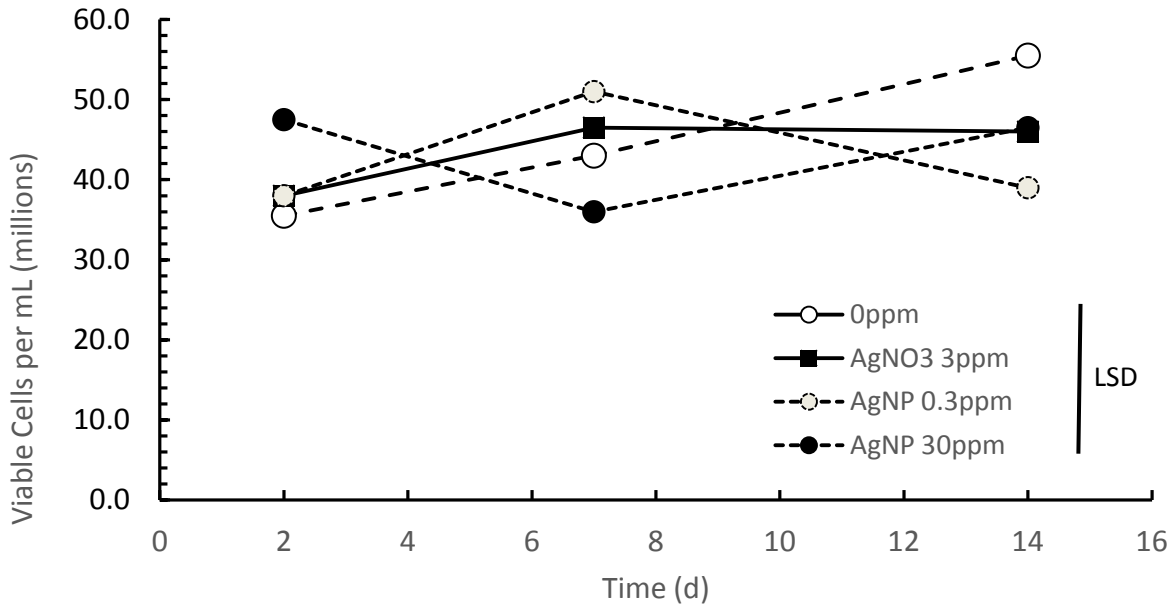

Figure 23: Average viable cell count in per mL.

5.3.2 Differential Cell Counts

5.3.2.1 Microscopy Studies

Coelomocyte slides prepared using the same volume of cells (20 µL) as used in the experiment exposure slides were stained with Wright-Giemsa stain and used to study the characteristics of the *A. caliginosa* coelomocyte cell types using the guidelines provided by Adamowicz (2005).

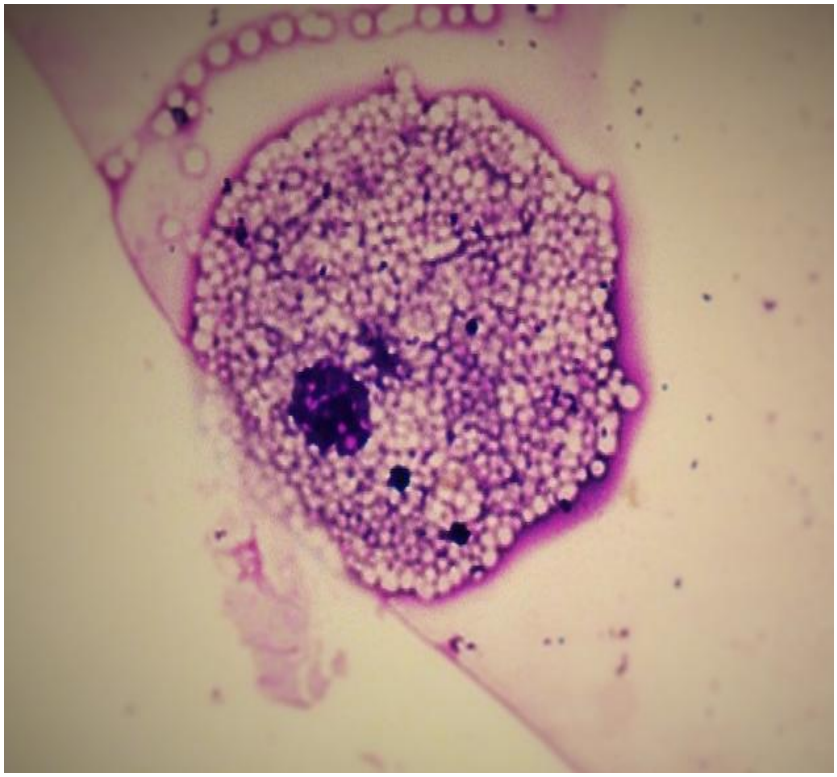

Figure 24: Eleocyte. 1000X magnification.

Eleocytes are the largest of the three cell types. These cells are easily identified by their size alone. The eleocyte in figure 24 shows the low nuclear-cytoplasm ratio. The nucleus is small and eccentrically located.

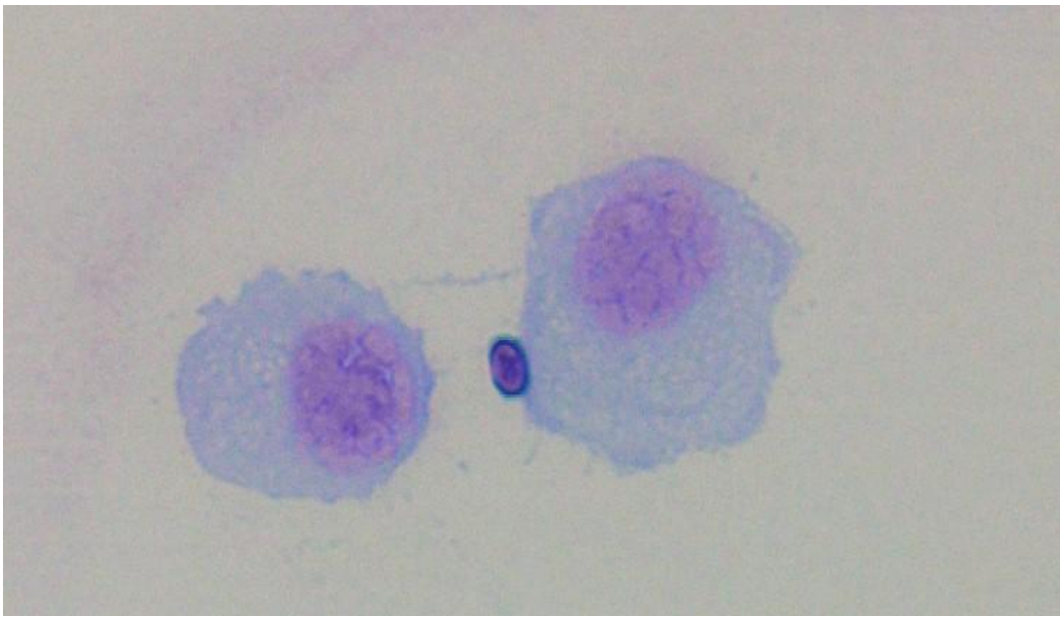

Figure 25: Amoebocytes. 1000X magnification

The amoebocytes and granulocytes are of similar size and other characteristics were used to distinguish between them. The amoebocytes in Figure 25 show the large oval shaped nucleus of amoebocytes. Visible pseudopodia were also used to differentiate amoebocytes. In Figure 25 the amoebocyte on the right appears to be bound to a bacterial cell in preparation for pinocytosis or phagocytosis. Another characteristic of amoebocytes is to form aggregates. Aggregates of amoebocytes were frequently observed both in preliminary studies and during differential cell counts. Figure 26 shows a typical aggregate of amoebocytes, composed of 7-8 cells. These aggregates were observed with both small quantities of 2-4 amoebocytes and with larger quantities of 10-20 amoebocytes. The amoebocytes also displayed a more purple tone in colour.

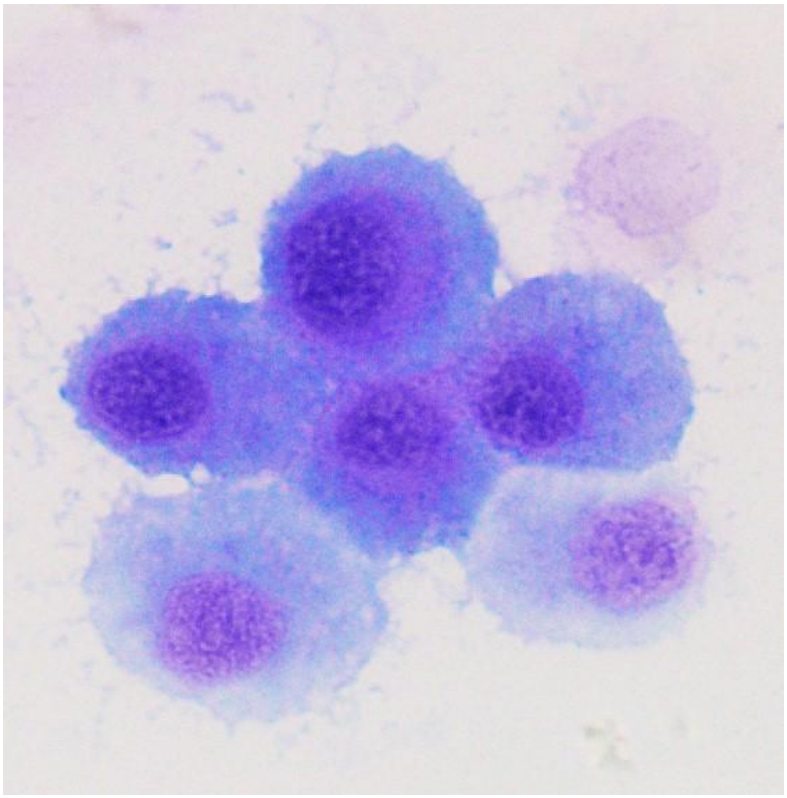

Figure 26: Aggregate of amoebocytes. 1000X magnification

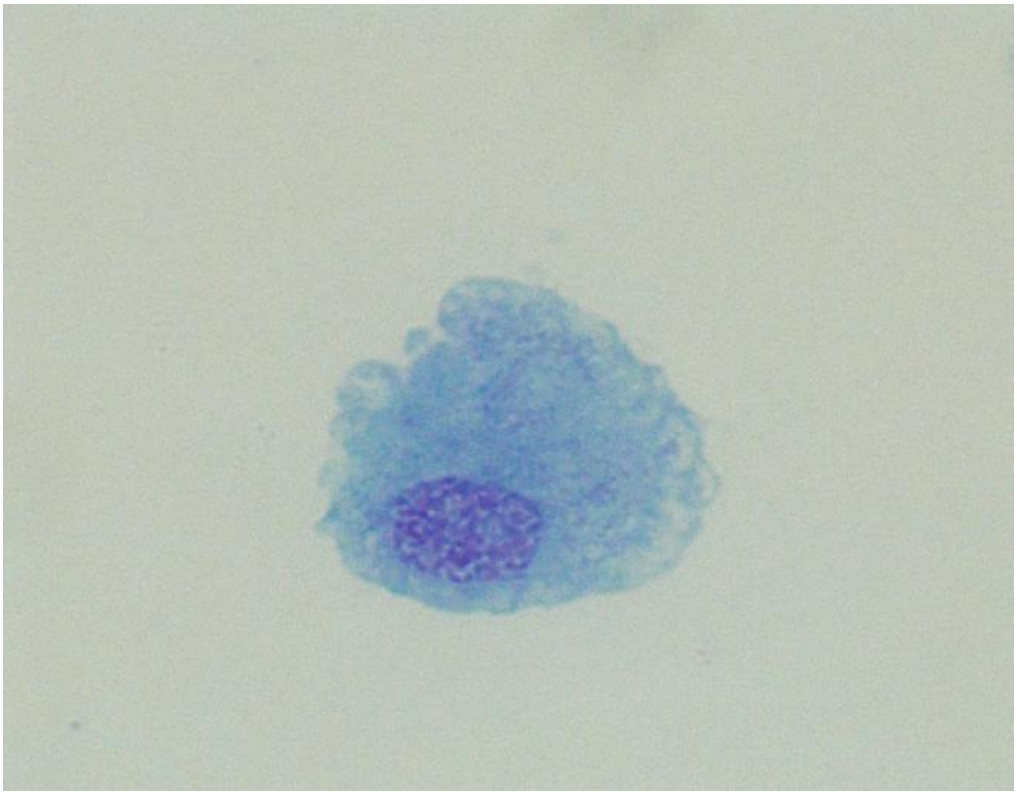

Figure 27: Granulocyte. 1000X magnification

Granulocytes were distinguished from amoebocytes by their smaller peripherally located nucleus and they were more of a blue colour. Granulocytes were not observed to form aggregates. Figure 27 shows the small peripherally located nucleus and the blue tone characteristic of granulocytes.

Each biological replicate was carefully analysed for differential cell counts. All cell counts began in the bottom left hand corner of the slides and cells were counted moving vertically up and down the slide as the slide was moved horizontally.

When a cell was observed that failed to display clear cell type characteristics, it was ignored. A total of 40 cells were counted per slide and cell types expressed as proportions (%).

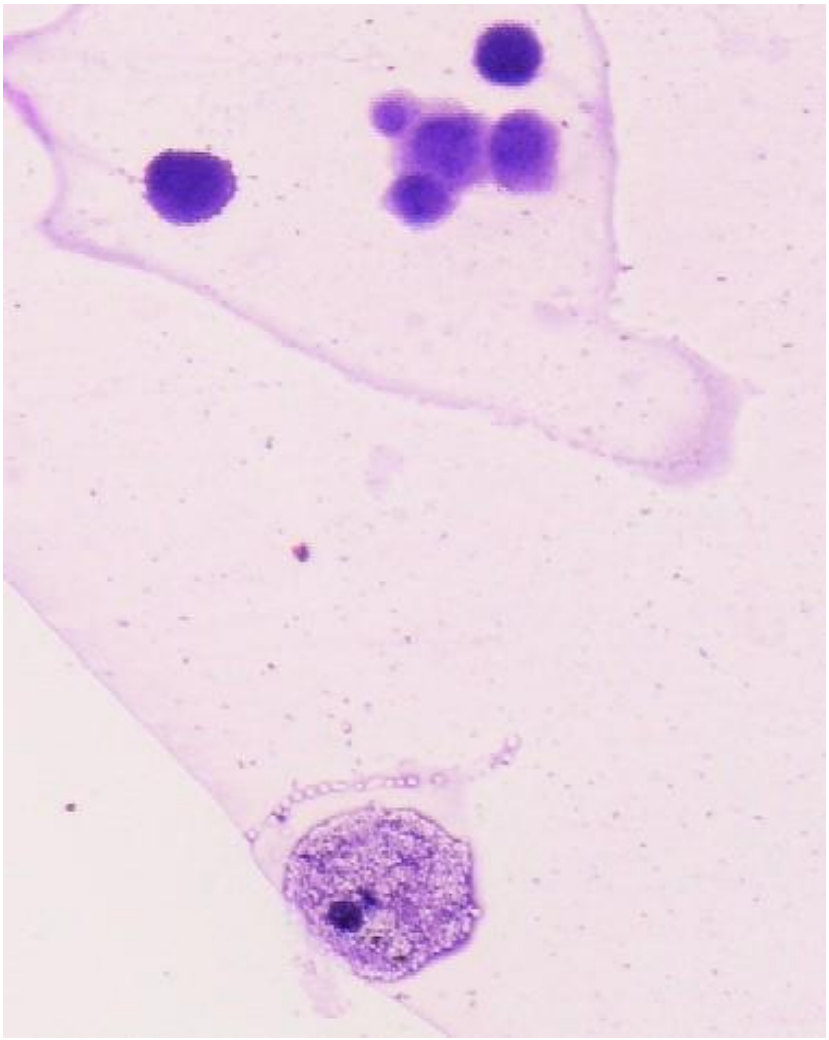

Figure 28: Size variation; eleocyte (bottom) and amoebocytes (top). 400X magnification.

The collective results from the biological replicates from each treatment and time point are expressed graphically below. For individual biological replicate data refer to Appendix 12. Figure 28 shows the size difference between eleocytes, bottom, and amoebocytes, top. This image also represents the relative proportion of eleocytes to amoebocytes. Amoebocytes were the most frequently observed cell type during both the preliminary studies and the biological replicate differential counts.

5.2.3.2 Differential Cell Count Results

The biological replicates of each treatment and time point were collectively analysed, table 6, using ANOVA and the LSD was determined for each cell type (Appendix A.5). Raw biological replicate results are shown in Appendix C.4.

Table 6: Differential Cell Count Results

Treatment	Time	Eleocytes %	Amoebocyte %	Granulocyte%	Total
0ppm	2 days	11.9	60.0	28.1	160
0ppm	7 days	10.0	68.1	21.9	160
0ppm	14 days	12.5	65.0	31.3	160
AgNO3 3ppm	2 days	11.9	59.4	28.8	160
AgNO3 3ppm	7 days	18.1	61.9	20.0	160
AgNO3 3ppm	14 days	7.5	73.1	19.4	160
AgNP 0.3ppm	2 days	10.0	60.0	30.0	160
AgNP 0.3ppm	7 days	10.0	63.8	26.3	160
AgNP 0.3ppm	14 days	11.9	73.1	15.0	160
AgNP 30ppm	2 days	6.3	67.5	26.3	160
AgNP 30ppm	7 days	10.6	59.4	30.0	160
AgNP 30ppm	14 days	8.8	75.6	15.6	160

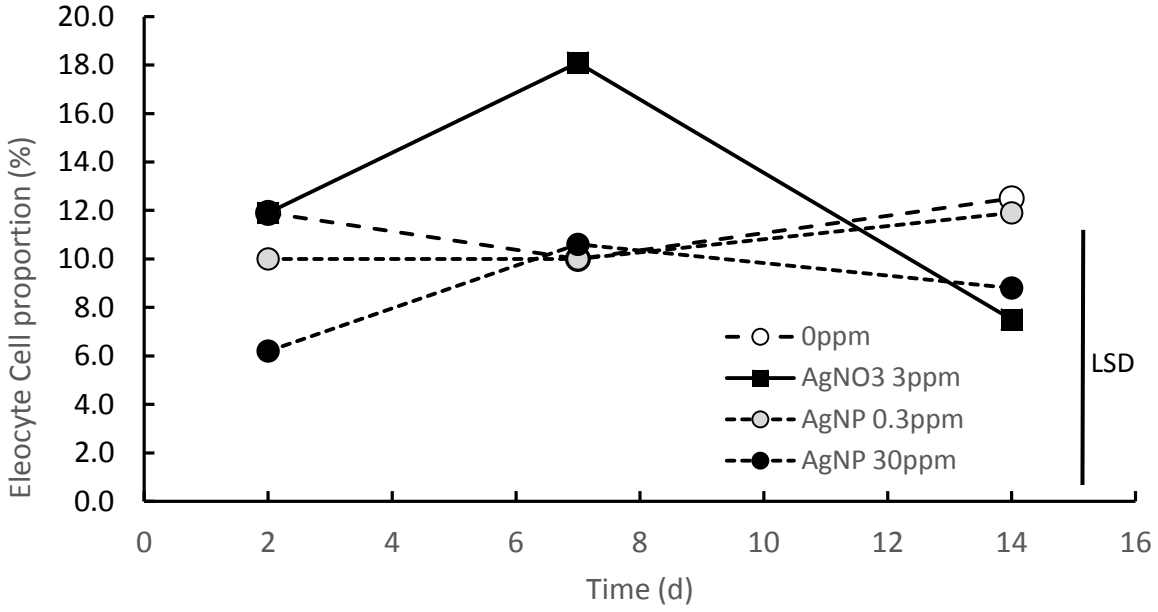

Figure 29: Eleocyte Proportions over Treatment and Time.

There was no significant effect on proportions of eleocytes across the treatments or the time points. In figure 29 there is a visible spike in eleocyte proportion at the 7 d time point for the $AgNO_3$ treatment. The proportion then shows a decline by the 14 d time point. However neither of these events are not significantly different to the other treatments.

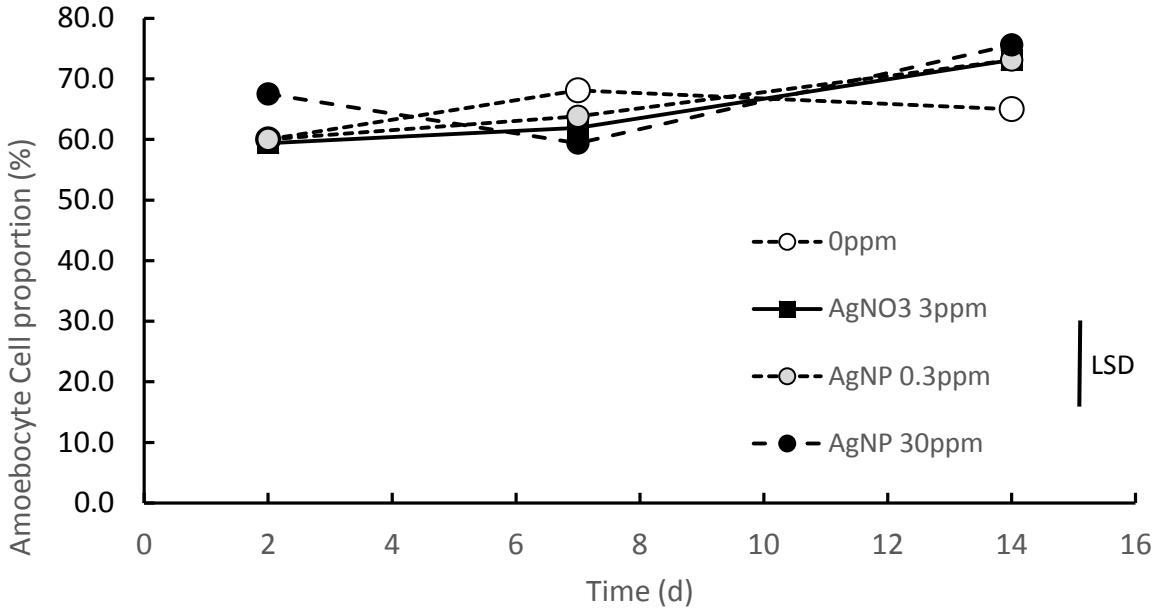

Figure 30: Amoebocyte Proportions over treatment and time.

There were significant effects on amoebocyte proportions over time. Amoebocyte proportions were significantly higher at the two week time point across all treatments. Figure 30 shows that the amoebocyte proportions across all the treatments at each time are relatively consistent.

Granulocytes proportions had a significant effect over time. Granulocytes were significantly higher at the two day time period across all treatments. The trend shown in figure 31 shows that over the 14 d period the proportion of granulocytes decline for each treatment, with exception to the slight flux at 7 d for the $AgNO_3$ treatment. However, as there was no significant effect on treatment the $AgNO_3$ treatment increase at 7d is not significantly different from the other treatments.

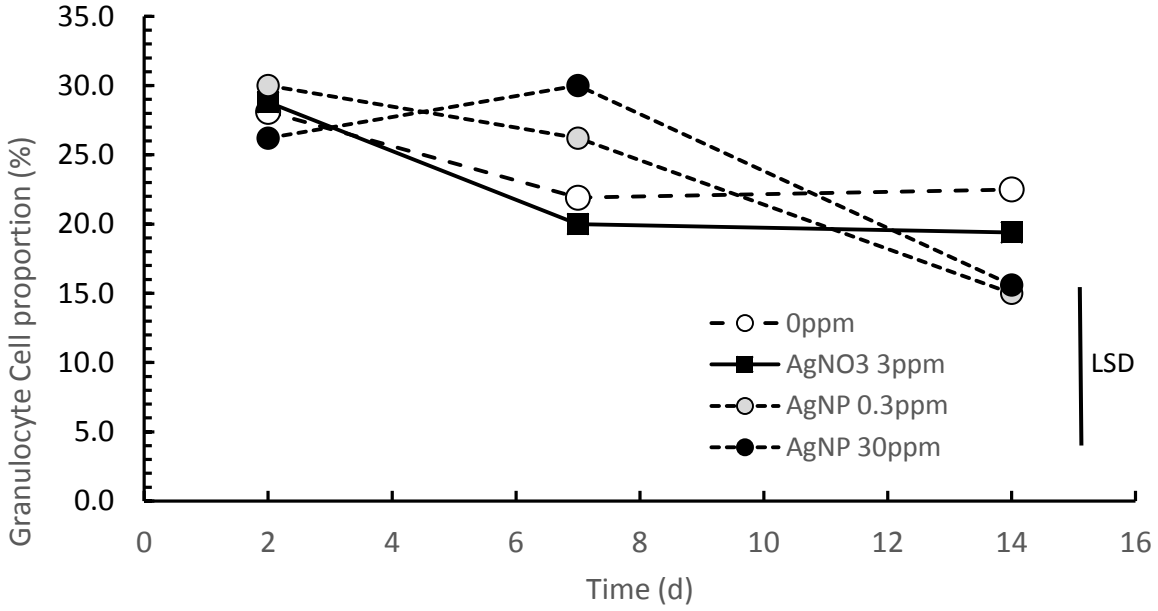

Figure 31: Granulocyte Proportions over Treatment and Time.

5.4 Discussion

This work was designed to observe any coelomocyte fluctuations in the earthworm *A. caliginosa* following exposure to environmentally relevant doses of AgNP in soil over a 14 d period. These methods have never been applied in published ecotoxicology studies using earthworms. Both cell viablities and differentital cell proportions were investigated. The results of the viable cell counts showed that there were no significant changes across treatments or time points. The differential cell counts revealed that there were some cell type proportion changes over time. Amoebocytes increased over time and the granulocytes decreased over time. This balanced fluctuation over time is likely to account for the steady viable cell counts over time.

When an earthworm is exposed to foreign material it is suggested that the amoebocyte cell proportions would increase as they are the dominant cell type involved in the removal of bacteria and other foreign materials (Adamowicz, 2005). The ratio of amoebocytes to eleocytes was shown to increase in the earthworm *Dendrobaena veneta* following exposure to Cd. It was also found that the expression of the metal detoxification enzyme, metallothionein (MT) was up-regulated in the amoebocytes but not in the eleocytes (Olchawa *et al.,* 2006).

The amoebocytes of the earthworm *L. rubellus* have been shown to be involved in Cd trafficking while the eleocytes are not (Morgan *et al.,* 2004).

It is important to understand the effects AgNPs have on the coelomocytes of the earthworm *A. caliginosa* as it is a dominant species in soils and has potential for bioassay developments. Heavy metal contaminated soil studies (Cd, Zn, Cu), using the earthworm *D. veneta* as a biological model, have shown that soils polluted with heavy metals lead to a decrease in coelomocytes. The effect of this decrease results in an elevated ocupancy of parasites and therefore earthworm productivity declines (Wieczorek-Olchawa *et al.,* 2003).

The amount of coelomocytes extruded from the earthworms *E. fetida* and *A. chlorotica* were found to decrease in a time-dependent manner following exposure to heavy metal (Cu, Pb and Cd) treatments. In the earthworm species *A. chlorotica,* the Cu exposures at low doses (0.33 and 0.66 μg/cm^2) to a significant decrease of eleocyte numbers (Homa *et al.,* 2007). The viability of coelomocytes, extruded from adult *E. fetida* earthworms, were found to decrease with increasing Ag^+ concentration (Hayashi *et al.,* 2012).

The literature shows that the tolerance of eartrhworm species to heavy metal expsoure is variable. A low dose that may disturb coelomocyte homestasis in one species may not have an effect on another.

There was no treatment effect in this work using environemntally relevant doses. The results of this work suggest the earthworms coelomocyte homestasis was not effected by any of the low heavy metal treatment doses. While there was no significant cell type proportion change observed, each of the three coelomocyte types of *A. caliginosa* were identified and characterised and would be of use in further *A. caliginosa* immune response studies.

Chapter 6

Discussion

In addition to the earthworm speciation studies, this study was conducted to investigate if there were toxic effects on the earthworm *A. caliginosa* following exposure to environmentally relevant doses of AgNPs and a theoretically comparative $AgNO_3$ dose.
It was evident from the speciation results of Chapter 2 that the majority of the established earthworm population at Lincoln University were *A. caliginosa.* Furthermore, the low dose exposures to AgNPs and $AgNO_3$ did not induce any adverse effects on *A. caliginosa* specimens based on the oxidative stress gene expressions of Chapter 4 and the immune cell viability measures of Chapter 5.

Before the genetic era, correctly identifying an earthworm species involved careful morphological observations, mostly of the sexual characteristics of adult species (Tsai *et al.,* 2000). When dealing with juvenile earthworms or coocoons the standard means of morphological identification are not possible as the sexual organs are not developed and it is possible incorrect identifications may occur, based on adult specimens present at sampling sites (Pérez-Losada *et al.,* 2009). Nowadays, by application of DNA barcoding or gene sequencing, standardised genes can be isolated, amplified and sequenced as long as a suitable gene reference is present in credible reference libraries (Caterino *et al.,* 2000; Hebert *et al.,* 2003; Klarica *et al.,* 2012) such as the NCBI GenBank which was utilised in this research. This approach allows for species identification at all life stages.
In a French study, the distribution of *Lumbricus* species was investigated across seven grasslands and six forest sites across France. Morphological analysis of adult specimens collected across these sites revealed four species, *L. terrestris*, *Lumbricus festivus, L. rubellus*

and *Lumbricus castaneus.* DNA sequences were collected for the mitochondrial COI gene across 131 samples, of theses both positively identified adult species and unidentified juveniles. The researchers cut a small segment of tissue (~1-2mm), extracted DNA and ran a PCR to amplify the COI gene from each sample, similar to the approach applied in Chapter 2 of this research.

The DNA sequence results were analysed to identify sample sequence clusters (DNA samples sharing the same sequence). The results showed that the unknown juvenile sequences were unequivocally identical with the known adult species sequences therefore identifying the species of the unknown juveniles (Richard *et al.,* 2010).

In a similar Chinese study, species of Chinese earthworms were examined by comparing the sequence diversity in the COI gene. The results revealed 28 species of earthworms, spanning six genera, and each earthworm specimen was successfully identified (Huang *et al.,* 2007).

The methods applied in the speciation studies to identify *A. caliginosa* from other species reported in chapter 2 are similar to the above mentioned studies, highlighting the benefits of genetic analysis for earthworm species identification in soil ecological research. It is important to be able to confidently and correctly identify earthworm species used in research (Lavelle *et al.,* 2006; Suthar, 2009), because earthworms are increasingly used in ecotoxicological research and using the same species is important to minimise variation between experimental groups (Nahmani *et al.,* 2006). DNA analysis is currently an unrivalled tool to meet this requirement. Currently there is no published literature where the GOIs of this research, (SOD, CAT, MT) have been measured in the earthworm *A. caliginosa* following exposure to either a chemical or environmental stress. This is not unsurprising considering the lack of gene sequences available on the species. The lack of

such a pivotal resource added complications to the GOI isolation process for the heterogeneous MT transcript.

Key toxicological factors are dose/concentration and the length of exposure. These two parameters can be measured easily, to determine the dose response of a specific chemical and threshold levels can then be classified to identify concentrations that are harmless or toxic (Elsaesser & Howard, 2012). Note however, that some toxicological dose responses can be complex and hard to interpret, particularly in the case of very low or very high doses (Rozman & Klaassen, 2007).

As soil biota play a fundamental role in maintaining soil health and productivity, biological properties of soil biota can be useful indicators in soil toxicity studies (Ritz *et al.,* 2009). Significantly however, the deliberate application of nanomaterials into soil from remediation technologies (Barnes *et al.,* 2010) and agricultural fertiliser applications (Tourinho *et al.,* 2012) highlight the relevance of this research.

The use of nanomaterials is unregulated and there is urgency to understand the effects these materials pose to the environment. Current research into the toxicological potential threat these materials pose struggles to keep up with the rapid expansion of the nanotechnology industry (Elsaesser & Howard, 2012).

Studies have been performed to investigate the toxicity of AgNPs on a wide range of organisms, including microbial, invertebrate, mammalian and human cells (Ahamed *et al.,* 2008; Hernández-Sierra *et al.,* 2008; Kawata *et al.,* 2009; Choi *et al.,* 2010; Hayashi *et al.,* 2014).

The application of biosolids onto land would account for a large majority of AgNP contamination into soils and was a significant factor of concern for the development of this research. Biosolid application onto land delivers both essential macro and micro nutrients for plant growth, but there are contaminates present which raise concern. Based on a 2003

report, in New Zealand, there were five biosolid schemes based in Nelson, Christchurch, Wellington, New Plymouth and Rotorua. Of the biosolids produced, half is discharged onto production forests and the remaining half is discharged onto agricultural land (New Zealand Water & Wastes Association, 2003).

However, research into chemical transition of AgNP following waste water treatment show that AgNPs in biosolids are found predominantly transformed as Ag sulphide (Ag_2S) particulates (Ma *et al.,* 2013; Kaegi *et al.,* 2011; Kaegi *et al.,* 2013; Lombi *et al.,* 2013; Impellitteri *et al.,* 2013). In a study by Levard *et al.* (2013) it was demonstrated that even partial sulphidation (0.073 S/Ag mol) dramatically reduces the toxicity of AgNP to killifish and duckweed species. Although AgNP transformation to Ag_2S in biosolids is shown to reduce immediate toxicity, there is also the potential for oxidative Ag^+ dissolution from Ag_2S over long periods of time (Ma *et al.,* 2013).

Pristine AgNPs mixed with biosolids and applied to soil were shown by Coleman *et al.* (2013) to have a more toxic effect. Coleman and colleagues (2013) set up mesocosms composed of soil and commonly occurring plant species and left them to establish for 2 months. On day 0, four experimental treatments were applied to the established mesocosms, namely, 1) 'control', 1.5 L deionised water; 2) 'slurry', 1.5 L biosolid slurry (1.5 mg total Ag); 3) 'slurry + AgNPs' (1.5 L biosolid slurry spiked with 9.9 mg Ag as AgNP; 11.4 mg total Ag); and 4) 'slurry + $AgNO_3$' (1.5 L biosolid slurry spiked with 44 mg of Ag as $AgNO_3$ (45.5 mg total Ag). These treatments, when homogenously distributed through soil, equated to 0.02, 0.14 and 0.56 mg Ag kg^{-1} soil respectively. All the treatment Ag concentrations were environmentally relevant based on US EPA guidelines (Stein *et al.,* 1995), and Ag additions were based on a recent national analysis of biosolids contaminants (EPA, 2009). The differences in soil microbial community biomass, composition and activity were determined between treatments as well

as plant biomass and photosynthesis and gas fluxes from soils. Based on previous results (Bradford *et al.,* 2009; Coleman *et al.,* 2012), Coleman and colleagues (2013) were expecting to see minimal effects in the 'slurry + AgNP' treatments compared to the 'slurry + $AgNO_3$' positive control. However, the microorganisms and plants showed adverse effects to the 'slurry + AgNP' treatment, and in the majority of measures these were similar, or even greater than the response measured in the 'slurry + $AgNO_3$' treatment. Coleman and colleges (2013) concluded that biosolids containing environmentally relevant concentrations of AgNP may also cause adverse effects on diverse terrestrial ecosystems. Therefore avenues of pristine AgNP applications onto land (eg. AgNP based fertilisers) could have adverse effects to soil ecosystems.

In my research, 'pristine' AgNPs were used at environmentally relevant doses to examine the effects on the soil dwelling earthworm species, *A. caliginosa*. While there is significant literature stating the potentially harmful effects AgNP soil pollution pose to earthworm species, the majority of these studies use relatively high and unrealistic doses of AgNP to achieve a detectable response. Current AgNP contamination in soil poses a greater threat to soil dwelling microorganism and indirect effects on the action of soil enzymes (Peyrot *et al.,* 2014). The potential consequences of AgNP contamination in soils of greatest concern is the interruption they may cause to numerous biochemical processes, especially the nutrient cycling pathways and other essential microbial mediated processes.

The current literature investigating the toxic effects of pristine AgNPs on soil ecosystems, employ relatively high doses of pristine AgNPs. In most of these soil toxicity studies, earthworms have been used as bio-indicators and AgNP treatments are typically run parallel with a $AgNO_3$ control. Hayashi *et al.* (2013) exposed *E. fetida* earthworms to 500 $mgkg^{-1}$ of Ag in two treatments as AgNP and $AgNO_3$ across four duration periods. At each duration period, genes responsible for oxidative stress, detoxification enzyme activity and immune regulation

responses were analysed between the two treatments. Comparisons of the molecular stresses were made between the two treatments across the different time points. The results showed unparalleled gene expression differences between the two Ag treatments ($AgNO_3$ and AgNP). The surface specific action and/or the differing levels of bioavailability between the two forms of Ag could explain this outcome (Liu *et al.,* 2011). This study provided evidence to support the induction of the antioxidant enzymes SOD and CAT as well as the metal detoxifying biomarker MT.

Reactive oxygen species are frequently detected in cells treated with AgNP as a result of oxidative stress (Foldbjerg *et al.,* 2011; AshaRani *et al.,* 2008; Wang *et al.,* 2009; Wei *et al.,* 2010; Farkas *et al.,* 2010; Wise *et al.,* 2010). The enzymes SOD, CAT and glutathione peroxidase (GPx) are enzymes of the cellular antioxidant defence system (Pigeolet *et al.,* 1990) that are induced to combat oxidative stress. Various cell types, both vertebrate and invertebrate, have been shown to have alterations in SOD and CAT transcription following acute and chronic exposure to low and high doses of AgNPs in comparison with controls (Kim *et al.,* 2009; Choi *et al.,* 2010; Wu & Zhou, 2013; Hayashi *et al.,* 2013 & 2012; Zhan, 2012; Li *et al.,* 2014). This cellular antioxidant cascade of enzymes are typically up regulated as a coping mechanism to counteract the ROS generated from the AgNP and/or Ag^+ within the cells (Ivask *et al.,* 2013). In addition, MT which have thiol groups, are responsible for binding heavy metals and scavenging free radicals including hydroxyl, superoxide and nitric oxide radicals in both mammalian and yeast models (Felix *et al.,* 1993; Hartmann & Weser, 2000).

The gene expression studies in *A. caliginosa* reported in chapter 4 were measured across the treatments and time points. The collective CAT expressions across the treated sample replicates (3 $mgkg^{-1}$ $AgNO_3$, 0.3 $mgkg^{-1}$ AgNP and 30 $mgkg^{-1}$ AgNP) were down-regulated at 7 d but up-regulated in the 3 $mgkg^{-1}$ $AgNO_3$ and 0.3 $mgkg^{-1}$ AgNP at 14d. Furthermore, both

the collective expression of the low and high AgNP treated replicates showed up-regulation of CAT expression at the 2 d time point while the $AgNO_3$ treated replicates were down regulation at 2 d. The ANOVA results of the gene expression studies in chapter 4 showed a significant effect for CAT expression (across treatments). At the 14 d time point, the CAT expression in *A. caliginosa* were significantly higher compared with the control (0mgkg^{-1}) by ~1.2 fold. While this fold difference is statistical significant in comparison to the control, it is not necessarily a high enough induction to suggest any significant response to oxidative stress.

The trend of SOD expression across both the treated and untreated replicates was to increase over time. The collective SOD expression of both the low and high AgNP treatments were more up-regulated at the 7 d time point in comparison with the $AgNO_3$ samples. ANOVA analysis showed a significant effect at 5% for SOD expression across time. The SOD expression values across all the treated and the untreated control (0 mgkg^{-1}) were significantly higher at the 14 d time point. There are two distinctive groupings, 1) $AgNO_3$ and 0.3 mgkg^{-1} AgNP and 2) untreated (0 mgkg^{-1}) and 30 mgkg^{-1} AgNP. Group 1 samples generated the greatest induction with >2-fold increase, while in the group 2 samples (controls) the induction was lower with <1.4- fold increase. As the induction is not significantly different between treated and untreated samples it is suggested this significant induction may be due to the unnatural glass jar experimental conditions. Accumulation over two weeks of earthworm excreta and/or lack of nutrients in soil (which is unlikely) may have had an effect on SOD expression at 14 d. The higher induction levels measured in the $AgNO_3$ and 0.3 mgkg^{-1} AgNP 14 d SOD expressions could be a result of both the exposure effect over time (glass jar conditions) and the treatment (3 mgkg^{-1} $AgNO_3$ and 0.3 mgkg^{-1} AgNP). The SOD induction in these two treatments was twice that of the untreated (0 mgkg^{-1}) and 30

$mgkg^{-1}$ AgNP treatment, which could be linked to a compounding effect of both exposure effect and a treatment effect over time.

The low molecular weight, cysteine-rich (~30%), ubiquitous MT proteins stem from an extremely heterogeneous super family. The evolution of these atypical metal binding proteins is obscure and not easily interpretable (Sigel *et al.,* 2009). There are three classes of MT (class I, class II and class III). MT sequences are classified based on their similarity to the first discovered MT sequence isolated from the kidneys of horses (Margoshes & Vallee, 1957). Class I and class II MTs are gene encoded proteins while class III MT are known as phytochelatins, these are non-gene-encoded plant proteins that are derived from glutathione (GSH) polymerization (Capdevila & Atrian, 2011). In the earthworm *E.fetida,* MT sequence is the annelid representative of MT. This protein has been shown to bind Cd and is composed of 75 amino acids with cysteine distributions in X-C-X and X-CC-X patterns and also one cysteine triplicate (Stürzenbaum, 2009). In the MT protein alignments (see appendix B5) composed of various *Lumbricidae* MT isoforms there was clear sequence diversity between both MT isoforms and Lumbricidae species.

In my research, the isolated MT fragment from the preliminary research was found not to be the correct MT isoform. *A. caliginosa* exposed to all treatments (0 $mgkg^{-1}$ [control], 3 $mgkg^{-1}$ $AgNO_3$, 0.3 $mgkg^{-1}$ AgNP, 30 $mgkg^{-1}$ AgNP – 2 d, 7 d and 14 d) were analysed along with CAT, SOD and reference ACT. Expression was not detected across the entire sample set. To validate this effect, the positive 48 h Cd exposure study was conducted because MT gene is markedly induced in earthworms exposed to Cd (Brulle *et al.,* 2006). The gene expression studies of this Cd exposure also showed a lack of MT induction in *A. caliginosa* highlighting that the MT isoform isolated and sequenced is unlikely to be the MT isoform involved in metal detoxification. While it could have been assumed that the lack of MT induction detected in the low dose Ag treatments was the result of adequate macromolecules

containing the thiol-bearing amino acid cysteine in the body systems and therefore up-regulation was not necessary, the Cd exposure results ruled out this suggestion. Further MT isoform isolation research is needed to determine if there is any MT isoform involved in metal detoxification in the *A. caliginosa* earthworm. That in combination with positive heavy metal doses would reveal whether there is a MT induction in this species at low environmentally relevant AgNP doses. A study by Hayashi *et al.* (2013) indicated that MT isoforms are Ag sensitive and the highest of the MT inductions from their study were correlated with high Ag body burdens. The above research suggests that *A. caliginosa* will most likely have a MT isoform sensitive to Ag, which will be inducible at certain Ag concentrations, but considering the vast sequence diversity between species, identifying this isoform will require in-depth genetic analysis research.

In earthworms, the free circulating coelomocytes of the coelom cavity are the first line of immune defence (Hamed *et al.,* 2002) and are therefore useful indicators of exposure to environmental toxins. Coelomocytes both maintain bacteria balance and also detoxify soil pollutants (Olchawa *et al.,* 2006). Coelomocytes have been found to engulf and store Cd, before it is excreted (Stürzenbaum *et al.,* 2004). Hayashi *et al.* (2012) compared the immune response of *E. fetida* coelomocytes and *Homo sapien* THP-1 and differentiated THP-1 cells following in vitro exposure to AgNPs and Ag^{+}. Coelomocytes were shown to be sensitive to Ag^{+}, with a dose responsive effect on coelomocyte viability. Transmission electron microscopic (TEM) imaging for AgNP accumulation suggested that the amoebocytes were the predominant AgNP scavenger cells with the greatest AgNP accumulation (Hayashi *et al.,* 2012).

The ratio of amoebocytes to eleocytes was shown to increase in the earthworm *D. veneta* following exposure Cd, along with upregulated expression of MT in amoebocytes suggesting that these celltypes are involved in metal detoxification (Olchawa *et al.,* 2006). It has been

shown that the amoebocytes of the earthworm *L. rubellus* are involved in Cd trafficking but not the eleocytes (Morgan *et al.,* 2004). These studies prompted the examination of coelomocyte cell viablilty counts and differential cell counts in this work. The results of the coelomocyte experiments described in Chapter 5 suggested that there is a differential cell type effect. Amoebocytes increased over time and the granulocytes decreased over time. This balanced fluctuation over time is likely to account for the steady total viable cell counts over time. There was no significant effect on the eleocyte proportions across the treatments or the time points. There was a visible spike in eleocyte proportion on day 7 for the $AgNO_3$ treatment. This declined by day 14. However neither of these events were significantly different between the treatments. There were significant effects on amoebocyte proportions over time. Amoebocyte proportions were significantly higher on day 14 across all treatments. Granulocytes were significantly higher on day 2 across all treatments. The declining trend in proportion of granulocytes from day 2 to 14 occurred with all treatments except for a slight flux on day 7 for the $AgNO_3$ treatment. It was apparent that higher doses of AgNP and $AgNO_3$ would be required to fully investigate the differential cell type and gene expression effects further. At the environemntally relevant doses used in this work there was only one significant effect based on treatment measure, the elevated CAT expression in the treated sample (3 $mgkg^{-1}AgNO_3$, 0.3 $mgkg^{-1}$ AgNP and 30 $mgkg^{-1}$ AgNP) compared to the untreated (0$mgkg^{-1}$) samples at 2 d and 14 d time points. There were significant effects associated with time but as these were across all the treatments including the untreated controls, this effect could be due to the exposure in glass jars. The type of soil used in experiments and the characteristics of the NPs are also significant factors to consider when investigating AgNP biotoxicity.

As discussed previously, the dose is a key parameter in toxicological research. With regard to nano-toxicology, it is vital to evaluate both relevant and realistic doses in order to conclude

meaningful effects for both in-vitro and in-vivo risk assessments. Therefore nano-toxicologists should be studying real-world doses, rather than unrealistically high doses, to draw accurate conclusions of the biological response (Song *et al.,* 2009). This approach was applied in this work to collect a realistic view of the genetic oxidative stress response and the effects AgNPs pose to the immune cells in the earthworm *A. caliginosa.* While there is significant literature stating the potentially harmful effects AgNP soil pollution pose to earthworm species, the majority of these studies use relatively high and unrealistic doses of AgNP to achieve a detectable response. Current AgNP contamination in soil poses a greater threat to soil dwelling microorganism and indirect effects on the action of soil enzymes (Peyrot *et al.,* 2014). The potential consequences of AgNP contamination in soils of greatest concern is the interruption they may cause to numerous biochemical processes, especially the nutrient cycling pathways and other essential microbial mediated processes.

6.1 Conclusion

The results of this research suggest that the low environmentally relevant AgNP doses do not pose an immediate threat to the soil dwelling earthworm *A. caliginosa.* Both the gene expression studies and the coelomocyte studies did not provide significant evidence to suggest that low dose AgNP contamination in organic soil is a concern to the productivity and health of *A. caliginosa*. However, there are reports in the literature that low environmentally relevant AgNP doses are a threat to soil dwelling microorganisms and could inflict adverse effects on important nutrient cycles. To understand the potentially negative toxicological effects, environmentally relevant doses of AgNP need to be used, and a more sensitive bio-indicator species needs to be found, *A.caliginosa* earthworms were not

sensitive enough to produce a response to any of the parameters tested at the low and environmentally relevant AgNP concentrations used in this study.

6.2 Future research

Successfully identifying the MT isoform in the earthworm *A. caliginosa* involved in metal detoxification would be a useful biomarker gene for future research on the effects of heavy metal NPs on this earthworm species. Implementing flow cytometry for differential coelomocyte counts, with cell type specific ligands would provide a more robust method for coelomocyte analysis and counting of a larger volume of cells would give a more accurate assessment. To investigate the long term consequences of low dose AgNP pollution in soil, the attention should also be on the interactions with microbial species especially those relevant to nutrient cycles and microbial enzymes involved in biogeochemical processes. Research is also required to investigate the effects of different AgNPs in different soil types to assess the effects of NP type and soil type with regard to bioavailability.

Soil microorganisms contribute to soil health and function from both intracellular enzymes and through the released extracellular enzymes in the surrounding soil (Tabatabai *et al.,* 2002). Hence an understanding of these enzymes would be useful to identify the microbial diversity and identify the functionality of various metabolic pathways and biogeochemical pathways (Nannipieri *et al.,* 2002) where interactions with AgNPs may take place.

Each manufactured NP possesses key physical and chemical characteristics Identifying these characteristics for each NP will enable a better understanding of their environmental fate and their ecotoxicity. The size of the NP is a key physical characteristic to consider, along with NP shape. The chemical characteristics consist of capping/coating agent chemistry, the acid-base behaviour of the surface coating and its effect on aqueous solubility, aggregation chemistry, electrostatic force between AgNPs, the dissolution of metallic ions and chemical

transformations. The combination of all these characteristics determine the overall bioavailability and may explain the behaviour of NP transport into surface waters, ground waters, sedimentation of surface water and/or the deposition into soil (Simonet & Valcárcel, 2009). Identifying these is important.

Understanding the physiochemical movements of heavy metal NPs in soil is relatively complex. In a suspended dissolved phase, chemical interaction and NP stability can be determined largely from aggregation rates. However, in a solid soil matrix NPs may interact between soild soil particle phases and aqueous phases (Tourinho *et al.,* 2012). Studying the movement of NPs in soil matrices is complicated but is necessary. Specialised procedures are necessary to characterise the various NP phase chemistries (Hassellöv *et al.,* 2008). Charged components will attract or repel the charged surface of NPs which will affect their association with the solid phase in soil (Tourinho *et al.,* 2012).

Metal based NPs have been found to weakly adsorb in low ionic strength soils with high dissolved organic matter loads. This suggests the ionic status and dissolved organic matter content are parameters which will affect the bioavailability of metal based NP in soil (Gimbert *et al.,* 2007). Therefore, an understanding of the ionic status is necessary to fully appreciate bioavailability of AgNPs.

Furthermore, it is suggested NPs interact with toxic organic compounds present in certain soils. This interaction could either amplify or allievate the overall toxicity of the toxin. This NP-toxin interacteration could lead to greater toxicity of the NP. A NP enters into a biological system and is adsorbed to a toxic pollutant, it could act as a vector delivering the toxin to the inside of cells (Nowack & Bucheli, 2007). Therefore an understanding the soil matrix to which AgNPs are released is also important.

Appendix A

Calculations and Statistics

A.1 Field Capacity Results

Sample	Diameter	Depth	Volume	Tare	GW	GD	BD	Gravimetric Moisture	Volumetric Moisture
	(cm)	(cm)	(cm^3)	(g)	(g)	(g)	(g/cm3)	(%)	(%)
1	10.40	3.10	263.34	118.56	475.96	379.94	0.99	36.74	36.46
2	10.50	2.65	229.29	117.76	548.86	432.77	1.37	36.85	50.63
3	10.50	3.29	284.45	117.83	533.36	418.70	1.06	36.11	40.31

Table A. 1: Field Capacity Results

The Average of the gravimetric moisture % was used to calculate dose delivery.
(36.74 + 36.85 + 36.11)/3 = 36.6 %
Mass of exposure soil = 600 g Gravimetric moisture % vol. (mL) = 600 x 36.6%
= 219.6 mL

A.2 FAAS Ag standards Graph and Dose Calculations

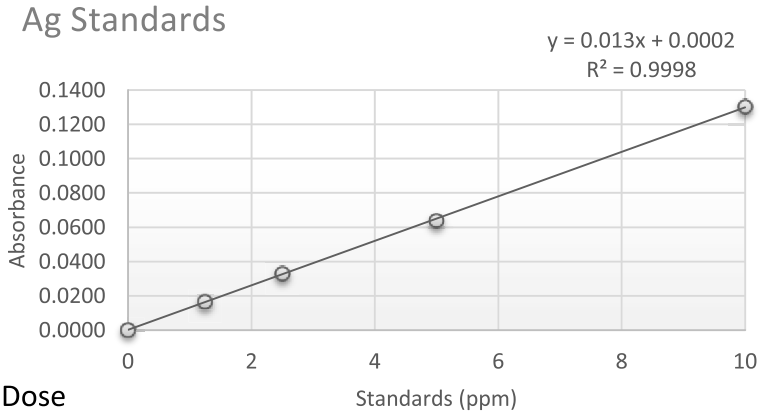

Standards(ppm)	Abs.
0	0.0002
1.25	0.0168
2.5	0.0331
5	0.0639
10	0.1304
Sample 1	0.1227
Sample 2	0.1294

Figure A. 1 FAAS Ag Standards

Dose Delivery Calculations:
219.6 mL x 4 (biological replicates) = 878.4 mL * 900mL prepared for each treatment.

$AgNO_3$ stock 1000 mgL^{-1}
$V_1 = \frac{3\ mgL^{-1} \times 900mL}{1000\ mgL^{-1}}$
= 2.7 mL $AgNO_3$ made up to 900 mL with deionised water

AgNP stock 13, 785 mgL^{-1}
$V_1 = \frac{30\ mgL^{-1} \times 900mL}{13,785\ mgL^{-1}}$
= 1.96 mL AgNP stock made up to 900 mL with deionised water

AgNP 30 mgL^{-1}
$V_1 = \frac{0.3\ mgL^{-1} \times 900mL}{30\ mgL^{-1}}$
= 9 mL AgNP 30 mgL^{-1} made up to 900 mL with deionised water

A.3 Statistical Analysis of Superoxide Dismutase (SOD)

Descriptive Statistics: SOD

Results for Time = 2

Variable	Treatment	Mean	SE Mean
SOD	0ppm	0.380	0.237
	AgNO3 3ppm	1.038	0.345
	AgNP 0.3ppm	1.002	0.335
	AgNP 30ppm	0.854	0.257

Results for Time = 7

Variable	Treatment	Mean	SE Mean
SOD	0ppm	1.312	0.471
	AgNO3 3ppm	0.866	0.161
	AgNP 0.3ppm	1.1333	0.0213
	AgNP 30ppm	2.097	0.662

Results for Time = 14

Variable	Treatment	Mean	SE Mean
SOD	0ppm	125	112
	AgNO3 3ppm	2238	2070
	AgNP 0.3ppm	500	386
	AgNP 30ppm	297	275

Analysis of variance

Variate: logSOD

Source of variation	d.f.	s.s.	m.s.	v.r.	F pr.
Treatment	3	5.2253	1.7418	2.79	0.054
Time	2	43.7897	21.8948	35.12	<.001
Treatment.Time	6	5.1823	0.8637	1.39	0.247
Residual	36	22.4412	0.6234		
Total	47	76.6385			

Least significant differences of means (5% level)

Table	Treatment	Time	Treatment Time
rep.	12	16	4
d.f.	36	36	36
l.s.d.	0.654	0.566	1.132

A.4 Statistical Analysis Catalase (CAT)

Descriptive Statistics: CAT

Results for Time = 2

Variable	Treatment	Mean	SE Mean
CAT	0ppm	0.549	0.268
	AgNO3 3ppm	1.821	0.783
	AgNP 0.3ppm	3.44	1.40
	AgNP 30ppm	1.877	0.418

Results for Time = 7

Variable	Treatment	Mean	SE Mean
CAT	0ppm	1.095	0.336
	AgNO3 3ppm	0.519	0.180
	AgNP 0.3ppm	1.093	0.716
	AgNP 30ppm	2.60	2.34

Results for Time = 14

Variable	Treatment	Mean	SE Mean
CAT	0ppm	0.387	0.322
	AgNO3 3ppm	2.467	0.322
	AgNP 0.3ppm	1.728	0.373
	AgNP 30ppm	0.872	0.190

Analysis of variance

Variate: logCAT

Source of variation	d.f.	s.s.	m.s.	v.r.	F pr.
Treatment	3	3.4186	1.1395	3.2	0.035
Time	2	0.5988	0.2994	0.84	0.44
Treatment.Time	6	4.5121	0.752	2.11	0.076
Residual	36	12.8337	0.3565		
Total	47	21.3632			

Least significant differences of means (5% level)

Table	Treatment	Time	Treatment Time
rep.	12	16	4
d.f.	36	36	36
l.s.d.	0.4944	0.4281	0.8562

A.5 Differential Cell Count Statistical Analysis

Analysis of variance

Variate: Amoebocyte_%

Source of variation	d.f.	s.s.	m.s.	v.r.	F pr.
Treatment	3	69.1	23	0.23	0.876
Time	2	926	463	4.6	0.017
Treatment.Time	6	531.2	88.5	0.88	0.52
Residual	36	3626.6	100.7		
Total	47	5153			

Tables of means

Variate: Amoebocyte_%

Grand mean 65.6

Treatment	0ppm	AgNO3 3ppm	AgNP 0.3ppm	AgNP 30ppm
	64.4	64.8	65.6	67.5

Time	2	7	14
	61.7	63.3	71.7

Time Treatment	0ppm	AgNO3 3ppm	AgNP 0.3ppm	AgNP 30ppm
2	60	59.4	60	67.5
7	68.1	61.9	63.8	59.4
14	65	73.1	73.1	75.6

Least significant differences of means (5% level)

Table	Treatment	Time	Treatment Time
rep.	12	16	4
d.f.	36	36	36
l.s.d.	8.31	7.2	14.39

Analysis of variance

Variate: Eleocytes_%

Source of variation	d.f.	s.s.	m.s.	v.r.	F pr.
Treatment	3	101.43	33.81	0.69	0.563
Time	2	47.66	23.83	0.49	0.618
Treatment.Time	6	241.93	40.32	0.82	0.559
Residual	36	1760.94	48.91		
Total	47	2151.95			

Tables of means

Variate: Eleocytes_%

Grand mean 10.8

Treatment	0ppm	AgNO3 3ppm	AgNP 0.3ppm	AgNP 30ppm
	11.5	12.5	10.6	8.5

Time	2	7	14
	10	12.2	10.2

Treatment	Time	2	7	14
0ppm		11.9	10	12.5
AgNO3 3ppm		11.9	18.1	7.5
AgNP 0.3ppm		10	10	11.9
AgNP 30ppm		6.2	10.6	8.8

Least significant differences of means (5% level)

Table	Treatment	Time	Treatment Time
rep.	12	16	4
d.f.	36	36	36
l.s.d.	5.79	5.01	10.03

Analysis of variance

Variate: Granulocyte_%

Source of variation	d.f.	s.s.	m.s.	v.r.	F pr.
Treatment	3	15.1	5.03	0.08	0.971
Time	2	844.01	422.01	6.61	0.004
Treatment.Time	6	402.86	67.14	1.05	0.41
Residual	36	2300	63.89		
Total	47	3561.98			

Tables of means

Variate: Granulocyte_%

Grand mean 23.6

Treatment	0ppm	AgNO3 3ppm	AgNP 0.3ppm	AgNP 30ppm
	24.2	22.7	23.8	24

Time	2	7	14
	28.3	24.5	18.1

Treatment	Time	2	7	14
0ppm		28.1	21.9	22.5
AgNO3 3ppm		28.8	20	19.4
AgNP 0.3ppm		30	26.2	15
AgNP 30ppm		26.2	30	15.6

Least significant differences of means (5% level)

Table	Treatment	Time	Treatment Time
rep.	12	16	4
d.f.	36	36	36
l.s.d.	6.62	5.73	11.46

A.6 Viable Cell Count Statistical Analysis

Analysis of variance

Variate: Viable_cells_per_mL_x10_6

Source of variation	d.f.	s.s.	m.s.	v.r.	F pr.
Treatment	3	24.9	8.3	0.06	0.98
Time	2	400.2	200.1	1.47	0.244
Treatment.Time	6	1341.8	223.6	1.64	0.165
Residual	36	4915	136.5		
Total	47	6681.9			

Tables of means

Variate: Viable_cells_per_mL_x10_6

Grand mean 43.5

Treatment	0ppm	AgNO3 3ppm	AgNP 0.3ppm	AgNP 30ppm
	44.7	43.5	42.7	43.3

Time	2	7	14
	39.8	44.1	46.8

Treatment	Time	2	7	14
0ppm		35.5	43	55.5
AgNO3 3ppm		38	46.5	46
AgNP 0.3ppm		38	51	39
AgNP 30ppm		47.5	36	46.5

Least significant differences of means (5% level)

Table	Treatment	Time	Treatment Time
rep.	12	16	4
d.f.	36	36	36
l.s.d.	9.67	8.38	16.76

Appendix B

Primer Design, Alignments and Sequences

B.1 Lumbricidae CAT mRNA Alignment and Primer Sites

```
EU407496.1      GCTTCCGTAACATGAACGGCTACGGCAGCCACACGTACAAGATGGTGAACGCTGCTGGCG
EU407494.1      GACATCGTCACATGGACGGATTCGGAAGCCACACATTCAAGTTGGTGAACGCCGAAGGAA
JQ782655.1      ----------------------------CACACGTACAAGATGGTGAACGATAAAGGAG
DQ286713        GATATCGTCATATGAATGGATACAGCAGTCACACCTACAAACTGGTGAACGCCGACGGAG
                                            ***** * ***  *********     **

EU407496.1      AGGCAGTCTACGTCAAGTTTCACTTCAAGACAAACCAGGGCATCAAGAACTTGTCTCGTA
EU407494.1      AGGCTGTGTACTGCAAATTCCACCACAAGACCAACCAAGGCCTTAAGAATTTGTCGGCTT
JQ782655.1      AACCTGTCTACTGCAAATTTCATCACAAGACCGACCAAGGCATCAAGAATTTGACGGCTG
DQ286713        AAGCTGTGTACTGCAAGTTCCATCACAAGACCAACCAAGGCATTAAGAATTTGACGGGTG
                *  * ** ***  *** ** **   ******  **** *** * ***** *** *   *

EU407496.1      AGCAAGCCGAGGAGCTCGCTGGGTCTGACCCGGACTATGCGTGTCGTGACCTGTACGAGT
EU407494.1      CTGAAGCCAATAGACTGGCCAGCGTTGACCCAGACTATTCCACTCGTGACCTTTACAATG
JQ782655.1      CCGAGGCTGACGCGCTTATCGTTCCTGACCCAGACTATGCGACACGTGACCTTTACAATG
DQ286713        CTGAGGCCGATCGACTGCTCGGTGTTGACCCAGACTATGCGACCCGTGACCTTTACAATG
                   * **  *    **         ****** ****** *    ******** *** *

EU407496.1      CCATCGCCAGCGGCAACTACCCTTCCTGGACTTTCTACATTCAAGTCATGACATTTGCTG
EU407494.1      CCATCGCTAATGGCAACTACCCGTCATGGACCACCTACATCCAGGTTATGACGTTCCAGG
JQ782655.1      CCATTGAGAATGGAAACTTCCCTTCGTGGACCACCCACATCCAGGTGATGACGTTCGAGG
DQ286713        CCATTGCGGATGGAAACTACCCTTCGTGGACCACCTACATCCAAGTGATGACGTTTGCGG
                **** *     ** **** *** ** *****   * **** ** ** ***** **    *

EU407496.1      AGGCCGAGCGCTTCCGCTGGAATCCATTCGACCTGACCAAGATTTGGCCTCATGCTGAGT
EU407494.1      AAGCGGAAAATTTCCGCTGGAATCCATTTGATTTGACAAAGATCTGGCCACTTAACGAAT
JQ782655.1      AAGCGGAAACGTTCCGCTGGAATCCATTCGA----------------------------
DQ286713        AAGCGGAAAGATTCCGCTTTAATCCATTTGACTTGACAAAGATCTGGCCACAGGCAGAAT
                * ** **    *******  ******** **

EU407496.1      ACCCGTTGATTCCGGTCGGTCGCTTCACTCTGAACCGCAACCCGAAGAATTTCTTCGCCG
EU407494.1      ATCCTTTGATTCCGGTTGGACGCTTTGTTCTCAATCGTAATCCAAGGAACTTCTTCGCCG
JQ782655.1      ------------------------------------------------------------
DQ286713        ATCCTCTGATTCCAGTGGGACGCTTTACTCTCAATCGTAATCCGAAGAACTACTTCGCCG


EU407496.1      AGGTGGAGCAGATCA
EU407494.1      AGGTGGAGCAGATCA
JQ782655.1      ---------------
DQ286713        AGGTGGAGCAGATCA
```

The yellow regions represent the CAT primer sites (CAT_caliginosa For: 5'- GGC CTT AAG AAT TTG TCG GC -3', CAT_caliginosa Rev: 5'- TCG AAT GGA TTC GAG CGG -3').

B.2 SOD Primer Locations in Lumbricidae SOD Alignment

```
DQ286712.1      ACAAGTGCAGGTGCTCACTTCAACCCATTTGGAAAGACTCATGGAGCTCCAGAAGATCAG
EU407497.1      ACAAGTGCAGGTGCTCACTTCAACCCATTCGGATTGACTCATGGAGCTCCTGAAGATAGG
EU407495.1      ACAAGTGCAGGTGCTCACTTCAACCCATTCGGATTGACTCATGGAGCTCCTGAAGATAGG
                **************************** ***  *************** ******  *

DQ286712.1      GAGAGGCATGTTGGGGATCTTGGTAATGTCATAGCTGATGAAAGTGGTGTTGCCAAGTTT
EU407497.1      GAGAGGCATGTTGGAGATCTTGGCAATGTGGTCGCTGATGAAAGTGGTGTTGCCAAGTTT
EU407495.1      GAGAGGCATGTTGGAGATCTTGGCAATGTGGTCGCTGACGAAAGTGGTGTTGCCAAGTTT
                ************** ******** *****  * ***** ********************

DQ286712.1      GAAGTGACGGATAAACTTCTGAACTTGACCGGGCCGAATTCAATCATTGGACGCACGGTG
EU407497.1      GAATTGACAGATAAACTTATCAATTTGACTGGACCAAACTCGATCATTGGACGTACAGTG
EU407495.1      GAACTGACGGACAAACTTCTCAATTTGACCGGACCAAACTCGATCATTGGACGTACAGTG
                *** **** ** ****** * ** ***** ** ** ** ** *********** ** ***

DQ286712.1      GTGGTACATGAGCTGGTGGACGATCTTGGCAAAGGTGGTCATGAGTTCAGCAAGACCACT
EU407497.1      GTGGTACATGAGCTGGTGGATGATCTTGGCAAGGGTGGTCACGAGTTTAGCAAGACCACG
EU407495.1      GTGGTACATGAGCTGGTGGATGATCTCGGCAAAGGTGGTCACGAGTTCAGCGAGACCACG
                ******************** ***** ***** ******** ***** *** *******
```

The yellow regions represent the SOD primers obtained from Y.Zhan, (2012)

(SOD_caliginosa For: 5'- GTG CTC ACT TCA ACC CAT T -3', SOD_caliginosa Rev: 5'- AGA TCR CCA CCA GCT CAT GT -3').

B.3 Lumbricidae MT Isoform Alignment and MT_Ann Primer Sites

```
AJ005822.1      GGATCAACATGTGCCTGCTCCAAATGCAGGTGTCCGAAAGATGACTGCGCGCCAAACTGC
AJ010263.1      GGGTCAACATGTGCCTGCTCCAAATGCAGGTGTCCAAAAGATGACTGCTTGCCAAACTGC
AJ236886.1      GGATCAACTTGTTGCTGCACAAACTGCAGATGTTTGAAAAGTGAGTGCTTGCCGGGCTGC
HM014116.1      ------ACCTGCTGCTGCACCAAATGCAGGTGTTTGAAAACTGAATGCCCACCAAACTGC
AJ005823.1      GGAGCTGCGTGTGCTTGCACCAACTGCAGATGCCTGAAAAGTGAATGTTCGCCAAACTGC
AJ010264.1      GGAGCTGCGTGTGCTTGCACCAACTGCAGATGCCTGAAAAGTGAATGTTCGCCAAACTAC
                       * **    *** * ** ***** **    ***  *** **    **   ** *

AJ005822.1      AAGAAGCTTTGCTGTGCTGATG---------CACAATGTGGAAATGCAAGCTGCAGTTGC
AJ010263.1      AAGAAGCTTTGCTGTGCTGATG---------CACAATGTGGAAATGCAGGCTGCAGTTGC
AJ236886.1      AAAAAGCTTTGCTGTGCTGACGCTGAGAAGGGCAAATGTGGAAATGCAGGCTGCAAGTGC
HM014116.1      AAAAAGAATTGCTGTGCTGATG---CCCAAGGAAAATGTGGAAATGCAAGCTGCAAGTGT
AJ005823.1      AGGAAGCTTTGCTGTGCTGATT---CCCAAGGAAAATGTGGAAATGCAGGCTGCAAGTGC
AJ010264.1      AGGAAGCTTTGCTGTGCTGATT---CCCAAGGAAAATGTGGAAATGCAGGCTGCAAGTGC
                *  ***  ************             ************** ******  **

AJ005822.1      GGGGCTGCATGCAAGTGCGCAGCTGGTTCATGCGCCTCAGGATGCAAGAAAGGATGCTGT
AJ010263.1      GGGGCTGCATGCAAGTGCGCAGCTGGTTCGTGCGCCTCAGGATGCAAGAAGGGATGCTGT
AJ236886.1      GGAGCTGCCTGCAAATGCTCGGCTGGTTCGTGCGCCGCAGGATGCAAGAAGGGGTGCTGT
HM014116.1      GGGGCTAGCTGTAAGTGTGCAGCTGGTTCGTGTGCCGCAGGATGTAAAAAAGGCTGCTGC
AJ005823.1      GGTGCTGCCTGCAAATGTGCCGCTGGTGCATGTGCCTCTGGATGCAAGAAAGGATGCTGT
AJ010264.1      GGTGCTGCCTGCAAATGTGCCGCTGGTGCATGTGCCTCTGGATGCAAGAAGGGATGCTGT
                ** ***   ** ** **  * ****** * ** *** * ***** ** ** ** *****
```

The yellow regions represent the degenerate MT primers designed (MT_Ann For: 5'- AAG SWT TGC TGT GST GRH RC -3', MT_Ann Rev: 5'- ACR YKC TTY CCY ACG ACA C -3').

B.4 Lumbricidae and *Mytilus* species MT Protein Sequences

```
CAA06548.1|              --MPAPCNCIETNVCIC-DTGCSGEGCRCG-DACKCSGADCKCSGCK-VVCKCSGRCECG 55
P80246.2|MT10A_MYTED     --MPAPCNCIETNVCIC-DTGCSGEGCRCG-DACKCSGADCKCSGCK-VVCKCSGRCECG 55
CAA06549.1|              --MPAPCNCIETNVCIC-DTGCSGEGCRCG-DACKCAGADCKCSGCK-VVCKCSGRCECG 55
O62554.3|MT10B_MYTED     --MPAPCNCIETNVCIC-DTGCSGEGCRCG-DACKCAGADCKCSGCK-VVCKCSGRCECG 55
CAA06550.1|              --MPAPCNCIETNVCIC-DTGCSGDGCRCG-DACKCSGADCKCSGCK-VVCKCSGSCECG 55
P80247.3|MT12_MYTED      --MPAPCNCIETNVCIC-DTGCSGDGCRCG-DACKCSGADCKCSGCK-VVCKCSGSCECG 55
CAA06551.1|              --MPAPCNCIESNVCIC-GTGCSGEGCRCG-DACKCSGADCKCSGCK-VVCKCSGSCACE 55
P80248.2|MT13_MYTED      --MPAPCNCIESNVCIC-GTGCSGEGCRCG-DACKCSGADCKCSGCK-VVCKCSGSCACE 55
CAA07546.1|              --MPAPCNCIETNVCIC-DTGCSGEGCRCG-DACKCSGADCKCSGCK-VVCKCSGSCACE 55
P80249.2|MT14_MYTED      --MPAPCNCIETNVCIC-DTGCSGEGCRCG-DACKCSGADCKCSGCK-VVCKCSGSCACE 55
CAA06553.1|              --MPGPCNCIETNVCIC-GTGCSGKCCRCG-DACKCASG-CGCSGCK-VVCKCSGTCACG 54
P80252.2|MT22_MYTED      --MPGPCNCIETNVCIC-GTGCSGKCCRCG-DACKCASG-CGCSGCK-VVCKCSGTCACG 54
P69154.2|MT23A_MYTGA     --MPGPCNCIETNVCIC-GTGCSGKCCQCG-DACKCASG-CGCSGCK-VVCRCSGTCACG 54
P80258.1|MT23B_MYTED     ---PGPCNCIETNVCIC-GTGCSGKCCQCG-DACKCASG-CGCSGCK-VVCRCSGTCACG 53
CAA06720.1|              MADASNTQCCGFDACPRRGAACACTNCRCLKSECSPNCRKLCCADSQ-GKCGNAG-CKCG 58
CAA09057.1|              ------TQCCGFDACPRRGAACACTNCRCLKSECSPNYRKLCCADSQ-GKCGNAG-CKCG 52
ADK62365.1|              --------------------TCCCTKCRCLKTECPPNCKKNCCADAQ-GKCGNAS-CKCG 38
P81695.1|                -----DTQCCGKSTCAREGSTCCCTNCRCLKSECLPGCKKLCCADAEKGKCGNAG-CKCG 54
CAC14313.1|              MADAFNTQCCGNKTCPREGSACACSKCRCPKDDCAPNCKKLCCADAQ---CGNAG-CSCG 56
CAC14312.1|              MADAFNTQCCGNKTCPREGSACACSKCRCPKDDCAPNCKKLCCADAQ---CGNAG-CSCG 56
CAA06719.1|              MADAFNTQCCGNKTCPREGSTCACSKCRCPKDDCAPNCKKLCCADAQ---CGNAS-CSCG 56
CAA09056.1|              ------TQCCGNKTCPREGSTCACSKCRCPKDDCLPNCKKLCCADAQ---CGNAG-CSCG 50
CAC14314.1|              MADALNTQCCGNKTCPREGSTCACSKCRCPKDDCLPNCKKLCCADAQ---CGNAG-CSCG 56
ADW27175.1|              ------------------GSTCACSKCRCPKDDCLPNCKKLCCADAQ---CGDAG-CSCG 38
                                             *.   *:*    *        *:..:   *  :. * *

CAA06548.1|              KGCTGPS-TCK--CAPGCSCK 73
P80246.2|MT10A_MYTED     KGCTGPS-TCK--CAPGCSCK 73
CAA06549.1|              KGCTGPS-TCK--CAPGCSCK 73
O62554.3|MT10B_MYTED     KGCTGPS-TCK--CAPGCSCK 73
CAA06550.1|              KGCTGPS-TCK--CAPGCSCK 73
P80247.3|MT12_MYTED      KGCTGPS-TCK--CAPGCSCK 73
CAA06551.1|              AGCTGPS-TCR--CAPGCSCK 73
P80248.2|MT13_MYTED      AGCTGPS-TCR--CAPGCSCK 73
CAA07546.1|              GGCTGPS-TCK--CAPGCSCK 73
P80249.2|MT14_MYTED      GGCTGPS-TCK--CAPGCSCK 73
CAA06553.1|              CDCTGPT-NCK--CESGCSCK 72
P80252.2|MT22_MYTED      CDCTGPT-NCK--CESGCSCK 72
P69154.2|MT23A_MYTGA     CDCTGPI-NCK--CESGCSCK 72
P80258.1|MT23B_MYTED     CDCTGPT-NCK--CDSGCSCK 71
CAA06720.1|              AACKCAAGACASGCKKGCCGD 79
CAA09057.1|              AACKCAAGACASGCKKGCCGD 73
ADK62365.1|              ASCKCAAGSCAAGCKKGCCG- 58
P81695.1|                AACKCSAGSCAAGCKKGCCGD 75
CAC14313.1|              AACKCAAGSCASGCKKGCCGD 77
CAC14312.1|              AACKCAAGSCASGCKKGCCGD 77
CAA06719.1|              AACKCAAGSCASGCKKGCCGD 77
CAA09056.1|              AACKCAAGSCASGCKKGCCGD 71
CAC14314.1|              AACKCAAGSCASGCKKGCCAD 77
ADW27175.1|              AAFKCAAGSCASGCKKGWCG- 58
                            . .   *   *  * .
```

Alignment showing no conservation shared between Lumbricidae and *Mytilus* species MT protein sequences.

B.5 Lumbricidae MT Protein Sequences

```
CAA09056.1|      ------TQCCGNKTCPREGSTCACSKCRCPKDDCLPNCKKLCCADAQ---CGNAGCSCGA 51
CAC14314.1|      MADALNTQCCGNKTCPREGSTCACSKCRCPKDDCLPNCKKLCCADAQ---CGNAGCSCGA 57
CAC14313.1|      MADAFNTQCCGNKTCPREGSACACSKCRCPKDDCAPNCKKLCCADAQ---CGNAGCSCGA 57
CAC14312.1|      MADAFNTQCCGNKTCPREGSACACSKCRCPKDDCAPNCKKLCCADAQ---CGNAGCSCGA 57
CAA06719.1|      MADAFNTQCCGNKTCPREGSTCACSKCRCPKDDCAPNCKKLCCADAQ---CGNASCSCGA 57
ADW27175.1|      ------------------GSTCACSKCRCPKDDCLPNCKKLCCADAQ---CGDAGCSCGA 39
CAA06720.1|      MADASNTQCCGFDACPRRGAACACTNCRCLKSECSPNCRKLCCADSQ-GKCGNAGCKCGA 59
CAA09057.1|      ------TQCCGFDACPRRGAACACTNCRCLKSECSPNYRKLCCADSQ-GKCGNAGCKCGA 53
ADK62365.1|      --------------------TCCCTKCRCLKTECPPNCKKNCCADAQ-GKCGNASCKCGA 39
P81695.1|        -----DTQCCGKSTCAREGSTCCCTNCRCLKSECLPGCKKLCCADAEKGKCGNAGCKCGA 55
                                     :*.*::*** * :* *. :* ****::   **:*.*.***

CAA09056.1|      ACKCAAGSCASGCKKGCCGD 71
CAC14314.1|      ACKCAAGSCASGCKKGCCAD 77
CAC14313.1|      ACKCAAGSCASGCKKGCCGD 77
CAC14312.1|      ACKCAAGSCASGCKKGCCGD 77
CAA06719.1|      ACKCAAGSCASGCKKGCCGD 77
ADW27175.1|      AFKCAAGSCASGCKKGWCG- 58
CAA06720.1|      ACKCAAGACASGCKKGCCGD 79
CAA09057.1|      ACKCAAGACASGCKKGCCGD 73
ADK62365.1|      SCKCAAGSCAAGCKKGCCG- 58
P81695.1|        ACKCSAGSCAAGCKKGCCGD 75
                 : **:**:**:***** *.
```

The blue regions represent the CW MT primers designed (MT.CW1 For: 5'- TGC TCC AAA TGC AGG TGC -3', MT.CW2 For: 5'- TGC TCA AAA TGC AGG TGT -3', MT.CW1 Rev: 5'- AGT CAC CAC AGC ATC CT -3'). The highlighted yellow regions represent the *E. fetida* qPCR primers (E.fetida_MT For: 5'- TCG CAA GAG AGG GAT CAA CT -3', E.fetida_MT Rev: 5'- CAT TTC CAC ATT TGC CCT TC -3') which amplified a MT product in *A. caliginosa.*

B.6 CW.MT Primer Alignments

```
CLUSTAL 2.1 multiple sequence alignment

rubellus2B          CSKCRC 6
rubellus2C          CSKCRC 6
rubellus2A          CSKCRC 6
rubellus.iso2       CSKCRC 6
terrestris          CSKCRC 6
fetida              CTNCRC 6
rubellus            CTNCRC 6
                    *::***
```

```
CLUSTAL 2.1 multiple sequence alignment

rubellus.iso2       TGCTCCAAATGCAGGTGT 18
rubellus2A          TGCTCCAAATGCAGGTGT 18
terrestris          TGCTCCAAATGCAGGTGT 18
rubellus2C          TGCTCAAAATGCAGGTGT 18
rubellus2B          TGCTCCAAATGCAGGTGC 18
fetida              TGCACAAACTGCAGATGT 18
rubellus            TGCACCAACTGCAGATGC 18
                    ***:*.**.*****.**
```

```
CLUSTAL 2.1 multiple sequence alignment

terrestris          KGCCGD 6
fetida              KGCCGD 6
rubellus            KGCCGD 6
rubellus.iso2       KGCCGD 6
rubellus2A          KGCCGD 6
rubellus2B          KGCCGD 6
rubellus2C          KGCCAD 6
                    ****.*
```

```
CLUSTAL 2.1 multiple sequence alignment

rubellus2B          AAGGGATGCTGTGGTGAC 18
rubellus2C          AAGGGATGCTGTGCTGAC 18
rubellus            AAAGGATGCTGTGGTGAC 18
rubellus.iso2       AAAGGATGCTGTGGTGAC 18
rubellus2A          AAAGGATGCTGTGGTGAC 18
terrestris          AAGGGATGCTGTGGTGAC 18
fetida              AAGGGGTGCTGTGGTGAC 18
                    **.**.******* ****
```

B.7 *Mytilus edulis* MT Protein Sequences

```
CAA06550.1|              MPAPCNCIETNVCICDTGCSGDGCRCGDACKCSGADCKCSGCKVVCKCSGSCECGKGCTG 60
P80247.3|MT12_MYTED      MPAPCNCIETNVCICDTGCSGDGCRCGDACKCSGADCKCSGCKVVCKCSGSCECGKGCTG 60
CAA06548.1|              MPAPCNCIETNVCICDTGCSGEGCRCGDACKCSGADCKCSGCKVVCKCSGRCECGKGCTG 60
P80246.2|MT10A_MYTED     MPAPCNCIETNVCICDTGCSGEGCRCGDACKCSGADCKCSGCKVVCKCSGRCECGKGCTG 60
CAA06549.1|              MPAPCNCIETNVCICDTGCSGEGCRCGDACKCAGADCKCSGCKVVCKCSGRCECGKGCTG 60
O62554.3|MT10B_MYTED     MPAPCNCIETNVCICDTGCSGEGCRCGDACKCAGADCKCSGCKVVCKCSGRCECGKGCTG 60
CAA06551.1|              MPAPCNCIESNVCICGTGCSGEGCRCGDACKCSGADCKCSGCKVVCKCSGSCACEAGCTG 60
P80248.2|MT13_MYTED      MPAPCNCIESNVCICGTGCSGEGCRCGDACKCSGADCKCSGCKVVCKCSGSCACEAGCTG 60
CAA07546.1|              MPAPCNCIETNVCICDTGCSGEGCRCGDACKCSGADCKCSGCKVVCKCSGSCACEGGCTG 60
P80249.2|MT14_MYTED      MPAPCNCIETNVCICDTGCSGEGCRCGDACKCSGADCKCSGCKVVCKCSGSCACEGGCTG 60
CAA06553.1|              MPGPCNCIETNVCICGTGCSGKCCRCGDACKCASG-CGCSGCKVVCKCSGTCACGCDCTG 59
P80252.2|MT22_MYTED      MPGPCNCIETNVCICGTGCSGKCCRCGDACKCASG-CGCSGCKVVCKCSGTCACGCDCTG 59
P69154.2|MT23A_MYTGA     MPGPCNCIETNVCICGTGCSGKCCQCGDACKCASG-CGCSGCKVVCRCSGTCACGCDCTG 59
P80258.1|MT23B_MYTED     -PGPCNCIETNVCICGTGCSGKCCQCGDACKCASG-CGCSGCKVVCRCSGTCACGCDCTG 58
                          *.******:*****.*****. *:*******:.. * ********:*** * *  .***

CAA06550.1|              PSTCKCAPGCSCK 73
P80247.3|MT12_MYTED      PSTCKCAPGCSCK 73
CAA06548.1|              PSTCKCAPGCSCK 73
P80246.2|MT10A_MYTED     PSTCKCAPGCSCK 73
CAA06549.1|              PSTCKCAPGCSCK 73
O62554.3|MT10B_MYTED     PSTCKCAPGCSCK 73
CAA06551.1|              PSTCRCAPGCSCK 73
P80248.2|MT13_MYTED      PSTCRCAPGCSCK 73
CAA07546.1|              PSTCKCAPGCSCK 73
P80249.2|MT14_MYTED      PSTCKCAPGCSCK 73
CAA06553.1|              PTNCKCESGCSCK 72
P80252.2|MT22_MYTED      PTNCKCESGCSCK 72
P69154.2|MT23A_MYTGA     PINCKCESGCSCK 72
P80258.1|MT23B_MYTED     PTNCKCDSGCSCK 71
                         * .*:* .*****
```

The yellow regions represent the regions used to design the *M. edulis* primers trialled on *A. caliginosa* for MT amplification.

B.8 *Mytilus edulis* MT mRNA alignment and Primer Sites

```
AJ005456.1      GATCTACTAAGCAGACCAGCTTTAACGAATAAAATGCCTGGACCTTGTAACTGCATTGAA
AJ005454.1      -------------------------ATTAAAAATGCCTGCACCTTGTAACTGTATCGAA
AJ007506.1      TACTACGACCACTGAGACCACTACGAATTAAACATGCCTGCACCTTGTAACTGTATCGAA
AJ005451.1      ------GACCACTGAGACCACTACAAATTAAACATGCCTGCACCTTGTAACTGTATCGAA
AJ005453.1      ------GACCACTGAGACCACTACAAATTAAACATGCCTGCACCTTGTAACTGTATCGAA
AJ005452.1      ------GACCACTGAGACCACTACAAATTAAACATGCCTGCACCTTGTAACTGTATCGAA
                                          ** ******* ********** ** ***

AJ005456.1      ACAAACGTGTGTATCTGTGGTACCGGATGCAGCGGGAAATGTTGTCGATGTGGAGACGCG
AJ005454.1      TCAAATGTGTGTATCTGTGGCACTGGGTGTAGCGGTGAAGGTTGTCGCTGTGGTGACGCC
AJ007506.1      ACAAATGTGTGTATATGTGACACTGGCTGCAGCGGTGAAGGTTGTCGCTGTGGTGACGCC
AJ005451.1      ACAAATGTGTGTATCTGTGACACTGGGTGCAGCGGTGAAGGTTGTCGCTGTGGTGACGCC
AJ005453.1      ACAAATGTGTGTATCTGTGACACTGGCTGCAGCGGTGACGGTTGTCGCTGTGGTGACGCC
AJ005452.1      ACAAATGTGTGTATCTGTGACACTGGCTGCAGCGGTGAAGGTTGTCGCTGTGGTGACGCC
                 **** ******** ****  ** ** ** *****  *  ******* ***** *****

AJ005456.1      TGCAAATGTGC---AAGTGGCTGTGGATGTTCCGGATGTAAAGTTGTTTGCAAATGTTCA
AJ005454.1      TGCAAGTGCTCGGGCGCCGACTGTAAATGTTCCGGTTGTAAAGTAGTTTGCAAGTGTTCA
AJ007506.1      TGCAAGTGCTCGGGCGCTGACTGTAAATGTTCTGGTTGTAAAGTAGTTTGCAAGTGTTCA
AJ005451.1      TGCAAGTGCTCGGGCGCTGACTGTAAATGTTCGGGTTGTAAAGTAGTTTGCAAGTGTTCA
AJ005453.1      TGCAAGTGCTCGGGCGCTGACTGTAAATGTTCTGGTTGTAAAGTAGTTTGCAAGTGTTCA
AJ005452.1      TGCAAGTGCGCGGGCGCTGACTGTAAATGTTCTGGTTGTAAAGTAGTTTGCAAGTGTTCA
                ***** **  *       * ****  ****** ** ******** ******** ******

AJ005456.1      GGTACATGTGCGTGTGGATGTGACTGCACTGGTCCGACAAACTGCAAATGTGAATCTGGA
AJ005454.1      GGTAGCTGTGCGTGTGAAGCAGGATGTACAGGACCTTCAACGTGTAGATGTGCACCTGGT
AJ007506.1      GGTAGCTGTGCGTGTGAAGGAGGATGTACAGGACCTTCAACGTGTAAATGTGCACCTGGC
AJ005451.1      GGTAGATGTGAGTGTGGCAAAGGATGTACAGGACCTTCAACGTGTAAATGTGCACCTGGC
AJ005453.1      GGTAGCTGTGAGTGTGGCAAAGGATGTACAGGACCTTCAACGTGTAAATGTGCACCTGGC
AJ005452.1      GGTCGCTGTGAGTGTGGCAAAGGATGTACAGGACCTTCAACGTGTAAATGTGCACCTGGC
                ***   **** *****     *  ** ** ** ** **  ***  ** * ***** * ****

AJ005456.1      TGCTCCTGCAAGTGACATAAAGCGAATCACATCACGTTCAATATAGTCATACTTGTAACT
AJ005454.1      TGCTCCTGCAAATGAATCAAAAAGACAATATACTCGAACTTATTCC---------------
AJ007506.1      TGTTCCTGCAAGTGAATCAAAAAGACAATATACTCGAACTTATTCC---------------
AJ005451.1      TGTTCCTGCAAGTGAATCAAAAAGACAATATACTCGAACTTATTCC---------------
AJ005453.1      TGTTCCTGCAAGTGAATCAAAAAGACAATATACTCGAACTTATTCC---------------
AJ005452.1      TGTTCCTGCAAGTGAATCAAAAAGACAATATACTCGAACTTATTCC---------------
                ** ******** ***   ***  **       * **  *    *
```

B.9 E. fetida MT qPCR Primers in E.fetida MT mRNA Sequence

GenBank: DQ286714.1

TCGCAAGAGAGGGATCAACTTGTTGCTGCACAAACTGCAGATGTTTGAAAAGTGAGTGCTTGCCAG
GCTGCAAAAAGCTTTGCTGTGCTGACGCTGAGAAGGGCAAATGTGGAAATGCAGGCTGCAAGTGCG
GGGCTGCCTGCAAATGCTCGGCCGGTTCGTGCGCTGCGGGATGCAAGAAGGGGTGCTGTGGTGACT
AG

B.10 Sequenced Templates and qPCR Primer sites

CATq Primers and CAT qPCR amplicon inside CAT template.

CACACGTACAAGATGGTGAACGATAAAGGAGAACCTGTCTACTGCAAATTTCATCACAAGACCGACCAAGGCA
TCAAGAATTTGACGGCTGCCGAGGCTGACGCGCTTATCGTTCCTGACCCAGACTATGCGACACGTGACCTTTAC
AATGCCATTGAGAATGGAAACTTCCCTTCGTGGACCACCCACATCCAGGTGATGACGTTCGAGGAAGCGGAAA
CGTTCCGCTGGAATCCATTCGA

ACTq Primers and ACT qPCR amplicon inside ACT template.

TTCGAGACCTTCAACTCCCCGGCCATGTATGTCGCCATCCAGGCCGTCCTCTCCCTGTACGCGTCCGGTCGTACC
ACCGGTATCGTGCTGGACTCCGGCGATGGTGTCACCCACACCGTCCCCATCTATGAGGGTTACGCCCTGCCCCA
TGCCATCCTTCGTCTCGACTTGGCCGGCAGAGATCTCACCGATTACCTGATGAAGATCCTGACGGAAAGAGGT
TACAGTTTCACCACCACGGCCGAGCGTGAAATCGTTCGTGACATCAAGGAGAAGCTGTGCTACGTCGCTCTGG
ACTTCGACCAGGAGATGGGAACGGCTGCCTCCTCCTCCTCCCTCGAGAAGAGCTACGAGCTTCCCGACGGTCA
GGTCATCACCATCGGAAACGAGCGCTTCCGTTGCCCAGAGTCCATGTTCCAGCCAGCCTTCCTGGGTATGGAG
TCGGCCGGTATCCATGAGACGACCTTCAACAGCATCATGAAGTGCGATGTCGATATCCGTAAGGATCTGTACG
CCAACACCGTCATGTCCGGAGGCACGACCATGTTCCCAGGTATCGCCGATCGTATGCAGAAAGAGATCACGAG
CATGGCTCCAAGCACGATGAAGATCAAGATCATTGCTCCACCTGAGCGCAAATACTCCGTATGGATCGGTGGA
TCCATCCTGGCCTCCCTGTCCACCTTCCAGCAGATGTGGATCAGCAAG

MTq Primers and MT qPCR amplicon inside MT template.

ACAAGTTTCGCAAGAGAGGGATCAACTTGTGTATGCACCAACTGCAGATGTTTGAAGAGTGAATGCCCACCAA
ATCTCATTAAAAT

SODq Primers and SOD qPCR amplicon inside SOD template.

CCTACACTCGTCCAATGATTGAGTTTGGCCCAGTCAAATTGAGGAGTTTATCTGTCAGTTCAAACTTGGCAACA
CCAGATTCATCAGCTACCACATTGCCAAGATCCCCAACATGCCTCTCCTGATCTTCTGGAGCTCCATGAGTCTTT
CCAAATGGGTTGAAGTGAGCAC

Appendix C

Raw Data

C.1 Biological Replicate RNA Concentrations and Quality

Treatment	Time	Rep	RNA Conc. (ngµL^{-1})	Abs. 260/280
0ppm	2 days	1	493	1.91
0ppm	2 days	2	376.7	1.83
0ppm	2 days	3	269.3	1.76
0ppm	2 days	4	350.1	1.94
0ppm	7 days	1	266	1.93
0ppm	7 days	2	637	1.86
0ppm	7 days	3	509	1.97
0ppm	7 days	4	329	1.93
0ppm	14 days	1	234	1.91
0ppm	14 days	2	195	1.94
0ppm	14 days	3	665	2.23
0ppm	14 days	4	282	2.02
$AgNO_3$ 3ppm	2 days	1	525.6	1.92
$AgNO_3$ 3ppm	2 days	2	469.2	2.06
$AgNO_3$ 3ppm	2 days	3	366.2	1.98
$AgNO_3$ 3ppm	2 days	4	121.8	1.67
$AgNO_3$ 3ppm	7 days	1	227	1.95
$AgNO_3$ 3ppm	7 days	2	670	2.04
$AgNO_3$ 3ppm	7 days	3	543	1.91
$AgNO_3$ 3ppm	7 days	4	344	1.84
$AgNO_3$ 3ppm	14 days	1	255	2.02
$AgNO_3$ 3ppm	14 days	2	486	2.14
$AgNO_3$ 3ppm	14 days	3	462	2.05
$AgNO_3$ 3ppm	14 days	4	735	1.96
AgNP 0.3ppm	2 days	1	316.9	1.79
AgNP 0.3ppm	2 days	2	206.8	1.50
AgNP 0.3ppm	2 days	3	179.2	1.55
AgNP 0.3ppm	2 days	4	133.5	1.45
AgNP 0.3ppm	7 days	1	241	1.79
AgNP 0.3ppm	7 days	2	396	1.87
AgNP 0.3ppm	7 days	3	155	1.53
AgNP 0.3ppm	7 days	4	416	1.79
AgNP 0.3ppm	14 days	1	265	2.06
AgNP 0.3ppm	14 days	2	325	1.90
AgNP 0.3ppm	14 days	3	172	1.96
AgNP 0.3ppm	14 days	4	387	2.05
AgNP 30ppm	2 days	1	389.1	1.85
AgNP 30ppm	2 days	2	188.3	1.73

AgNP 30ppm	2 days	3	522	1.86
AgNP 30ppm	2 days	4	363.7	1.82
AgNP 30ppm	7 days	1	229	1.77
AgNP 30ppm	7 days	2	733	1.95
AgNP 30ppm	7 days	3	785	1.96
AgNP 30ppm	7 days	4	238	1.61
AgNP 30ppm	14 days	1	341	1.97
AgNP 30ppm	14 days	2	105	1.77
AgNP 30ppm	14 days	3	105	2.08
AgNP 30ppm	14 days	4	691	2.00

C.2 Biological Replicate CAT and SOD Expressions

Treatment	Time	Replicate	CAT	SOD	logCAT	logSOD
Control 0ppm	2	1	1.03	0.50	0.012	-0.298
Control 0ppm	2	2	0.10	0.01	-1.011	-2.223
Control 0ppm	2	3	1.00	1.00	0.000	0.000
Control 0ppm	2	4	0.07	0.01	-1.150	-2.019
Control 0ppm	7	1	0.97	0.65	-0.013	-0.187
Control 0ppm	7	2	1.59	2.63	0.201	0.421
Control 0ppm	7	3	1.63	1.34	0.212	0.128
Control 0ppm	7	4	0.19	0.62	-0.716	-0.206
Control 0ppm	14	1	1.35	461.01	0.130	2.664
Control 0ppm	14	2	0.15	35.75	-0.823	1.553
Control 0ppm	14	3	0.00	0.26	-2.661	-0.580
Control 0ppm	14	4	0.05	2.23	-1.320	0.347
$AgNO_3$ 3ppm	2	1	1.51	1.01	0.179	0.005
$AgNO_3$ 3ppm	2	2	0.07	0.08	-1.178	-1.098
$AgNO_3$ 3ppm	2	3	1.84	1.42	0.266	0.152
$AgNO_3$ 3ppm	2	4	3.86	1.64	0.587	0.215
$AgNO_3$ 3ppm	7	1	0.36	0.60	-0.445	-0.221
$AgNO_3$ 3ppm	7	2	1.04	1.33	0.015	0.125
$AgNO_3$ 3ppm	7	3	0.21	0.75	-0.675	-0.125
$AgNO_3$ 3ppm	7	4	0.47	0.78	-0.329	-0.108
$AgNO_3$ 3ppm	14	1	2.19	8447.48	0.340	3.927
$AgNO_3$ 3ppm	14	2	2.24	168.13	0.351	2.226
$AgNO_3$ 3ppm	14	3	2.02	154.88	0.305	2.190
$AgNO_3$ 3ppm	14	4	3.42	179.97	0.534	2.255
AgNP 0.3ppm	2	1	2.34	0.76	0.368	-0.116
AgNP 0.3ppm	2	2	3.67	1.87	0.564	0.271
AgNP 0.3ppm	2	3	7.19	1.10	0.857	0.043
AgNP 0.3ppm	2	4	0.57	0.27	-0.242	-0.563
AgNP 0.3ppm	7	1	0.28	1.16	-0.546	0.065
AgNP 0.3ppm	7	2	0.06	1.12	-1.258	0.051

AgNP 0.3ppm	7	3	3.18	1.08	0.503	0.032
AgNP 0.3ppm	7	4	0.85	1.17	-0.070	0.069
AgNP 0.3ppm	14	1	1.96	216.78	0.291	2.336
AgNP 0.3ppm	14	2	2.19	71.08	0.339	1.852
AgNP 0.3ppm	14	3	2.15	1653.67	0.333	3.218
AgNP 0.3ppm	14	4	0.62	59.66	-0.208	1.776
AgNP 30ppm	2	1	2.07	0.49	0.317	-0.311
AgNP 30ppm	2	2	0.98	0.45	-0.007	-0.343
AgNP 30ppm	2	3	2.94	0.92	0.468	-0.036
AgNP 30ppm	2	4	1.51	1.56	0.179	0.192
AgNP 30ppm	7	1	0.22	1.82	-0.664	0.260
AgNP 30ppm	7	2	0.12	3.84	-0.913	0.584
AgNP 30ppm	7	3	0.45	0.63	-0.346	-0.202
AgNP 30ppm	7	4	9.61	2.11	0.983	0.323
AgNP 30ppm	14	1	0.51	22.21	-0.291	1.347
AgNP 30ppm	14	2	0.58	46.14	-0.237	1.664
AgNP 30ppm	14	3	1.24	1120.46	0.093	3.049
AgNP 30ppm	14	4	1.16	0.27	0.064	-0.562

C.3 Biological Replicate Viable Cell Counts

Treatment	Time	Replicate	Viable cells per mL x10^6	Viable cells per mL
0ppm	2 days	1	26	26,000,000
0ppm	2 days	2	34	34,000,000
0ppm	2 days	3	48	48,000,000
0ppm	2 days	4	34	34,000,000
0ppm	7 days	1	40	40,000,000
0ppm	7 days	2	38	38,000,000
0ppm	7 days	3	38	38,000,000
0ppm	7 days	4	56	56,000,000
0ppm	14 days	1	50	50,000,000
0ppm	14 days	2	56	56,000,000
0ppm	14 days	3	56	56,000,000
0ppm	14 days	4	60	60,000,000
$AgNO_3$ 3ppm	2 days	1	42	42,000,000
$AgNO_3$ 3ppm	2 days	2	34	34,000,000
$AgNO_3$ 3ppm	2 days	3	38	38,000,000
$AgNO_3$ 3ppm	2 days	4	38	38,000,000
$AgNO_3$ 3ppm	7 days	1	56	56,000,000
$AgNO_3$ 3ppm	7 days	2	72	72,000,000
$AgNO_3$ 3ppm	7 days	3	28	28,000,000
$AgNO_3$ 3ppm	7 days	4	30	30,000,000
$AgNO_3$ 3ppm	14 days	1	36	36,000,000
$AgNO_3$ 3ppm	14 days	2	44	44,000,000
$AgNO_3$ 3ppm	14 days	3	52	52,000,000

$AgNO_3$ 3ppm	14 days	4	52	52,000,000
AgNP 0.3ppm	2 days	1	36	36,000,000
AgNP 0.3ppm	2 days	2	24	24,000,000
AgNP 0.3ppm	2 days	3	40	40,000,000
AgNP 0.3ppm	2 days	4	52	52,000,000
AgNP 0.3ppm	7 days	1	46	46,000,000
AgNP 0.3ppm	7 days	2	50	50,000,000
AgNP 0.3ppm	7 days	3	50	50,000,000
AgNP 0.3ppm	7 days	4	58	58,000,000
AgNP 0.3ppm	14 days	1	54	54,000,000
AgNP 0.3ppm	14 days	2	22	22,000,000
AgNP 0.3ppm	14 days	3	36	36,000,000
AgNP 0.3ppm	14 days	4	44	44,000,000
AgNP 30ppm	2 days	1	42	42,000,000
AgNP 30ppm	2 days	2	40	40,000,000
AgNP 30ppm	2 days	3	46	46,000,000
AgNP 30ppm	2 days	4	62	62,000,000
AgNP 30ppm	7 days	1	52	52,000,000
AgNP 30ppm	7 days	2	40	40,000,000
AgNP 30ppm	7 days	3	34	34,000,000
AgNP 30ppm	7 days	4	18	18,000,000
AgNP 30ppm	14 days	1	66	66,000,000
AgNP 30ppm	14 days	2	30	30,000,000
AgNP 30ppm	14 days	3	56	56,000,000
AgNP 30ppm	14 days	4	34	34,000,000

C.4 Biological Replicate Differential Cell Counts

Treatment	Time	Replicate	Eleocytes %	Amoebocyte %	Granulocyte %
0ppm	2 days	1	10	60	30
0ppm	2 days	2	25	50	25
0ppm	2 days	3	10	52.5	37.5
0ppm	2 days	4	2.5	77.5	20
0ppm	7 days	1	7.5	75	17.5
0ppm	7 days	2	5	75	20
0ppm	7 days	3	20	57.5	22.5
0ppm	7 days	4	7.5	65	27.5
0ppm	14 days	1	7.5	72.5	20
0ppm	14 days	2	20	55	25
0ppm	14 days	3	12.5	62.5	25
0ppm	14 days	4	10	70	20
$AgNO_3$ 3ppm	2 days	1	17.5	65	17.5
$AgNO_3$ 3ppm	2 days	2	2.5	62.5	35
$AgNO_3$ 3ppm	2 days	3	10	57.5	32.5
$AgNO_3$ 3ppm	2 days	4	17.5	52.5	30

$AgNO_3$ 3ppm	7 days	1	30	40	30
$AgNO_3$ 3ppm	7 days	2	20	60	20
$AgNO_3$ 3ppm	7 days	3	10	72.5	17.5
$AgNO_3$ 3ppm	7 days	4	12.5	75	12.5
$AgNO_3$ 3ppm	14 days	1	15	50	35
$AgNO_3$ 3ppm	14 days	2	2.5	77.5	20
$AgNO_3$ 3ppm	14 days	3	7.5	87.5	5
$AgNO_3$ 3ppm	14 days	4	5	77.5	17.5
AgNP 0.3ppm	2 days	1	5	62.5	32.5
AgNP 0.3ppm	2 days	2	15	47.5	37.5
AgNP 0.3ppm	2 days	3	15	55	30
AgNP 0.3ppm	2 days	4	5	75	20
AgNP 0.3ppm	7 days	1	7.5	62.5	30
AgNP 0.3ppm	7 days	2	2.5	57.5	40
AgNP 0.3ppm	7 days	3	17.5	65	17.5
AgNP 0.3ppm	7 days	4	12.5	70	17.5
AgNP 0.3ppm	14 days	1	22.5	67.5	10
AgNP 0.3ppm	14 days	2	5	67.5	27.5
AgNP 0.3ppm	14 days	3	7.5	85	7.5
AgNP 0.3ppm	14 days	4	12.5	72.5	15
AgNP 30ppm	2 days	1	5	65	30
AgNP 30ppm	2 days	2	7.5	62.5	30
AgNP 30ppm	2 days	3	10	77.5	12.5
AgNP 30ppm	2 days	4	2.5	65	32.5
AgNP 30ppm	7 days	1	0	62.5	37.5
AgNP 30ppm	7 days	2	10	55	35
AgNP 30ppm	7 days	3	7.5	70	22.5
AgNP 30ppm	7 days	4	25	50	25
AgNP 30ppm	14 days	1	5	75	20
AgNP 30ppm	14 days	2	10	77.5	12.5
AgNP 30ppm	14 days	3	10	80	10
AgNP 30ppm	14 days	4	10	70	20

C5 Primer Efficency Standards and Melt Curves

Table C 1: qPCR Primer Efficency CT Values

Concentration ($ngµL^{-1}$)	Ct Value		Ct Value		Ct Value		Ct Value	
	ACTq		**CATq**		**SODq**		**MTq**	
0.1	7.904	8.010	7.520	7.407	6.452	6.526	6.879	7.066
0.001	15.555	15.445	14.329	14.608	12.605	12.778	13.302	13.445
0.0001	18.827	19.052	17.528	17.341	15.672	16.031	16.758	16.982
0.00001	22.057	22.033	20.739	20.573	18.687	19.404	20.117	20.244
0.000001	25.105	24.987	23.905	24.035	21.950	22.732	23.071	23.215
0.00000001	31.430	32.047	30.667	30.448	28.499	28.809	29.646	31.063

ACTq Melt Curve (Tm)

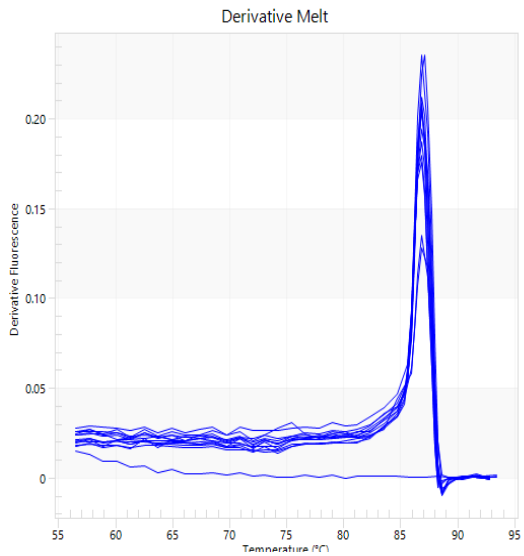

MTq Melt Curve (Tm)

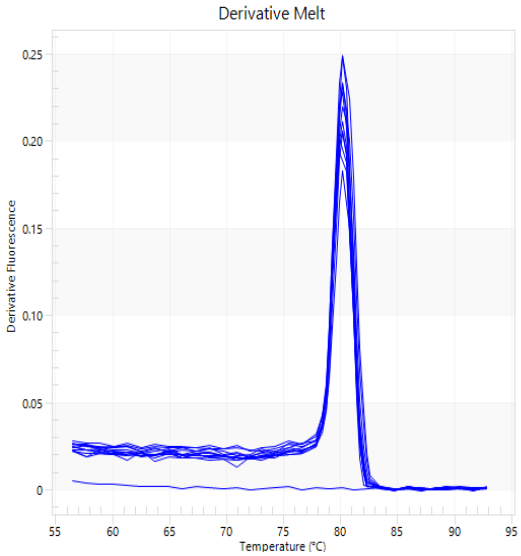

SODq Melt Curve (Tm)

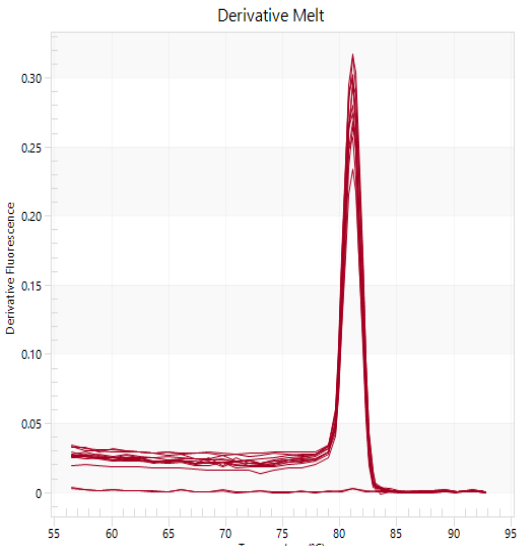

CATq Melt Curve (Tm)

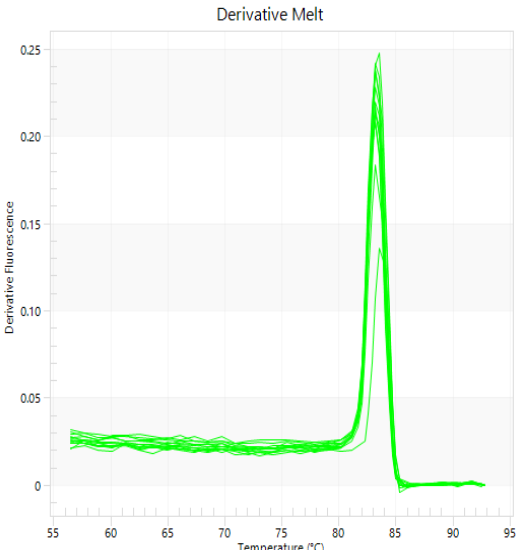

Figure C 1: qPCR Primer Melt Curves

References

Adamowicz, A. (2005). Mophology and ultrastructure of the earthworm Dendrobaena veneta (Lumbricidae) coelomocytes. *Tissue and Cell*, *37*(2), 125-133.

Afshari, C. A., Hamadeh, H. K., & Bushel, P. R. (2010). The evolution of bioinformatics in toxicology: advancing toxicogenomics. *Toxicological Sciences*, kfq373.

Ahamed, M., AlSalhi, M. S., & Siddiqui, M. K. J. (2010). Silver nanoparticle applications and human health. *Clinica Chimica Acta*, *411*(23), 1841-1848.

Ahamed, M., Karns, M., Goodson, M., Rowe, J., Hussain, S. M., Schlager, J. J., & Hong, Y. (2008). DNA damage response to different surface chemistry of silver nanoparticles in mammalian cells. *Toxicology and Applied Pharmacology*, *233*(3), 404-410.

Ahn, J. M., Eom, H. J., Yang, X., Meyer, J. N., & Choi, J. (2014). Comparative toxicity of silver nanoparticles on oxidative stress and DNA damage in the nematode, Caenorhabditis elegans. *Chemosphere*, *108*, 343-352.

Anjum, N. A., Gill, S. S., Duarte, A. C., Pereira, E., & Ahmad, I. (2013). Silver nanoparticles in soil–plant systems. *Journal of Nanoparticle Research*, *15*(9), 1-26.

Asensio, V., Rodriguez-Ruiz, A., Garmendia, L., Andre, J., Kille, P., Morgan, A. J., Soto, M., & Marigomez, I. (2013). Towards an integrative soil health assessment strategy: a three tier (integrative biomarker response) approach with Eisenia fetida applied to soils subjected to chronic metal pollution. *Science of the Total Environment*, *442*, 344-365.

AshaRani, P. V., Low Kah Mun, G., Hande, M. P., & Valiyaveettil, S. (2008). Cytotoxicity and genotoxicity of silver nanoparticles in human cells. *ACS nano*, *3*(2), 279-290.

Barnes, C. A., Elsaesser, A., Arkusz, J., Smok, A., Palus, J., Lesniak, A., & Howard, C. V. (2008). Reproducible comet assay of amorphous silica nanoparticles detects no genotoxicity. *Nano Letters*, *8*(9), 3069-3074.

Barnes, R. J., Riba, O., Gardner, M. N., Scott, T. B., Jackman, S. A., & Thompson, I. P. (2010). Optimization of nano-scale nickel/iron particles for the reduction of high concentration chlorinated aliphatic hydrocarbon solutions. *Chemosphere*, *79*(4), 448-454.

Beer, C., Foldbjerg, R., Hayashi, Y., Sutherland, D. S., & Autrup, H. (2012). Toxicity of silver nanoparticles—nanoparticle or silver ion?. *Toxicology letters*, *208*(3), 286-292.

Benn, T. M., & Westerhoff, P. (2008). Nanoparticle silver released into water from commercially available sock fabrics. *Environmental science & technology*, *42*(11), 4133-4139.

Benoit, R., Wilkinson, K. J., & Sauvé, S. (2013). Partitioning of silver and chemical speciation of free Ag in soils amended with nanoparticles. *Chem Cent J*, *7*, 75.

Bergeson, L. L. (2010). Nanosilver: US EPA's pesticide office considers how best to proceed. *Environmental Quality Management*, *19*(3), 79-85.

Bianchini, A., Bowles, K. C., Brauner, C. J., Gorsuch, J. W., Kramer, J. R., & Wood, C. M. (2002). Evaluation of the effect of reactive sulfide on the acute toxicity of silver (I) to Daphnia magna. part 2: Toxicity results. *Environmental toxicology and chemistry*, *21*(6), 1294-1300.

Blaser, S. A., Scheringer, M., MacLeod, M., & Hungerbühler, K. (2008). Estimation of cumulative aquatic exposure and risk due to silver: Contribution of nano-functionalized plastics and textiles. *Science of the total environment*, *390*(2), 396-409.

Blaser, S. A., Scheringer, M., MacLeod, M., & Hungerbühler, K. (2008). Estimation of cumulative aquatic exposure and risk due to silver: Contribution of nano-functionalized plastics and textiles. *Science of the total environment*, *390*(2), 396-409.

Blaser, S. A., Scheringer, M., MacLeod, M., & Hungerbühler, K. (2008). Estimation of cumulative aquatic exposure and risk due to silver: Contribution of nano-functionalized plastics and textiles. *Science of the total environment*, *390*(2), 396-409.

Boese, K. (1920). Uber Collargol, seine Anwendung, und Wirkung und die Erfolge dieser Behandlung in der Chirurgie und Gynakologie.

, M. (2009). Impact of silver nanoparticle contamination on the genetic diversity of natural bacterial assemblages in estuarine sediments. *Environmental science & technology*, *43*(12), 4530-4536.

Brulle, F., Lemière, S., Waterlot, C., Douay, F., & Vandenbulcke, F. (2011). Gene expression analysis of 4 biomarker candidates in Eisenia fetida exposed to an environmental metallic trace elements gradient: a microcosm study. *Science of the Total Environment*, *409*(24), 5470-5482.

Brulle, F., Mitta, G., Cocquerelle, C., Vieau, D., Lemiere, S., Leprêtre, A., & Vandenbulcke, F. (2006). Cloning and real-time PCR testing of 14 potential biomarkers in Eisenia fetida following cadmium exposure. *Environmental science & technology*, *40*(8), 2844-2850.

Brulle, F., Mitta, G., Leroux, R., Lemière, S., Leprêtre, A., & Vandenbulcke, F. (2007). The strong induction of metallothionein gene following cadmium exposure transiently affects the expression of many genes in Eisenia fetida: A trade-off mechanism?.

Comparative Biochemistry and Physiology Part C: Toxicology & Pharmacology, *144*(4), 334-341.

Bundy, J. G., Sidhu, J. K., Rana, F., Spurgeon, D. J., Svendsen, C., Wren, J. F., Stürzenbaum, S. R., Morgan, A. J., & Kille, P. (2008). 'Systems toxicology'approach identifies coordinated metabolic responses to copper in a terrestrial non-model invertebrate, the earthworm Lumbricus rubellus. *BMC biology*, *6*(1), 25.

Burgos, M. G., Winters, C., Stürzenbaum, S. R., Randerson, P. F., Kille, P., & Morgan, A. J. (2005). Cu and Cd effects on the earthworm Lumbricus rubellus in the laboratory: multivariate statistical analysis of relationships between exposure, biomarkers, and ecologically relevant parameters. *Environmental science & technology*, *39*(6), 1757-1763.

Burleson, D. J., Driessen, M. D., & Penn, R. L. (2004). On the characterization of environmental nanoparticles. *Journal of Environmental Science and Health, Part A*, *39*(10), 2707-2753.

Byrne, J. D., Betancourt, T., & Brannon-Peppas, L. (2008). Active targeting schemes for nanoparticle systems in cancer therapeutics. *Advanced drug delivery reviews*, *60*(15), 1615-1626.

Calisi, A., Zaccarelli, N., Lionetto, M. G., & Schettino, T. (2013). Integrated biomarker analysis in the earthworm Lumbricus terrestris: application to the monitoring of soil heavy metal pollution. *Chemosphere*, *90*(11), 2637-2644.

Capdevila, M., & Atrian, S. (2011). Metallothionein protein evolution: a miniassay. *JBIC Journal of Biological Inorganic Chemistry*, *16*(7), 977-989.

Carlson, C., Hussain, S. M., Schrand, A. M., K. Braydich-Stolle, L., Hess, K. L., Jones, R. L., & Schlager, J. J. (2008). Unique cellular interaction of silver nanoparticles: size-dependent generation of reactive oxygen species. *The Journal of Physical Chemistry B*, *112*(43), 13608-13619.

Caterino, M. S., Cho, S., & Sperling, F. A. (2000). The current state of insect molecular systematics: a thriving Tower of Babel. *Annual review of entomology*, *45*(1), 1-54.

Chaperon, S., & Sauve, S. (2007). Toxicity interaction of metals (Ag, Cu, Hg, Zn) to urease and dehydrogenase activities in soils. *Soil biology and Biochemistry*, *39*(9), 2329-2338.

Chen, C., Zhou, Q., Liu, S., & Xiu, Z. (2011). Acute toxicity, biochemical and gene expression responses of the earthworm Eisenia fetida exposed to polycyclic musks. Chemosphere, 83(8), 11471154

Choi, J. E., Kim, S., Ahn, J. H., Youn, P., Kang, J. S., Park, K., Yi, J., & Ryu, D. Y. (2010). Induction of oxidative stress and apoptosis by silver nanoparticles in the liver of adult zebrafish. *Aquatic Toxicology*, *100*(2), 151-159.

Choi, O., Clevenger, T. E., Deng, B., Surampalli, R. Y., Ross, L., & Hu, Z. (2009). Role of sulfide and ligand strength in controlling nanosilver toxicity. *Water research*, *43*(7), 1879-1886.

Choi, O., Deng, K. K., Kim, N. J., Ross, L., Surampalli, R. Y., & Hu, Z. (2008). The inhibitory effects of silver nanoparticles, silver ions, and silver chloride colloids on microbial growth. *Water research*, *42*(12), 3066-3074.

Colman, B. P., Arnaout, C. L., Anciaux, S., Gunsch, C. K., Hochella Jr, M. F., Kim, B., Lowry, G. V., & Bernhardt, E. S. (2013). Low concentrations of silver nanoparticles in biosolids cause adverse ecosystem responses under realistic field scenario. *PLoS One*, *8*(2), e57189.

Colman, B. P., Wang, S. Y., Auffan, M., Wiesner, M. R., & Bernhardt, E. S. (2012). Antimicrobial effects of commercial silver nanoparticles are attenuated in natural streamwater and sediment. *Ecotoxicology*, *21*(7), 1867-1877.

Çotuk, A., & Dales, R. P. (1984). Lysozyme activity in the coelomic fluid and coelomocytes of the earthworm Eisenia foetida Sav. in relation to bacterial infection. *Comparative Biochemistry and Physiology Part A: Physiology*, *78*(3), 469-474.

Croteau, M. N., Misra, S. K., Luoma, S. N., & Valsami-Jones, E. (2011). Silver bioaccumulation dynamics in a freshwater invertebrate after aqueous and dietary exposures to nanosized and ionic Ag. *Environmental science & technology*, *45*(15), 6600-6607.

Das, P., Williams, C. J., Fulthorpe, R. R., Hoque, M. E., Metcalfe, C. D., & Xenopoulos, M. A. (2012). Changes in bacterial community structure after exposure to silver nanoparticles in natural waters. *Environmental science & technology*, *46*(16), 9120-9128.

Demuynck, S., Grumiaux, F., Mottier, V., Schikorski, D., Lemiere, S., & Leprêtre, A. (2007). Cd/Zn exposure interactions on metallothionein response in Eisenia fetida (Annelida, Oligochaeta). *Comparative Biochemistry and Physiology Part C: Toxicology & Pharmacology*, *145*(4), 658-668.)

Egger, S., Lehmann, R. P., Height, M. J., Loessner, M. J., & Schuppler, M. (2009). Antimicrobial properties of a novel silver-silica nanocomposite material. *Applied and environmental microbiology*, *75*(9), 2973-2976.

Eisen, G. (1874). Bidrag till Kannedomen om New Englands och Canadas Lumbricider. Ofv. Vet. Akad. Forh 31: 41-49.

El Badawy, A. M., Silva, R. G., Morris, B., Scheckel, K. G., Suidan, M. T., & Tolaymat, T. M. (2010). Surface charge-dependent toxicity of silver nanoparticles. *Environmental science & technology*, *45*(1), 283-287.

Elsaesser, A., & Howard, C. V. (2012). Toxicology of nanoparticles. *Advanced drug delivery reviews*, *64*(2), 129-137.

El-Temsah, Y. S., & Joner, E. J. (2012). Impact of Fe and Ag nanoparticles on seed germination and differences in bioavailability during exposure in aqueous suspension and soil. *Environmental toxicology*, *27*(1), 42-49.

Engelmann, P., Molnár, L., Pálinkás, L., Cooper, E. L., & Németh, P. (2004). Earthworm leukocyte populations specifically harbor lysosomal enzymes that may respond to bacterial challenge. *Cell and tissue research*, *316*(3), 391-401.

EPA (2009). *Biosolids: targeted national sewage sludge survey report.* Retrieved on the 16th of July 2013 from http://water.epa.gov/scitech/wastetech/biosolids/tnsss-fs.cfm

Erickson, R. J., Brooke, L. T., Kahl, M. D., Venter, F. V., Harting, S. L., Markee, T. P., & Spehar, R. L. (1998). Effects of laboratory test conditions on the toxicity of silver to aquatic organisms. *Environmental toxicology and chemistry*, *17*(4), 572-578.

Evans, A. C. (1946). X.—A new species of earthworm of the genus Allolobophora. *Journal of Natural History*, *13*(98), 98-101.

Fabrega, J., Luoma, S. N., Tyler, C. R., Galloway, T. S., & Lead, J. R. (2011). Silver nanoparticles: behaviour and effects in the aquatic environment. *Environment international*, *37*(2), 517-531.

Fabrega, J., Renshaw, J. C., & Lead, J. R. (2009). Interactions of silver nanoparticles with Pseudomonas putida biofilms. *Environmental science & technology*, *43*(23), 9004-9009.

Farkas, J., Christian, P., Urrea, J. A. G., Roos, N., Hassellöv, M., Tollefsen, K. E., & Thomas, K. V. (2010). Effects of silver and gold nanoparticles on rainbow trout (Oncorhynchus mykiss) hepatocytes. *Aquatic Toxicology*, *96*(1), 44-52.

Felix, K., Lengfelder, E., Hartmann, H. J., & Weser, U. (1993). A pulse radiolytic study on the reaction of hydroxyl and superoxide radicals with yeast Cu (I)-thionein. *Biochimica et Biophysica Acta (BBA)-Protein Structure and Molecular Enzymology*, *1203*(1), 104-108.

Fisher, N. S., & Wang, W. X. (1998). Trophic transfer of silver to marine herbivores: A review of recent studies. *Environmental toxicology and chemistry*, *17*(4), 562-571.

Fisker, K. V., Holmstrup, M., & Sørensen, J. G. (2013). Variation in metallothionein gene expression is associated with adaptation to copper in the earthworm Dendrobaena octaedra. *Comparative Biochemistry and Physiology Part C: Toxicology & Pharmacology*, *157*(2), 220-226.

Foldbjerg, R., Dang, D. A., & Autrup, H. (2011). Cytotoxicity and genotoxicity of silver nanoparticles in the human lung cancer cell line, A549. *Archives of toxicology*, *85*(7), 743-750.

Fung, M. C., & Bowen, D. L. (1996). Silver products for medical indications: risk-benefit assessment. *Clinical Toxicology*, *34*(1), 119-126.

Garnett, M. C., & Kallinteri, P. (2006). Nanomedicines and nanotoxicology: some physiological principles. *Occupational Medicine*, *56*(5), 307-311.

Gimbert, L. J., Hamon, R. E., Casey, P. S., & Worsfold, P. J. (2007). Partitioning and stability of engineered ZnO nanoparticles in soil suspensions using flow field-flow fractionation. *Environmental Chemistry*, *4*(1), 8-10.

Glover, R. D., Miller, J. M., & Hutchison, J. E. (2011). Generation of metal nanoparticles from silver and copper objects: nanoparticle dynamics on surfaces and potential sources of nanoparticles in the environment. *Acs Nano*, *5*(11), 8950-8957.

Gomes, S. I., Soares, A. M., Scott-Fordsmand, J. J., & Amorim, M. J. (2013). Mechanisms of response to silver nanoparticles on Enchytraeus albidus (Oligochaeta): survival, reproduction and gene expression profile. *Journal of hazardous materials*, *254*, 336-344.

Gottschalk, F., & Nowack, B. (2011). The release of engineered nanomaterials to the environment. *Journal of Environmental Monitoring*, *13*(5), 1145-1155.

Gottschalk, F., Scholz, R. W., & Nowack, B. (2010). Probabilistic material flow modeling for assessing the environmental exposure to compounds: Methodology and an application to engineered nano-TiO< sub> 2</sub> particles. *Environmental Modelling & Software*, *25*(3), 320-332.

Gottschalk, F., Sonderer, T., Scholz, R. W., & Nowack, B. (2009). Modeled environmental concentrations of engineered nanomaterials (TiO2, ZnO, Ag, CNT, fullerenes) for different regions. *Environmental Science & Technology*, *43*(24), 9216-9222.

Gruber, C., Stürzenbaum, S., Gehrig, P., Sack, R., Hunziker, P., Berger, B., & Dallinger, R. (2000). Isolation and characterization of a self-sufficient one-domain protein. *European Journal of Biochemistry*, *267*(2), 573-582.

Hamed, S. S., Kauschke, E., & Cooper, E. L. (2002). Cytochemical properties of earthworm coelomocytes enriched by Percoll. *A new model for analyzing antimicrobial peptides with biomedical applications*, 29-37.

Hartmann, H. J., & Weser, U. (2000). Copper-release from yeast Cu (I)-metallothionien by nitric oxide (NO). *BioMetals*, *13*(2), 153-156.

Hassellöv, M., Readman, J. W., Ranville, J. F., & Tiede, K. (2008). Nanoparticle analysis and characterization methodologies in environmental risk assessment of engineered nanoparticles. *Ecotoxicology*, *17*(5), 344-361.

Hayashi, Y., Engelmann, P., Foldbjerg, R., Szabó, M., Somogyi, I., Pollák, E., Molnár, L., Autrup, H., Sutherland, D. S., Scott-Fordsmand, J., & Heckmann, L. H. (2012). Earthworms and humans in vitro: characterizing evolutionarily conserved stress and immune responses to silver nanoparticles. *Environmental science & technology*, *46*(7), 4166-4173.

Hayashi, Y., Heckmann, L. H., Simonsen, V., & Scott-Fordsmand, J. J. (2013). Time-course profiling of molecular stress responses to silver nanoparticles in the earthworm< i> Eisenia fetida</i>. *Ecotoxicology and environmental safety*, *98*, 219-226.

Hebert, P. D., Cywinska, A., & Ball, S. L. (2003). Biological identifications through DNA barcodes. *Proceedings of the Royal Society of London. Series B: Biological Sciences*, *270*(1512), 313-321.

Heckmann, L. H., Hovgaard, M. B., Sutherland, D. S., Autrup, H., Besenbacher, F., & Scott-Fordsmand, J. J. (2011). Limit-test toxicity screening of selected inorganic nanoparticles to the earthworm Eisenia fetida. *Ecotoxicology*, *20*(1), 226-233.

Hernández-Sierra, J. F., Ruiz, F., Pena, D. C. C., Martínez-Gutiérrez, F., Martínez, A. E., Guillén, A. D. J. P., Tapia-Pérez, H., & Castañón, G. M. (2008). The antimicrobial sensitivity of Streptococcus mutans to nanoparticles of silver, zinc oxide, and gold. *Nanomedicine: Nanotechnology, Biology and Medicine*, *4*(3), 237-240.

Hogstrand, C., & Wood, C. M. (1998). Toward a better understanding of the bioavailability, physiology, and toxicity of silver in fish: implications for water quality criteria. *Environmental toxicology and chemistry*, *17*(4), 547-561.

Homa, J., Klimek, M., Kruk, J., Cocquerelle, C., Vandenbulcke, F., & Plytycz, B. (2010). Metal-specific effects on metallothionein gene induction and riboflavin content in coelomocytes of Allolobophora chlorotica. Ecotoxicology and Environmental Safety, 73(8), 1937-1943.

Homa, J., Stürzenbaum, S. R., Morgan, A. J., & Plytycz, B. (2007). Disrupted homeostasis in coelomocytes of Eisenia fetida and Allolobophora chlorotica exposed dermally to heavy metals. *European Journal of Soil Biology*, *43*, S273-S280.

Homa, J., Zorska, A., Wesolowski, D., & Chadzinska, M. (2013). Dermal exposure to immunostimulants induces changes in activity and proliferation of coelomocytes of Eisenia andrei. *Journal of Comparative Physiology B*, *183*(3), 313-322.

Hooper, H. L., Jurkschat, K., Morgan, A. J., Bailey, J., Lawlor, A. J., Spurgeon, D. J., & Svendsen, C. (2011). Comparative chronic toxicity of nanoparticulate and ionic zinc to the earthworm< i> Eisenia veneta</i> in a soil matrix. *Environment international*, *37*(6), 1111-1117.

Hostetter, R. K., & Cooper, E. L. (1974). Earthworm coelomocyte immunity. In *Contemporary topics in immunobiology* (pp. 91-107). Springer US.

Hou, L., Li, K., Ding, Y., Li, Y., Chen, J., Wu, X., & Li, X. (2012). Removal of silver nanoparticles in simulated wastewater treatment processes and its impact on COD and NH< sub> 4</sub> reduction. *Chemosphere*, *87*(3), 248-252.

Hu, C., Li, M., Wang, W., Cui, Y., Chen, J., & Yang, L. (2012). Ecotoxicity of silver nanoparticles on earthworm Eisenia fetida: responses of the antioxidant system, acid phosphatase and ATPase. *Toxicological & Environmental Chemistry*, *94*(4), 732-741.

Hu, C.W., Li, M., Cui, Y.B., Li, D.S., Chen, J. & Yang, L.Y. (2010). Toxicological effects of TiO(2) and ZnO nanoparticles in soil on earthworm Eisenia fetida. *Soil Biology & Biochemistry, 42, 586–591.*

Huang, J., Xu, Q., Sun, Z. J., Tang, G. L., & Su, Z. Y. (2007). Identifying earthworms through DNA barcodes. *Pedobiologia*, *51*(4), 301-309.

Hussain, S. M., Hess, K. L., Gearhart, J. M., Geiss, K. T., & Schlager, J. J. (2005). In vitro toxicity of nanoparticles in BRL 3A rat liver cells. *Toxicology in vitro*, *19*(7), 975-983.

Impellitteri, C. A., Harmon, S., Silva, R. G., Miller, B. W., Scheckel, K. G., Luxton, T. P., Schupp, D., & Panguluri, S. (2013). Transformation of silver nanoparticles in fresh, aged, and incinerated biosolids. *Water research*, *47*(12), 3878-3886.

Ivask, A., Juganson, K., Bondarenko, O., Mortimer, M., Aruoja, V., Kasemets, K., Blinova, I., Heinlaan, M., & Kahru, A. (2013). Mechanisms of toxic action of Ag, ZnO and CuO nanoparticles to selected ecotoxicological test organisms and mammalian cells in vitro: A comparative review. *Nanotoxicology*, *8*(S1), 57-71.

Jo, Y. K., Kim, B. H., & Jung, G. (2009). Antifungal activity of silver ions and nanoparticles on phytopathogenic fungi. *Plant Disease*, *93*(10), 1037-1043.

Kaegi, R., Voegelin, A., Ort, C., Sinnet, B., Thalmann, B., Krismer, J., Hagendorfer, H., Elumelu, M., & Mueller, E. (2013). Fate and transformation of silver nanoparticles in urban wastewater systems. *Water Research*, *47*(12), 3866-3877.

Kaegi, R., Voegelin, A., Sinnet, B., Zuleeg, S., Hagendorfer, H., Burkhardt, M., & Siegrist, H. (2011). Behavior of metallic silver nanoparticles in a pilot wastewater treatment plant. *Environmental Science & Technology*, *45*(9), 3902-3908.

Karlsson, H. L. (2010). The comet assay in nanotoxicology research. *Analytical and Bioanalytical Chemistry*, *398*(2), 651-666.

Kawata, K., Osawa, M., & Okabe, S. (2009). In vitro toxicity of silver nanoparticles at noncytotoxic doses to HepG2 human hepatoma cells. *Environmental Science & Technology*, *43*(15), 6046-6051.

Keller, A. A., McFerran, S., Lazareva, A., & Suh, S. (2013). Global life cycle releases of engineered nanomaterials. *Journal of Nanoparticle Research*, *15*(6), 1-17.

Kim, J., Kim, S., & Lee, S. (2011). Differentiation of the toxicities of silver nanoparticles and silver ions to the Japanese medaka (Oryzias latipes) and the cladoceran Daphnia magna. *Nanotoxicology*, *5*(2), 208-214.

Kim, S., Choi, J. E., Choi, J., Chung, K. H., Park, K., Yi, J., & Ryu, D. Y. (2009). Oxidative stress-dependent toxicity of silver nanoparticles in human hepatoma cells. *Toxicology In Vitro*, *23*(6), 1076-1084.

Klaine, S. J., Alvarez, P. J., Batley, G. E., Fernandes, T. F., Handy, R. D., Lyon, D. Y., Mahendra, S., McLaughlin, M. J., & Lead, J. R. (2008). Nanomaterials in the environment: behavior, fate, bioavailability, and effects. *Environmental Toxicology and Chemistry*, *27*(9), 1825-1851.

Klarica, J., Kloss-Brandstätter, A., Traugott, M., & Juen, A. (2012). Comparing four mitochondrial genes in earthworms–implications for identification, phylogenetics, and discovery of cryptic species. *Soil Biology and Biochemistry*, *45*, 23-30.

Kurek, A., Homa, J., & Plytycz, B. (2002). Earthworm coelomocytes: convenient model for basic and applied sciences. *A new model for analyzing antimicrobial peptides with biomedical applications. IOS press, Ohmsha*, 38-46.

Kvitek, L., Vanickova, M., Panacek, A., Soukupova, J., Dittrich, M., Valentova, E., Prucek, R., Bancirova, M., Milde, D., & Zboril, R. (2009). Initial study on the toxicity of silver nanoparticles (NPs) against Paramecium caudatum. *The Journal of Physical Chemistry C*, *113*(11), 4296-4300.

Lapied, E., Moudilou, E., Exbrayat, J. M., Oughton, D. H., & Joner, E. J. (2010). Silver nanoparticle exposure causes apoptotic response in the earthworm Lumbricus terrestris (Oligochaeta). *Nanomedicine*, *5*(6), 975-984.

Lapied, E., Nahmani, J. Y., Moudilou, E., Chaurand, P., Labille, J., Rose, J., Exbrayat, J.M., Oughton, D.H., & Joner, E. J. (2011). Ecotoxicological effects of an aged TiO< sub> 2</sub> nanocomposite measured as apoptosis in the anecic earthworm< i> Lumbricus terrestris</i> after exposure through water, food and soil. *Environment International*, *37*(6), 1105-1110.

Lavelle, P., Decaëns, T., Aubert, M., Barot, S., Blouin, M., Bureau, F., Margerie, P., Mora, P., & Rossi, J. P. (2006). Soil invertebrates and ecosystem services. *European journal of Soil Biology*, *42*, S3-S15.

Lea, M. C. (1889). On allotropic forms of silver. *American Journal of Science*, 37, 476–491.

Lead, J. R., & Wilkinson, K. J. (2006). Aquatic colloids and nanoparticles: current knowledge and future trends. *Environmental Chemistry*, *3*(3), 159-171.

Levard, C., Hotze, E. M., Colman, B. P., Dale, A. L., Truong, L., Yang, X. Y., Bone, A. J., & Lowry, G. V. (2013). Sulfidation of silver nanoparticles: natural antidote to their toxicity. *Environmental Science & Technology*, *47*(23), 13440-13448.

Levard, C., Reinsch, B. C., Michel, F. M., Oumahi, C., Lowry, G. V., & Brown Jr, G. E. (2011). Sulfidation processes of PVP-coated silver nanoparticles in aqueous solution: impact on dissolution rate. *Environmental Science & Technology*, *45*(12), 5260-5266.

Li, L., Wu, H., Peijnenburg, W. J., & van Gestel, C. A. (2014). Both released silver ions and particulate Ag contribute to the toxicity of AgNPs to earthworm Eisenia fetida. *Nanotoxicology*, (0), 1-10.

Liang, S.-H., Chen, S.-C., Chen, C.-Y., Kao, C.-M., Yang, J.-I., Shieh, B.-S., Chen, J.-H., & Chen, C.-C. (2011). Cadmium-induced earthworm metallothionein-2 is associated with metal accumulation and counteracts oxidative stress. *Pedobiologia*, *54(5–6), 333-340. Liebig*

Lim, D., Roh, J. Y., Eom, H. J., Choi, J. Y., Hyun, J., & Choi, J. (2012). Oxidative stress-related PMK-1 P38 MAPK activation as a mechanism for toxicity of silver nanoparticles to reproduction in the nematode Caenorhabditis elegans. *Environmental Toxicology and Chemistry*, *31*(3), 585-592.

Lionetto, M. G., Calisi, A., & Schettino, T. (2012). Earthworm biomarkers as tools for soil pollution assessment. *Soil Health and Land Use and Management*, 305-332.

Liu, J., Pennell, K. G., & Hurt, R. H. (2011). Kinetics and mechanisms of nanosilver oxysulfidation. *Environmental Science & Technology*, *45*(17), 7345-7353.

Lombi, E., Donner, E., Taheri, S., Tavakkoli, E., Jämting, Å. K., McClure, S., Naidu, R., Miller, B. W., Scheckel, K. G., & Vasilev, K. (2013). Transformation of four silver/silver chloride nanoparticles during anaerobic treatment of wastewater and post-processing of sewage sludge. *Environmental Pollution*, *176*, 193-197.

Lorenz, C., Windler, L., Von Goetz, N., Lehmann, R. P., Schuppler, M., Hungerbühler, K., Heuberger, M., & Nowack, B. (2012). Characterization of silver release from commercially available functional (nano) textiles. *Chemosphere*, *89*(7), 817-824.

Lowry, G. V., Espinasse, B. P., Badireddy, A. R., Richardson, C. J., Reinsch, B. C., Bryant, L. D., Bone, A., Deonarine, A., Chae, S., Therezien, M., Colman, B. P., Hsu-Kim, H., Bernhardt, E., Matson, C. W., & Wiesner, M. R. (2012a). Long-term transformation and fate of manufactured Ag nanoparticles in a simulated large scale freshwater emergent wetland. *Environmental science & technology*, *46*(13), 7027-7036.

Lowry, G. V., Gregory, K. B., Apte, S. C., & Lead, J. R. (2012b). Transformations of nanomaterials in the environment. *Environmental science & technology*, *46*(13), 6893-6899.

Lubick, N. (2008). Nanosilver toxicity: ions, nanoparticles□ or both?. *Environmental Science & Technology*, *42*(23), 8617-8617.

Luoma, S. N. (2008). Silver nanotechnologies and the environment. *The Project on Emerging Nanotechnologies Report*, *15*.

Ma, R., Levard, C., Judy, J. D., Unrine, J. M., Durenkamp, M., Martin, B., Jefferson, B., & Lowry, G. V. (2013). Fate of zinc oxide and silver nanoparticles in a pilot wastewater treatment plant and in processed biosolids. *Environmental science & technology*, *48*(1), 104-112.

Marambio-Jones, C., & Hoek, E. M. (2010). A review of the antibacterial effects of silver nanomaterials and potential implications for human health and the environment. *Journal of Nanoparticle Research*, *12*(5), 1531-1551.

Margoshes, M., & Vallee, B. L. (1957). A cadmium protein from equine kidney cortex. *Journal of the American Chemical Society*, *79*(17), 4813-4814.

Morgan, A. J., Stürzenbaum, S. R., Winters, C., Grime, G. W., Aziz, N. A. A., & Kille, P. (2004). Differential metallothionein expression in earthworm (Lumbricus rubellus) tissues. *Ecotoxicology and environmental safety*, *57*(1), 11-19.

Muangphra, P., & Gooneratne, R. (2011). Comparative genotoxicity of cadmium and lead in earthworm coelomocytes. *Applied and Environmental Soil Science*, *2011*.

Mueller, N. C., & Nowack, B. (2008). Exposure modeling of engineered nanoparticles in the environment. *Environmental Science & Technology*, *42*(12), 4447-4453.

Mustonen, M., Haimi, J., Väisänen, A., & Knott, K. E. (2014). Metallothionein gene expression differs in earthworm populations with different exposure history. *Ecotoxicology*, *23*(9), 1732-1743.)

Nahmani, J., Hodson, M. E., & Black, S. (2007). A review of studies performed to assess metal uptake by earthworms. *Environmental Pollution*, *145*(2), 402-424.

Nahmani, J., Lavelle, P., & Rossi, J. P. (2006). Does changing the taxonomical resolution alter the value of soil macroinvertebrates as bioindicators of metal pollution?. *Soil Biology and Biochemistry*, *38*(2), 385-396.

Nannipieri, P., Kandeler, E., & Ruggiero, P. (2002). Enzyme activities and microbiological and biochemical processes in soil. *Enzymes in the environment. Marcel Dekker, New York*, 1-33.

Navarro, E., Baun, A., Behra, R., Hartmann, N. B., Filser, J., Miao, A. J., Quigg, A., Santschi, P. H., & Sigg, L. (2008a). Environmental behavior and ecotoxicity of engineered nanoparticles to algae, plants, and fungi. *Ecotoxicology*, *17*(5), 372-386.

Nel, A. E., Mädler, L., Velegol, D., Xia, T., Hoek, E. M., Somasundaran, P., Klaessig, F., Castranova, V., & Thompson, M. (2009). Understanding biophysicochemical interactions at the nano–bio interface. *Nature materials*, *8*(7), 543-557.

New Zealand Water & Wastes Association (2003). *Guidelines for the Safe Application of Biosolids to Land in New Zealand*. Retrieved on the 20th of July 2013 from http://www.waternz.org.nz/Folder?Action=View%20File&Folder_id=280&File=Workshop%20Handout.pdf

Nowack, B., & Bucheli, T. D. (2007). Occurrence, behavior and effects of nanoparticles in the environment. *Environmental Pollution*, *150*(1), 5-22.

Nowack, B., Krug, H. F., & Height, M. (2011). 120 years of nanosilver history: implications for policy makers. *Environmental science & technology*, *45*(4), 1177-1183.

Nuwaysir, E. F., Bittner, M., Trent, J., Barrett, J. C., & Afshari, C. A. (1999). Microarrays and toxicology: the advent of toxicogenomics. *Molecular carcinogenesis*, *24*(3), 153-159.

Mahadevan, B., Snyder, R. D., Waters, M. D., Benz, R. D., Kemper, R. A., Tice, R. R., & Richard, A. M. (2011). Genetic toxicology in the 21st century: reflections and future directions. *Environmental and Molecular Mutagenesis*, *52*(5), 339-354.

Olchawa, E., Bzowska, M., Stürzenbaum, S. R., Morgan, A. J., & Plytycz, B. (2006). Heavy metals affect the coelomocyte-bacteria balance in earthworms: Environmental interactions between abiotic and biotic stressors. *Environmental pollution*, *142*(2), 373-381.

Oukarroum, A., Barhoumi, L., Pirastru, L., & Dewez, D. (2013). Silver nanoparticle toxicity effect on growth and cellular viability of the aquatic plant Lemna gibba. *Environmental Toxicology and Chemistry*, *32*(4), 902-907.

Pal, S., Tak, Y. K., & Song, J. M. (2007). Does the antibacterial activity of silver nanoparticles depend on the shape of the nanoparticle? A study of the gram-negative bacterium Escherichia coli. *Applied and Environmental Microbiology*, *73*(6), 1712-1720.

Pan, B., & Xing, B. (2010). Chapter three-manufactured nanoparticles and their sorption of organic chemicals. *Advances in Agronomy*, *108*, 137-181.

Pan, B., & Xing, B. (2012). Applications and implications of manufactured nanoparticles in soils: a review. *European Journal of Soil Science*, *63*(4), 437-456.

Park, M. V., Neigh, A. M., Vermeulen, J. P., de la Fonteyne, L. J., Verharen, H. W., Briedé, J. J., van Loveren, H., & de Jong, W. H. (2011). The effect of particle size on the cytotoxicity, inflammation, developmental toxicity and genotoxicity of silver nanoparticles. *Biomaterials*, *32*(36), 9810-9817.

Pérez-Losada, M., Ricoy, M., Marshall, J. C., & Domínguez, J. (2009). Phylogenetic assessment of the earthworm< i> Aporrectodea caliginosa</i> species complex (Oligochaeta: Lumbricidae) based on mitochondrial and nuclear DNA sequences. *Molecular Phylogenetics and Evolution*, *52*(2), 293-302.

Perrier, E. (1872). *Recherches pour servir a l'histoire des lombriciens terrestres*. Bouvier.

Peyrot, C., Wilkinson, K. J., Desrosiers, M., & Sauvé, S. (2014). Effects of silver nanoparticles on soil enzyme activities with and without added organic matter. *Environmental Toxicology and Chemistry*, *33*(1), 115-125.

Pigeolet, E., Corbisier, P., Houbion, A., Lambert, D., Michiels, C., Raes, M., Zachery, M., & Remacle, J. (1990). Glutathione peroxidase, superoxide dismutase, and catalase inactivation by peroxides and oxygen derived free radicals. *Mechanisms of Ageing and Development*, *51*(3), 283-297.

Purcell, T. W., & Peters, J. J. (1998). Sources of silver in the environment. *Environmental Toxicology and Chemistry*, *17*(4), 539-546.

Rai, M., Yadav, A., & Gade, A. (2009). Silver nanoparticles as a new generation of antimicrobials. *Biotechnology Advances*, *27*(1), 76-83.

Reinsch, B. C., Levard, C., Li, Z., Ma, R., Wise, A., Gregory, K. B., Brown, G. E., & Lowry, G. V. (2012). Sulfidation of silver nanoparticles decreases Escherichia coli growth inhibition. *Environmental Science & Technology*, *46*(13), 6992-7000.

Richard, B., Decaëns, T., Rougerie, R., James, S. W., Porco, D., & Hebert, P. D. N. (2010). Re-integrating earthworm juveniles into soil biodiversity studies: species identification through DNA barcoding. *Molecular Ecology Resources*, *10*(4), 606-614.

Ritz, K., Black, H. I., Campbell, C. D., Harris, J. A., & Wood, C. (2009). Selecting biological indicators for monitoring soils: a framework for balancing scientific and technical opinion to assist policy development. *Ecological Indicators*, *9*(6), 1212-1221.)

Rivero, A. (2006). Nitric oxide: an antiparasitic molecule of invertebrates. *Trends in Parasitology*, *22*(5), 219-225.

Römer, I., White, T. A., Baalousha, M., Chipman, K., Viant, M. R., & Lead, J. R. (2011). Aggregation and dispersion of silver nanoparticles in exposure media for aquatic toxicity tests. *Journal of Chromatography A*, *1218*(27), 4226-4233.

Rozman, K. K., & Klaassen, C. D. (2007). Casarett and Doull's Toxicology: The Basic Science of Poisons.

Sanudo-Wilhelmy, S. A., & Flegal, A. R. (1992). Anthropogenic silver in the Southern California Bight: a new tracer of sewage in coastal waters. *Environmental Science & Technology*, *26*(11), 2147-2151.

Sathis, K. K., Suresh, K. U., & Neelanarayanan, P. (2013). Mitochondrial 16s RNA sequence for earthworm identification from semi evergreen forest type of Puliyancholai reserved forest in Kolli Hill, Tamil Nadu, South India. *Journal of Microbiology and Biotechnology Research, 3, 40-45.*

S v C (1826) s ’u é su s L b c s p Cuv *Mem. Acad. Sci. Inst. Fr*, *5*, 176-184.

Sawada, H., Takami, K., & Asahi, S. (2005). A toxicogenomic approach to drug-induced phospholipidosis: analysis of its induction mechanism and establishment of a novel in vitro screening system. *Toxicological Sciences*, *83*(2), 282-292.

Sayes, C. M., & Warheit, D. B. (2009). Characterization of nanomaterials for toxicity assessment. *Wiley Interdisciplinary Reviews: Nanomedicine and Nanobiotechnology*, *1*(6), 660-670.

Shahrokh, S., & Emtiazi, G. (2009). Toxicity and unusual biological behavior of nanosilver on Gram positive and negative bacteria assayed by microtiter-plate. *Eur J Biol Sci*, *1*(3), 28-31.

Shoults-Wilson, W. A., Reinsch, B. C., Tsyusko, O. V., Bertsch, P. M., Lowry, G. V., & Unrine, J. M. (2011a). Role of particle size and soil type in toxicity of silver nanoparticles to earthworms. *Soil Science Society of America Journal*, *75*(2), 365-377.

Shoults-Wilson, W. A., Zhurbich, O. I., McNear, D. H., Tsyusko, O. V., Bertsch, P. M., & Unrine, J. M. (2011b). Evidence for avoidance of Ag nanoparticles by earthworms (Eisenia fetida). *Ecotoxicology*, *20*(2), 385-396.

Sigel, A., Sigel, H., & Sigel, R. K. (Eds.). (2009). *Metallothioneins and related chelators* (Vol. 5). Royal Society of Chemistry.

Silva, T., Pokhrel, L. R., Dubey, B., Tolaymat, T. M., Maier, K. J., & Liu, X. (2014). Particle size, surface charge and concentration dependent ecotoxicity of three organo-coated silver nanoparticles: comparison between general linear model-predicted and observed toxicity. *Science of the Total Environment*, *468*, 968-976.

Simonet, B. M., & Valcárcel, M. (2009). Monitoring nanoparticles in the environment. *Analytical and bioanalytical chemistry*, *393*(1), 17-21.

Song, Y., Li, X., & Du, X. (2009). Exposure to nanoparticles is related to pleural effusion, pulmonary fibrosis and granuloma. *European Respiratory Journal*, *34*(3), 559-567.

Spurgeon, D. J., Svendsen, C., Lister, L. J., Hankard, P. K., & Kille, P. (2005). Earthworm responses to Cd and Cu under fluctuating environmental conditions: a comparison with results from laboratory exposures. *Environmental pollution*, *136*(3), 443-452.

Stein, L., Boulding, R., Helmick, J., & Murphy, P. (1995). Process design manual: land application of sewage sludge and domestic septage. *Cincinnati, Ohio: US Environmental Protection Agency*.

Stensberg, M. C., Wei, Q., McLamore, E. S., Porterfield, D. M., Wei, A., & Sepúlveda, M. S. (2011). Toxicological studies on silver nanoparticles: challenges and opportunities in assessment, monitoring and imaging. *Nanomedicine*, *6*(5), 879-898.

Strange, R. N., & Scott, P. R. (2005). Plant disease: a threat to global food security. *Phytopathology*, *43*.

Stürzenbaum, S. R. (2009). Earthworm and nematode metallothioneins. *Metal ions in life sciences*, *5*, 183-197.

Stürzenbaum, S. R., Andre, J., Kille, P., & Morgan, A. J. (2009). Earthworm genomes, genes and proteins: the (re) discovery of Darwin's worms. *Proceedings of the Royal Society B: Biological Sciences*, *276*(1658), 789-797.

Stürzenbaum, S. R., Georgiev, O., Morgan, A. J., & Kille, P. (2004). Cadmium detoxification in earthworms: from genes to cells. *Environmental science & technology*, *38*(23), 6283-6289.

Stürzenbaum, S. R., Kille, P., & Morgan, A. J. (1998). The identification, cloning and characterization of earthworm metallothionein. *Febs Letters*, *431*(3), 437-442.

Suthar, S. (2009). Earthworm communities a bioindicator of arable land management practices: a case study in semiarid region of India. *Ecological indicators*, *9*(3), 588-594.

Tabatabai, M. A., Dick, W. A., Burns, R. G., & Dick, R. P. (2002). Enzymes in soil: research and developments in measuring activities. *Enzymes in the environment: activity, ecology, and applications*, 567-596.

Tourinho, P. S., Van Gestel, C. A., Lofts, S., Svendsen, C., Soares, A. M., & Loureiro, S. (2012). Metal-based nanoparticles in soil: Fate, behavior, and effects on soil invertebrates. *Environmental Toxicology and Chemistry*, *31*(8), 1679-1692.

Tsai, C. F., Tsai, S. C., & Liaw, G. J. (2000). Two new species of protandric pheretimoid earthworms belonging to the genus Metaphire (Megascolecidae: Oligochaeta) from Taiwan. *Journal of Natural History*, *34*(9), 1731-1741.

Tsyusko, O. V., Hardas, S. S., Shoults-Wilson, W. A., Starnes, C. P., Joice, G., Butterfield, D. A., & Unrine, J. M. (2012). Short-term molecular-level effects of silver nanoparticle exposure on the earthworm,< i> Eisenia fetida</i>. *Environmental Pollution*, *171*, 249-255.

Umh, H. N., & Kim, Y. (2013). Spectroscopic and microscopic studies of vesicle rupture by AgNPs attack to screen the cytotoxicity of nanomaterials. *Journal of Industrial and Engineering Chemistry*.

Unrine, J. M., Colman, B. P., Bone, A. J., Gondikas, A. P., & Matson, C. W. (2012). Biotic and abiotic interactions in aquatic microcosms determine fate and toxicity of Ag nanoparticles. Part 1. Aggregation and dissolution. *Environmental science & technology*, *46*(13), 6915-6924.

Valko, M. M. H. C. M., Morris, H., & Cronin, M. T. D. (2005). Metals, toxicity and oxidative stress. *Current medicinal chemistry*, *12*(10), 1161-1208.

van der Ploeg, M. J., Handy, R. D., Heckmann, L. H., van der Hout, A., & Van Den Brink, N. W. (2013). C60 exposure induced tissue damage and gene expression alterations in the earthworm Lumbricus rubellus. *Nanotoxicology*, *7*(4), 432-440.

van der Ploeg, M. J., van den Berg, J. H., Bhattacharjee, S., de Haan, L. H., Ershov, D. S., Fokkink, R. G., Zuilhof, H., Rietjens, I., & van den Brink, N. W. (2014). In vitro nanoparticle toxicity to rat alveolar cells and coelomocytes from the earthworm Lumbricus rubellus. *Nanotoxicology*, *8*(1), 28-37.

van der Wal, A., Norde, W., Zehnder, A. J., & Lyklema, J. (1997). Determination of the total charge in the cell walls of Gram-positive bacteria. *Colloids and surfaces B: Biointerfaces*, *9*(1), 81-100.

VandeVoort, A. R., Arai, Y., & Sparks, D. L. (2012). Environmental chemistry of silver in soils: current and historic persective. *Advances in agronomy*, *114*, 59-90.

Wang, D., Kou, R., Choi, D., Yang, Z., Nie, Z., Li, J., Saraf, L. V., Hu, D. H., Zhang, J. G., Graff, G. L., Liu, J., Pope, M. A., & Aksay, I. A. (2010). Ternary self-assembly of x − p c p s s c c c s *ACS nano*, *4*(3), 1587-1595.

Wang, J., Rahman, M. F., Duhart, H. M., Newport, G. D., Patterson, T. A., Murdock, R. C., Hussain, S. M., Schlager, J. J., & Ali, S. F. (2009). Expression changes of dopaminergic system-related genes in PC12 cells induced by manganese, silver, or copper nanoparticles. *Neurotoxicology*, *30*(6), 926-933.

Wang, Y., Westerhoff, P., & Hristovski, K. D. (2012). Fate and biological effects of silver, titanium dioxide, and C< sub> 60</sub>(fullerene) nanomaterials during simulated wastewater treatment processes. *Journal of hazardous materials*, *201*, 16-22.

Wei, L., Tang, J., Zhang, Z., Chen, Y., Zhou, G., & Xi, T. (2010). Investigation of the cytotoxicity mechanism of silver nanoparticles in vitro. *Biomedical Materials*, *5*(4), 044103.

Wieczorek-Olchawa, E., Niklinska, M., Miedzobrodzki, J., & Plytycz, B. (2003). Effects of temperature and soil pollution on the presence of bacteria, coelomocytes and brown bodies in coelomic fluid of Dendrobaena veneta: The 7th international symposium on earthworm ecology· Cardiff· Wales· 2002. *Pedobiologia*, *47*(5), 702-709.

Wigginton, N. S., Haus, K. L., & Hochella Jr, M. F. (2007). Aquatic environmental nanoparticles. *Journal of Environmental Monitoring*, *9*(12), 1306-1316.

Wilson, K. H. (1995). Molecular biology as a tool for taxonomy. *Clinical infectious diseases*, *20*(Supplement 2), S117-S121.

Wise, J. P., Goodale, B. C., Wise, S. S., Craig, G. A., Pongan, A. F., Walter, R. B., Thompson, W. D., Ng, A. K., Aboueissa, A. M., Mitani, H., Spalding, M. J., & Mason, M. D. (2010). Silver nanospheres are cytotoxic and genotoxic to fish cells. *Aquatic Toxicology*, *97*(1), 34-41.

Woodrow Wilson Database (2010). (http://www.nanotechproject. org). Accessed 02 July 2013.

Wu, Y., & Zhou, Q. (2013). Silver nanoparticles cause oxidative damage and histological changes in medaka (Oryzias latipes) after 14 days of exposure. *Environmental Toxicology and Chemistry*, *32*(1), 165-173.

Yacobi, N. R., Malmstadt, N., Fazlollahi, F., DeMaio, L., Marchelletta, R., Hamm-Alvarez, S. F., Borok, Z., Kim, K., & Crandall, E. D. (2010). Mechanisms of alveolar epithelial

translocation of a defined population of nanoparticles. *American journal of respiratory cell and molecular biology*, *42*(5), 604-614.

Yu, S. J., Yin, Y. G., & Liu, J. F. (2013). Silver nanoparticles in the environment. *Environmental Science: Processes & Impacts*, *15*(1), 78-92.

Zhan, Y. (2012). *Effects of silver nanoparticles on bacteria and earthworms* (Doctoral dissertation, Lincoln University)

Zhang, Z., Kong, F., Vardhanabhuti, B., Mustapha, A., & Lin, M. (2012). Detection of engineered silver nanoparticle contamination in pears. *Journal of agricultural and food chemistry*, *60*(43), 10762-10767.